AN ABSTRACT OF THE THESIS OF

Alok Tripathi for the degree of Doctor of Philosophy in Electrical and Computer Engineering presented on April 2, 1999.

Title: Modeling and Characterization of Multiple Coupled Lines

Abstract approved: _____
V. K. Tripathi

A configuration-oriented circuit model for multiple coupled lines in an inhomogeneous medium is developed and presented in this thesis. This circuit model consists of a network of uncoupled transmission lines and is readily modeled with simulation tools like LIBRA© and SPICE©. It provides an equivalent circuit representation which is simple and topologically meaningful as compared to the model based on modal decomposition. The configuration-oriented model is derived by decomposing the immittance matrices associated with an n coupled line $2n$-port system. Time- and frequency-domain simulations of typical coupled line multiports are included to exemplify the utility of the model. The model is useful for the simulation and design of general single and multilayer coupled line components, such as filters and couplers, and for the investigation of signal integrity issues including crosstalk in interconnects associated with high speed digital and mixed signal electronic modules and packages.

It is shown that multiconductor lossless structures in an inhomogeneous medium can be characterized by multiport time-domain reflection (TDR) measurements. A synthesis technique of an equivalent lossless (non-dispersive) uniform multiconductor n coupled lines (UMCL) $2n$-port system from the measured discrete time-domain reflection response is presented. This procedure is based on the decomposition of the characteristic immittance matrices of the UMCL in terms of partial mode immittance matrices. The decomposition scheme leads to the discrete transition matrix function of a UMCL $2n$-port system. This in turn establishes a relationship between the normal-mode parameters of the UMCL and the measured impulse reflection and transmission response. Equivalence between the synthesis procedure presented in this thesis and the solution

of a special form of an algebraic Riccati matrix equation whose solution can lead to the normal-mode parameters and a real termination network is illustrated. In order to demonstrate the procedure, a typical microstrip structure with three lines is synthesized from the time-domain reflection (TDR) data.

In order to compliment known field theoretic techniques for characterization of multiconductor structures a network analog method is employed to solve the magnetic vector potential equation to characterize multilayer Metal-Insulator-Semiconductor (MIS) transmission line structures. This approach leads to the frequency dependent distributed inductance and the resistance matrices of a multilayer MIS transmission line structure. It is shown that the frequency dependent transmission line parameters can be modeled by an efficient quasi-static formulation for all propagating modes including the slow-wave and skin-effect modes. To demonstrate the proposed approach for single and multilevel structures, the frequency dependent distributed inductance and resistance matrices corresponding to the propagating modes classified as the slow-wave and skin-effect modes are calculated and validated by comparison with full-wave solutions.

Modeling and Characterization of Multiple Coupled Lines

by

Alok Tripathi

A THESIS

submitted to

Oregon State University

in partial fulfillment of the

requirements for the degree of

Doctor of Philosophy

Completed April 2, 1999

Commencement June 1999

Doctor of Philosophy thesis of Alok Tripathi presented on April 2, 1999

APPROVED:

Major Professor, representing Electrical and Computer Engineering

Head of Department of Electrical and Computer Engineering

Redacted for Privacy

Dean of Graduate School

I understand that my thesis will become part of the permanent collection of Oregon State University libraries. My signature below authorizes release of my thesis to any reader upon request.

Redacted for Privacy

Alok Tripathi, Author

ACKNOWLEDGEMENTS

First of all, I would like to express my gratitude to Prof. V. K. Tripathi for his valuable guidance, constant support, encouragement and patience during the entire course of this research.

I would also like to thank Prof. Weisshaar for his help, guidance and patience, and Prof. Temes, Prof. Miller, Prof. Kolodziej, Dr. Settaluri for serving on my graduate committee and reviewing the manuscript.

I am also grateful to my friends and colleagues, Rick, Maynard, Bhanu, Ed, John, Paul, Kate, Zheng, Seoy, Kim, Hahm and many others for their valuable discussions, cooperation and encouragement.

Additionally, I would like to acknowledge support of Dr. Arabi whose whole hearted involvement as Intel project mentor and also Intel Corporation for the project which lead this research work to the present form.

Last but not the least I would like to express my gratitude to Prof. T. S. Vedavathy (IISc, Bangalore) for her guidance and to my parents for the encouragement, support and patience that they had evinced for my long absence from home.

TABLE OF CONTENTS

TABLE OF CONTENTS (CONTINUED)

TABLE OF CONTENTS (CONTINUED)

LIST OF FIGURES

LIST OF FIGURES (CONTINUED)

LIST OF FIGURES (CONTINUED)

LIST OF TABLES

Chapter 1
INTRODUCTION

For the last several decades, modeling and characterization techniques for multiconductor transmission line (MTL) system have been a topic of active research. Application of this research, in general, includes several important fields of electrical engineering. One of the prominent applications of MTL system is in power systems for efficient transmission of electrical energy from one point to another as in case of two/multiconductor power line. Multilevel interconnects present on the multilayer printed circuit boards (PCBs) and in high-speed digital and high-frequency RF integrated circuits are also examples of nonuniform MTLs. MTLs also have several useful applications in the area of microwave engineering, especially in MMIC's (Monolithic Microwave Integrated Circuits), where they are widely used as basic building block element in some of the passive structures [5], [6], [7]. Furthermore, in the field of signal processing and system identification, the propagation and electrical characteristics of MTLs can also be indirectly linked with the development of several, now widely used algorithms. The well established theory of design of lattice filters [8], [9] (digital filters) pertaining to signal processing can be interpreted in terms of propagation and electrical characteristics of transmission lines. Another example is in the solution (e.g. single and multidimensional peeling algorithm [10], [11]) of several problems explicitly classified as single or multi-dimension inverse problems in the present system identification literature [8], [9], [12].

Several CAD-oriented (Computer-Aided-Design) models for application specific MTLs based systems have been proposed and investigated in the past. In general, most of these MTLs based systems have different CAD-oriented equivalent circuit models for modeling their electrical characteristics despite the fact that all of these systems can be described by the identical governing differential equations such as the transmission

line equations. The same holds true for the electrical characterization techniques associated with these application specific equivalent circuit models of MTL systems. The dependence of CAD-oriented equivalent circuit models and similarly the corresponding characterization techniques are due to the exploitation or emphasis of different aspects of the electromagnetic boundary value problems associated with these different application. This results in different frequency, time and spatial variations in the corresponding line parameters of the transmission line equations. For example, recent spectacular advances in the processing technology of semiconductors has lead to the reduction of active device sizes on digital and RF integrated circuits. The reduction of the device sizes such as MOSFET and BJT has made the associated parasitics smaller resulting in significant improvement in switching speed and the high frequency analog operational capabilities. Furthermore, demands of inclusion of more functionalities on die or on the same board, for better cost effectiveness, has lead to the increase in density and electrical lengths of interconnects used in connecting the high-speed circuit devices. These interconnects now occupy a major area (real-state) of the die in a modern day integrated circuit. The electrical characteristics of these high performance interconnects are influenced by several factors which includes spatial variation of the interconnect metallization, inhomogeneity of dielectric layers, conductor and dielectric losses and various discontinuities such as vias, steps and bends.

The high speed interconnects are designed with the objective to maintain the signal integrity and the timing constraints (noise margins and timing budgets) at very high frequency. Thereby, interconnects performance can significantly get affected by the high frequency electromagnetic issues associated with these structures. Unlike interconnects, in power transmission lines EMC and the non-ideal ground effects (due to the earth) are of significance and here the main emphasis is on the reduction of transmission losses. In such systems low frequency electromagnetic issues are more important and the transmission lines are uniform or can have spatial variation along the direction of propagation. High frequency effects (on the corresponding MTLs line parameters) are more dominant in applications involving usage of coupled transmission lines as passive components in MMICs. Here the MTLs are uniform or sometimes have spatial varia-

tion along the direction of the propagation. In all of the above mentioned applications, MTL systems are designed to reduce all type of losses which include the radiation loss (to reduce EMC related effects). In contrast to these applications, in antenna systems (e.g. dipole, microstrip antenna etc.) which can be considered as a transmission line systems the objective is to enhance and modify the radiation pattern. From the above discussion it is apparent that different dominant effects as well as system specifications for different applications determines the equivalent circuit CAD models as well as the characterization techniques linked with the MTLs based system to only specific sets of applications.

1.1 OVERVIEW OF THESIS

In this thesis fundamental theory of coupled transmission line is revisited and some new and significant results applicable to general MTL system are illustrated. These results further reinforce the validity and importance of already existing formulation based on the normal-mode parameters [13], [14],[15]. The presented work broadly addresses the following key areas:

- An overview of current state of art in the modeling techniques for MTL systems in microwave and high-speed interconnect applications.
- A new equivalent circuit CAD model (configuration-oriented model [2], [4]) for uniform MTL system based on the single transmission lines.
- Relationship of this model (configuration-oriented model) with respect to already existing equivalent circuit models for MTL system.
- Synthesis technique for a uniform lossless non-dispersive MTL system from the measured time-domain reflection response.
- A quasi-TEM based network analog approach for extraction of line parameters of MIS (Metal-Insulator-Semiconductor substrate) based multilayer multilevel transmission line structures.

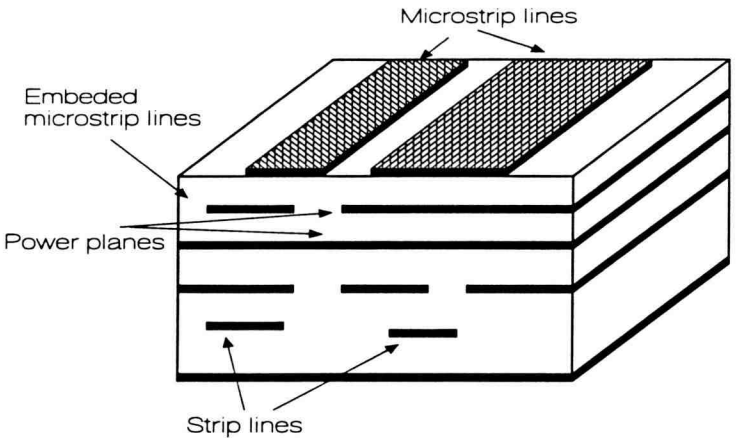

Figure 1.1. A typical multilayer multilevel interconnect structure.

The presented results are useful in modeling and characterization of typical uniform multiconductor transmission line structures in a multilayer dielectric and multilevel metallization type of interconnect environment typically encountered on integrated circuits or in high performance digital, RF or mixed signal printed-circuit boards. Such a schematic of a typical multilayer, multilevel interconnect structure is shown in Fig. 1.1.

1.2 THESIS ORGANIZATION

A general review of MTLs from the historical perspective for modeling, characterization, synthesis and the extraction of characteristics parameters by electromagnetic simulation is presented in Chapter-2. In Chapter-3, a new CAD-oriented model is proposed for the MTLs. This model consists of a system of transmission lines and has simpler SPICE input data requirements as compared to the modal decomposition based models. It is shown that this configuration-oriented model can, in general, be implemented for the simulation of lossy and dispersive multiconductor inhomogeneous

structures. The derivation of the circuit model is based on decomposition of the admittance or impedance matrix of the n coupled lines $2n$-port system. Closed form expressions for the model parameters for the important cases of asymmetric coupled lines and symmetrical three coupled line structures are included in this chapter. Time- and frequency-domain simulation results for typical structures are presented to demonstrate the applications of the configuration-oriented SPICE models.

The problem of synthesis of an equivalent $2n$-port system (for n uniform coupled lines) from the reflection response of a uniform MTL system is a subset of classical problems defined as multi-dimensional inverse problems. In Chapter-4, a synthesis procedure for equivalent $2n$-port system associated with n coupled lossless non-dispersive transmission lines from the measured reflection response of a uniform MTL system is proposed. An entirely new transition matrix function of a uniform MTL system in the discrete Fourier transform domain (z-domain) is derived. The relationship between the measured reflection response and the normal-mode parameters of MTL system are studied. Later, equivalence between the solution of special class of polynomial algebraic Riccati matrix equation [120] and the synthesis procedure proposed in this chapter is illustrated. Furthermore, to exemplify this procedure coupled three microstrip line 6-port system is synthesized from the measured time-domain reflection response.

In Chapter-5, a new approach based on network analog approach is proposed for extraction of frequency dependent transmission line parameters of a MIS transmission line structure. This formulation is based on the vector magnetic potential equation applicable to MIS structure. A detailed description of how the magnetic potential equation can be discretized and various boundary conditions implemented for a MIS transmission line structures is illustrated. The proposed approach is then applied to several useful MIS transmission line structures to demonstrate the validity and accuracy of the approach.

Conclusions and recommendations for possible future work based on the work reported in this thesis are summarized in Chapter-6.

Chapter 2
INTRODUCTION TO MULTIPLE COUPLED LINES

The analysis and modeling of coupled transmission systems including multiconductor transmission lines has been a topic of considerable interest in recent years. Advances in planar and layered interconnect and propagation structures and components in microwave, high speed digital and mixed signal circuits have resulted in increased interest in efficient, accurate analysis and design of these circuits and systems. In this chapter, a general discussion of the coupled transmission line formulation and some typical applications of coupled transmission lines in MMICs is presented. The various CAD-oriented models proposed for MTL systems in the current literature relevant to the usage of MTLs as interconnects and passive components on integrated circuits or on printed-circuit boards are summarized. An overview of existing techniques for the synthesis of transmission lines from the measured reflection and transmission response data are reported. Additionally, a brief description of the techniques currently available for the extraction of transmission line parameters of a multilayer transmission line structure with special emphasis to MIS transmission line structures are discussed.

2.1 COUPLED TRANSMISSION LINE FORMULATION

A general (n+1) multiconductor line system including the reference conductor plane is shown in Fig. 2.1. Assuming the given multiconductor transmission lines are uniform along the length and the propagation modes are quasi-TEM, the electrical characteristics of this system are described by matrix telegraphers equations (or coupled transmission line equations) as,

$$\frac{\partial v]}{\partial z} = -([R(\omega)] + j\omega[L(\omega)])i] \tag{2.1}$$

$$\frac{\partial i]}{\partial z} = -([G(\omega)] + j\omega[C(\omega)])v]. \tag{2.2}$$

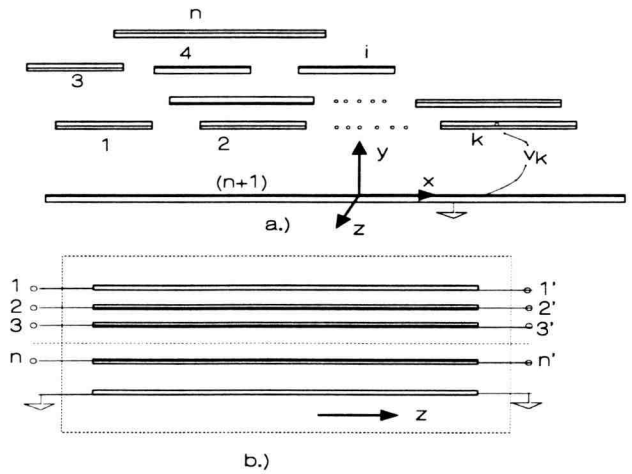

Figure 2.1. A general MTLs system, and the corresponding $2n$-port MTL system.

Here the kth element of vectors $v]$ represents the voltage between the kth conductor and the reference conductor. Similarly, the kth element of vector $i]$ represents the current flowing on the kth conductor. The matrices $[R(\omega)]$, $[G(\omega)]$, $[L(\omega)]$ and $[C(\omega)]$ are in general frequency dependent resistance, conductance, inductance and capacitance matrices respectively corresponding to the given multiconductor coupled line system. From the circuit point of view, the From the circuit point of view, desired form of solution for (1) and (2) is to describe the given n uniform multiconductor transmission line system in terms of $2n$-port (algebraic) system which is independent of the boundary conditions associated with the transmission line equations. This leads to an equivalent $2n$-port circuit block element, general enough to allow any terminal conditions in terms of linear as well as nonlinear circuit elements at the ports. The procedure for extraction of $2n$-port algebraic system corresponding to the partial differential equations given in (1) and (2) is carried out by assuming $e^{j\omega t-\gamma z}$ variation along the direction of propagation. This assumption partially decouples the coupled transmission line equations. The resulting equations are further transformed by using linear transformations and leads to a generalized matrix eigenvalue problem and the corresponding decoupled transmission line equations. The solution of the generalized matrix eigenvalue problem and the

associated decoupled transmission line equations can be described in terms of $2n$-port algebraic system. Moreover, this $2n$-port system can be expressed in terms of well know $2n$-port impedance, admittance, $ABCD$ or the scattering matrix parameters [13], [14], [15].

In general, the circuit simulation and design of these structures is normally based on the characteristic parameters derived from a rigorous frequency dependent electromagnetic solution, or the line constants derived from quasi-static solutions. The quasi-static solutions lead to the [R], [L], [G], and [C] matrices associated with the multiconductor system. The frequency dependent full wave solutions lead to the computation of eigenvalues, eigenvectors and eigenfunctions from which equivalent frequency dependent elements of the [R],[L],[G] and [C] matrices can also be calculated. Discussion of capacitance and inductance matrices in terms of modal power is presented in [16]. Similarly, in [17] the quasi-TEM analysis of lossless coupled transmission line system in an inhomogeneous medium is reviewed. Starting from the generalized telegraphers equations the characteristic impedance of the normal-mode parameters using power-current, power-voltage and voltage-current is defined and computed. Some examples of quasi-static and full wave approach based on one of these definition can be found in [3], [15], [18], [19]. Despite availability of procedure for representing coupled transmission line equations as a $2n$-port system in terms of normal-mode parameters, survey of recent literature reveals several different formulations [20]. Many of the formulations can lead to nonphysical values for the normal-mode parameters associated with the $2n$-port system and was explicitly demonstrated in [21]. The details of the procedure for representing coupled transmission line system in terms of $2n$-port system and the physical significance of normal-mode parameters are reported in [3], [4], [13], [14], [15].

2.2 SOME APPLICATIONS OF MULTIPLE COUPLED LINES

As alluded, earlier interconnects are composed of nonuniform MTLs and therefore MTLs are the essential components of integrated circuits and the printed-circuit boards for connecting various active devices. Also, in case of microwave integrated circuits,

MTLs are also used in the design of passive devices. Despite several advancement in the design and wide usage of these passive (devices) structures several issues still remain unresolved and are at present subject of ongoing research. Here, some of the typical recent advances in the applications of MTLs in various passive structures are briefly reviewed.

Application of coupled line in the design of couplers have been widely investigated and reported in the literature. Design procedure for asymmetric couplers (based on coupled transmission line) with equal phase velocity have been derived in [22]. Gunton in [23] has derived design equations for the S-parameters for 4-port couplers with non-mode converting impedances based on the formulation for inhomogeneous coupled transmission lines given by Tripathi [13]. A more general formulation based on the optimization has been reported by Chin [24] for the design of couplers with real termination impedances. Sellberg [25] derived explicit formulas for the synthesis and the optimization of general uniform contra-directional couplers having complex termination impedances. Thereby the known method of compensating different phase velocities (c and π modes) using shunt capacitors can now also be included in the design procedure using this formulation. Couplers based on coupled dielectric waveguide, microstrips and coupled finline structure with co-directional or/and contra-directional coupling has been reported in [5], [6], [22], [23], [26], [27], [28]. Except for some special cases, a general solution to the problem of synthesis of asymmetric coupled line coupler remains unresolved and is an area of active research.

In [29], [30], [31] a design procedure for edge-coupled transmission line transformers for designing networks to provide DC isolation for biasing active circuits in MMIC applications has been reported. Quirarte has in [7] demonstrated how different configurations of coupled lines or parallel connected coupled lines can be used together to obtain differential phase shifters. Yansheng has shown that several short sections of two or more coupled lines when alternatively connected together can achieve the needed performance of a single-section coupler and phase shifter [32]. This analysis is restricted to symmetrical structures. Applications and design procedures for filters based on special cases of MTLs are described in [33], [34] [35].

In recent years design procedures for the reduction of crosstalk for coupled interconnects is also being actively investigated. Use of substrate compensation to control crosstalk and coupling was reported in [36]. A layout technique which reduces the nearest neighbor crosstalk for multiconductor signal buses is presented in [37]. A technique to analyze two conductor transmission lines with rectangular notch in the dielectric layer between the two strip for reduction of the crosstalk is presented in [38]. In general, much of the work reported regarding application of MTLs as circuit elements concerns only with few special cases of a general MTLs system. Application of general normal-mode formulation [13], [14] to various MTLs based devices is still a subject of active research.

2.3 CAD-ORIENTED MODELING TECHNIQUES

Computer-Aided-Design (CAD) methodologies for the design, simulation and optimization of integrated circuits are presently an integral part of integrated circuit design cycle. Sophisticated and accurate SPICE models for basic circuit elements or device model libraries are essential elements for a successful design. MTLs as interconnects or passive devices are now important structures and can significantly affect the performance of integrated circuits. Crosstalk, noise due to reflections, skews, absolute delays and ground bounce limits the performance of digital and RFICs and have now become important issues to be included in the design cycle. Thereby, accurate and computationally efficient CAD models of MTLs are essential and are at present an active area of research. CAD models based on the equivalent circuits (model is generated using existing SPICE elements) and transfer function based techniques are the two distinct ways addressed in the current literature for modeling the MTLs based systems. We here review the current state of art in the modeling techniques for MTLs and also their evolution with time. Modeling techniques for MTLs from the perspective of interconnects modeling and passive structures modeling in microwave and RF systems are only considered.

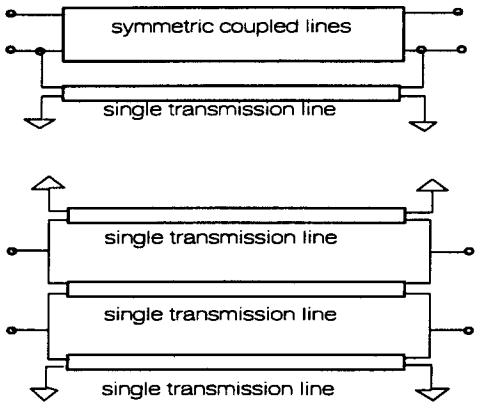

Figure 2.2. Equivalent circuit of coupled transmission lines in a homogeneous medium based on [1] and [2].

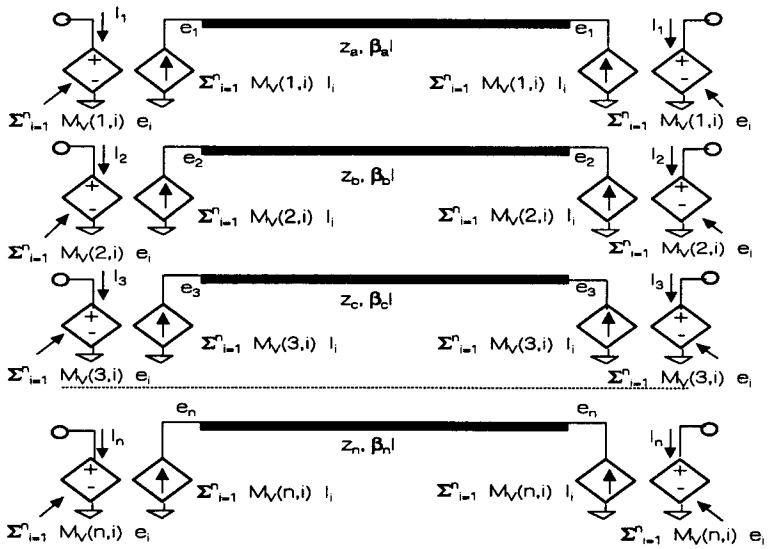

Figure 2.3. Equivalent circuit of multiconductor transmission lines based on modal decomposition [3]. $[M_V]$ is the modal voltage eigenvector matrix, z_i are the corresponding model characteristic impedances and β_i are the associated modal delays.

2.3.1 Equivalent Circuit Models

Several circuit models based on the solution of coupled transmission line equations have been proposed in the past. For a lossless multiconductor transmission line structure in a homogeneous media Seviora [39] presented an n coupled transmission line equivalent circuit which requires only single transmission lines. Approximate synthesis procedures for a $2n$-port admittance matrix associated with coupled transmission lines using transmission lines and short-circuit stubs was reported in [40], [41]. These methods had negative characteristic immittance in the equivalent circuit. Equivalent circuit based on a pair of non-symmetrical coupled lines where the coupling between the neighboring lines were taken into the account was reported by Grayzel [42]. A general equivalent circuit for n coupled lines in homogeneous media based on the generalization of [42] was presented in [1]. An example of such an equivalent circuit for the case of coupled transmission line system is shown in Fig. 2.2. The basic element of this equivalent circuit consists of symmetrical coupled lines and transmission lines to model a general n coupled transmission line structure excluding the reference conductor. The number of elements needed in the equivalent circuit is at most $(n^2 - n + 2)/2$. For the case of lossless coupled transmission lines in inhomogeneous media with frequency-independent line constants, a SPICE model based on modal decompositions was proposed in [19]. This model represents the congruent transformer bank [43] by dependent sources and leads to a circuit model consisting of linear dependent sources and ideal delay elements representing uncoupled transmission lines (ref. Fig. 2.3). This model was also extended to lossy MTL system in [19]. The disadvantage of this model is that the linear dependent source elements vary with frequency. This means that the model is not appropriate for the transient analysis usually performed on time- domain circuit simulators.

Simplified versions of the model valid for special cases of homogeneous, electrically identical lines with near neighbor coupling only have also been reported [44], [45]. A rigorous procedure leading to the configuration-oriented equivalent circuit model, consisting of a system of transmission lines only, was reported for the case of homogeneous media in [2] (ref. Fig. 2.2). The number of transmission lines elements needed in

the equivalent circuit is at most $n(n+1)/2$. Similar useful models valid for special cases of inhomogeneous structures have also been proposed and used in the design of coupled lines circuits [34], [46], [47], [48], [49]. These models are not suitable for a general multiconductor transmission line structure. A general configuration-oriented equivalent circuit model for multiconductor transmission lines in an inhomogeneous medium is reported in [4] (ref. Fig. 2.4). This circuit model demonstrates that the multiconductor coupled line system can be represented in terms of uncoupled transmission lines. These uncoupled transmission lines are connected in a configuration-oriented fashion. The number of transmission line elements needed in the equivalent circuit is at most $n^2(n+1)/2$. Modeling of lossy and lossless uncoupled transmission lines in this circuit model can be performed via several, widely available and reported CAD oriented models for single transmission line system in the present literature. For example, with configuration-oriented model a very useful and most commonly used algorithm for transient analysis of lossless transmission line system based on the method of characteristics proposed in [50] can be used in the simulation of lossless uncoupled transmission lines. The method of characteristics has been also extended to lossy transmission lines system in [51], [52]. Here the transfer function of lossy line is approximated in terms of lumped and distributed circuit elements which again can be used for simulating the lossy uncoupled transmission lines present in the configuration-oriented equivalent circuit model.

2.3.2 Alternate Modeling Techniques: for MTLs

As an alternative to the equivalent circuit methods where the emphasis is on obtaining the equivalent circuit of MTLs with the already existing SPICE circuit elements, several modeling techniques for MTLs which needs some preprocessing before SPICE implementation has been proposed in the current literature. In this section, some of these alternative methods are reviewed.

Approximating transmission lines in terms of simplified pole-zero description has been investigated in [53], [54]. In [55], a distributed interconnect model is proposed for

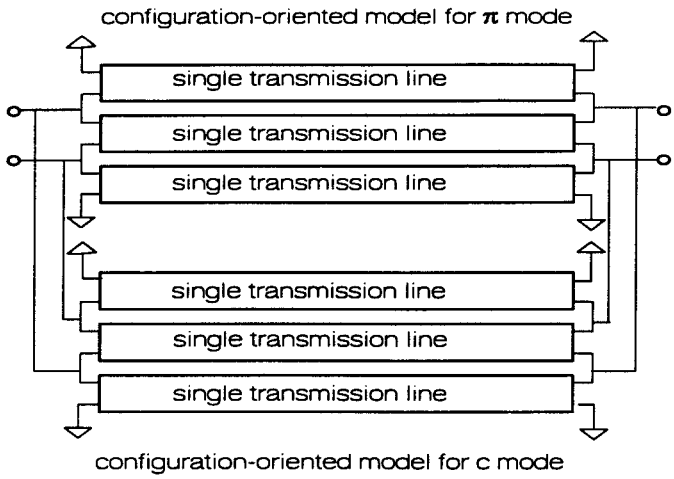

Figure 2.4. Equivalent circuit of coupled transmission lines in an inhomogeneous media based on the configuration-oriented model [4]. Here the uncoupled transmission lines in the π and c part are of different electrical lengths.

a self-damped lossy transmission lines. A method for transient analysis of lossy transmission lines with an arbitrary nonlinear terminal networks is presented in [56], [57]. Here the time-domain Green function is evaluated for the multiconductor transmission lines by terminating the ports with the quasi-match loads to ensure short duration of Green function response. A procedure based on the method of characteristic for simulating lossless coupled line was demonstrated by Chang [43] and later extended to multiconductor lossy coupled transmission lines structure by Orhanovic and Chang [58], [59], [60]. A new approach for the time-domain simulation of transient on a dispersive and lossy coupled transmission lines terminated with the active devices was reported in [61], [62]. This method combines scattering matrix of an arbitrary line and the nonlinear causal impedance functions at load ends to derive expressions for the signals at the near and the far end. Numerical inversion of Laplace transform has been an important tool for time-domain analysis of high speed VLSI interconnects modeled by transmission line network. A procedure based on inversion of Laplace transform is presented for analysis

of lossy coupled transmission lines with arbitrary linear termination and interconnecting network is proposed in [63], [64]. Methods based on this procedure leads to slow decaying functions during Laplace inversion and therefore the convergence of inversion procedure in [63], [64] can be computationally inefficient.

For a nonuniform MTL systems also several CAD oriented modeling techniques have been proposed in the literature. In [65], time-domain scattering parameters of MTLs are formulated and the nonuniform section is modeled by cascaded uniform sections for simulating nonuniform MTL system. This procedure can lead to a very large number of cascaded uniform sections making the approach computationally inefficient. A procedure based on asymptotic waveform evaluation (AWE) technique is reported in [66], [67], [68]. In this procedure, Pade's moment-matching methods are used to approximate the frequency-domain transfer function of linear circuit by an equivalent circuit with fewer number of poles and residues. The disadvantage of this method is that the moment matching is done at the single point and leads to fewer number of poles. This is due to the ill conditioning of the Hankel matrix resulted in the solution of unknown terms in the equivalent circuit. Multi-point moment matching techniques such as Complex-Frequency-Hopping (CFH) or multi-point Pade's approximation [69] has been suggested as an alternative to AWE. For a lossy coupled line system, moment matching with Pade and CFH has been applied to obtain dominant poles of an equivalent network for frequency- and time-domain simulation is illustrated in [70]. This approach can be computationally inefficient and requires multiple expansions. To model transient response of nonuniform coupled line system a method of convolution-characteristics is reported in [71]. Based on Chebyshev expansion for the spatial variations of line parameters in transmission line equations a all purpose multiconductor transmission line model is described in [72], [73], [74] for efficient and robust interconnect simulation using a nonlinear circuit simulator such as SPICE.

In general, most of these alternative approach are based on the theory of approximations and are ideal for nonuniform coupled transmission line interconnects structures. The disadvantage of some of these methods is that they are unsuitable for the broad range of interconnects typically encountered in different substrate environment. Some

discussion where the need for an alternative approach, especially based on the equivalent circuit model approximation have been discussed in [75], [76]. Additionally, many of the alternative approaches sometimes can lead to an equivalent transfer function which violates some of the inherent properties related to physical systems such as symmetry and energy conservation present in the coupled transmission line equations. This results in unstable or physically unrealizable MTLs transfer functions.

2.4 SYNTHESIS TECHNIQUES

Synthesis techniques of a nonuniform transmission line system based on the inverse scattering (based on linear equations: 'layer-adjoining approach' and its dual the Schur-type algorithms: 'layer-peeling algorithm') has fascinated both the engineering and mathematical community alike. This is due to the linkage of these techniques to the solution of some of the very complex engineering problems. In general, the synthesis techniques for lossless nonuniform transmission line system, classified as one-dimension inverse problem, are now well established and are routinely and extensively used for many diverse applications. Some examples of these applications include interconnect modeling [10], [11], in signal processing for modeling of vocal tract for speech synthesis, in image processing and non-destructive testing for biomedical and material science applications. A brief overview of some of the significant historical contributions in the synthesis methods of transmission lines based on the inverse scattering techniques is presented here.

In [77], using a discrete inverse scattering technique, impedance-profile of a nonuniform transmission line is synthesized which reflects an arbitrary waveform. Youla [78] and Wohlers [79] developed the realizability and uniqueness proofs for uniform transmission lines with resistive and inductive terminations in frequency-domain. A synthesis procedure for a tapered line has been proposed in [80]. Gopinath [81] presented a treatise on the existence and uniqueness of nonuniform transmission lines in time-domain with the constraints on the propagation velocity to be constant. Orlov [82] developed the theory for nonuniform lines of arbitrary impedance profile. A detail de-

scription of theory reported in [82] and several other practical inversion and synthesis techniques is provided by Bruckstein [8], [9]. In this paper relationships between the layer-peeling algorithm and layer-adjoining algorithms proposed for solutions of one-dimensional inverse scattering problems are illustrated. An approximate synthesis procedure for a lossy nonuniform transmission line system from the measured time-domain reflection and transmission data has been proposed in [83]. Unlike lossless case, a general solution to the problem of synthesis of lossy nonuniform transmission line still remains unresolved.

The synthesis techniques developed for a single nonuniform transmission lines have been also extended to several useful special cases, such as coupled symmetric transmission lines and the multiconductor coupled lines in a homogeneous media [10], [11], [84]. In case of coupled line system, an optimization based approach is proposed in [85] for modeling the board-level and package-level interconnect circuitry based on the measured time-domain reflectometry data. In [86] an experimental technique based on principle of causality has been proposed for circuit modeling and synthesis of multiconductor transmission lines. In this paper only symmetrical coupled line structure is used as a test vehicle to demonstrate the approach which can be easily reduced to a problem of synthesis of single line using the constraint of symmetry. An approximate design procedure for the planar microwave filters based on theory of inverse scattering has been proposed in [87].

Approximate characterization techniques both in the frequency- and time-domain for a general lossless uniform MTL system from the measured reflection (and transmission) data using optimization have been proposed with a limited success [88], [89]. In [90] a general synthesis procedure for lossless uniform MTL system from the measured reflection data is proposed. Here the necessary and sufficiency conditions for the extraction of all the normal-mode parameters of uniform multiconductor transmission lines from the measured reflection data are derived [90]. A lossless uniform MTL $2n$-port system terminated in a resistive network is only considered. A general solution to the problem of synthesis of lossless/lossy nonuniform MTL system which can be classified as multi-dimensional inverse problem still remains unresolved.

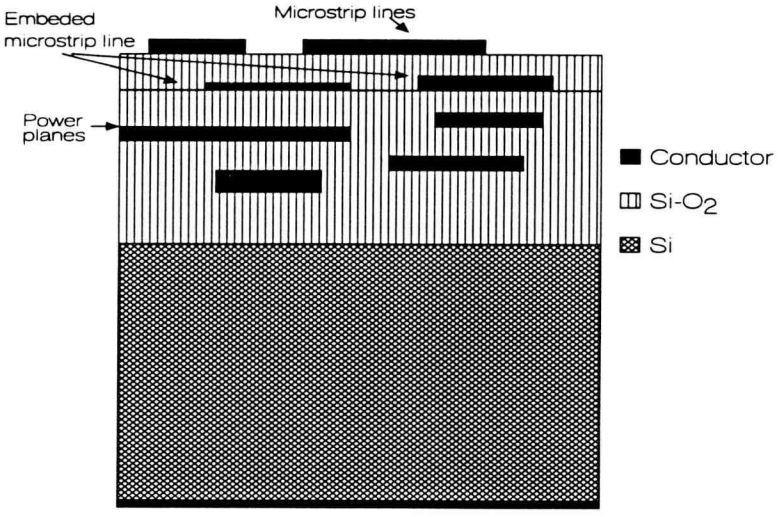

Figure 2.5. A typical die cross-section of MIS ($Si - SiO_2$) structure.

2.5 MODELING OF MULTILAYER TRANSMISSION LINES

Among the several, some of the general criteria for the selection of a CAD-oriented EM simulation tools for a particular application are:

- Accuracy and easy in implementation.
- Computational efficiency.
- Output parameter format (i.e. the extracted parameters of these tools should directly lead to the SPICE circuit elements which can then be easily incorporated in the circuit design tools).
- Range of validity (i.e. the extracted values should be valid over the wide range of input parameters values).

Although, several EM-simulators which use accurate full-wave techniques ([91], [92], [93], [94], [95]) are available, the EM simulation tools based on the quasi-static

approximations satisfy all of the above criteria for the present RF and digital applications. Therefore, the EM simulation tools based on the quasi-static techniques ([96], [97], [98], [99], [100], [101], [102], [103], [104]) are widely preferred for modeling and design of planar multilayer transmission lines or similar structures. Examples of these similar structures which are subset of general multilayer transmission line structure includes stripline, microstrip line, edge-coupled microstrip line and broad-side coupled microstrip line.

Accurate CAD-oriented electromagnetic (EM) simulation tools for the characterization of CMOS or GaAs multilayer MIS transmission lines structure are important for the design of high speed digital and RFIC's. An example of a typical Si-SiO_2 transmission structure is illustrated in Fig. 2.5 [105]. The propagation characteristics of such structures with lossy media depends on the conductivity of substrate layer. In case of single transmission line on a CMOS substrate (Si-SiO_2), the propagating mode can be classified as quasi-TEM, slow-wave and the skin-effect mode. This classification is based on the propagation characteristics of the mode [106]. Similarly, for n coupled lines in a multilevel Si-SiO_2 structure (CMOS), the n propagating modes can also be classified into the three mode categories as defined in case of single transmission line [91]. The modal characteristics of these n coupled transmission lines, and hence, the distributed transmission line matrix parameters exhibit significant frequency dependence. In general, the modes classified as the skin-effect modes are the dominant modes of propagation for these transmission lines at the RF frequencies, particularly for IC's in CMOS technology. The associated frequency dependent modal characteristics of this mode can also be expressed in terms of frequency dependent distributed transmission line parameters. Quasi-static techniques proposed in [103], [104], [107], evaluate the distributed inductance matrix by replacing the dielectric media by an air media and then solving the Laplace equation associated with the corresponding boundary-value problem. Therefore, in these implementations the effect of substrate current on the inductance matrix of a multilayer MIS transmission lines structure with lossy substrates are hence not included in the simulation. The efficient quasi-static techniques in [100], [108] which readily lead to the normal-mode parameters [13] required in the circuit

design of MTL system based interconnection and passive structures in the CMOS technology such as inductors and transformers are only limited to the quasi-TEM and the slow-wave modes. Several measurement based characterization techniques for the transmission lines on Si-SiO_2 substrate has been also investigated in [109], [110], to study their propagation and the impedance characteristics. Many new CAD models based on optimization of the electrical response (limited to a particular structure) or based on modification of existing closed form formulas for special cases of MIS transmission line structures are proposed in [111], [112], [113], [114]. In [115] the effect of substrate current is included via a quasi-static formulation based on the magneto-static potential equation. Based on this formulation a CAD-oriented spiral model valid for quasi-TEM, slow-wave and skin-effect region is demonstrated in [116].

Several full-wave methods for evaluating the propagation characteristics of MIS transmission lines structures have been also actively investigated. Techniques based on the hybrid methods have been also proposed for the characterization of multilayer transmission line structure. Some recent work in this direction is briefly reviewed here. The full-wave method based on Spectral-domain approach is an important technique widely preferred for CAD based EM simulators (e.g. Momentum: HP EEsoF). Some of the main advantages of this approach are: computationally efficient, numerically stabile and easy to implement. In [91], [93] the full-wave Spectral-domain technique has been applied to analyze MIS based microstrip line, symmetric and asymmetric coupled microstrip lines. In these formulations the thickness of conductors are not taken into the account which can significantly affect the electrical characteristics of MTL system. Furthermore, it is only suitable for planar layered structures. Hybrid mode formulations which, in general, are combinations of two or more techniques have been proposed for more practical interconnection structures. In [94], lossy coplanar type transmission lines are analyzed using a hybrid mode formulation based on the full-wave Spectral-domain approach and the perturbation method. Ching-Kuang [95] has proposed a full-wave mixed potential based mode matching approach for the analysis of planar transmission lines. For homogeneous and inhomogeneous doping profile a hybrid mode analysis is presented in [117] to characterize the propagation properties of uniplanar slow-wave

MIS coplanar transmission lines. A rigorous procedure for evaluating the frequency dependent propagation characteristics of lossless and lossy open coupled polygonal conductor transmission lines, which includes the case of thick conductors is presented [92]. Similarly, Jun-Wu [118] has presented a full-wave technique for evaluating the propagation and losses in a lossy line system. A full-wave mode matching procedure for analysis of planar transmission line structure is reported in [95]. The full-wave methods can accurately model the propagation characteristics of MIS transmission line structure but are generally computationally inefficient and therefore not suitable for CAD implementation.

2.6 COMMENTS

In this thesis, multiconductor transmission lines are revisited with particular emphasis to address the present requirement of general CAD-oriented model and theoretical framework for efficient transient analysis of uniform MTLs on time-domain simulators. A new CAD-oriented equivalent circuit model (configuration-oriented model) is proposed which consists of single transmission lines. Although, several CAD models had been already proposed in the past, this model provides more physical insight into the normal-mode theory proposed in [13] for coupled transmission lines. It also includes the case of lossy dispersive uniform MTL system. The requirement of this model in better understanding of normal-mode theory for the design of general asymmetric coupled microstrip line filters was particularly alluded in [34]. Equivalence between this model [4], the model based on modal decomposition [3] and the normal-mode parameters [13], [14] is illustrated. Later, using this equivalence a synthesis procedure for uniform MTL $2n$-port system from the measured time-domain reflection response is reported [90]. Also, a new approach based on the magneto-static potential equation and solved via network analog approach is described for modeling multilayer multilevel layered MIS transmission line structure.

Chapter 3
A CONFIGURATION-ORIENTED SPICE MODEL

3.1 INTRODUCTION

In this chapter, the configuration-oriented SPICE model for a general case of inhomogeneous multilayer multiconductor lines is reported. This model is an extension of the earlier configuration-oriented model proposed in [20] for uniform MTL system in a homogeneous media to a more general case of inhomogeneous media [4]. The proposed equivalent circuit model consists of uncoupled transmission lines connected in the configuration-oriented fashion as was the case in the earlier model [20]. A general formulation and the extraction procedure for equivalent circuit based on the configuration-oriented model for n multiconductor transmission line system is described. This procedure is based on the admittance matrix of $2n$-port system associated with the n coupled lines and leads to a configuration-oriented model based on the π-type of topology [4], [119]. A similar procedure based on the impedance matrix can also be derived and leads to a configuration-oriented model based on the T-type of topology [4], [119]. The T-type of topology is the dual of π-type of topology [119]. The procedure is then illustrated by applying it to a case of general asymmetric coupled line. Network models based on the π and T type of configuration-oriented model topologies are demonstrated and equivalence with the similar models proposed in past for special cases of coupled lines is shown. Another procedure for obtaining the configuration-oriented model based on the decomposition of characteristic admittance matrix is exemplified by applying it to a case of three symmetric coupled microstrip lines [14]. The applicability of the configuration-oriented model to a multiconductor lossy coupled line system is discussed. Several examples of typical applications of configuration-oriented models in microwave and digital realms are presented to demonstrate the accuracy and the versatility of the proposed equivalent circuit model. This chapter includes the derivations and proofs of the results used in the chapter.

3.2 EQUIVALENT CIRCUIT MODEL

The configuration-oriented SPICE model consists of a network of uncoupled transmission lines characterized by their propagation constants and impedances. The model can be readily derived from the admittance (impedance) matrix characterizing the $2n$-port system, as described in this section.

The procedure for deriving the expression for the admittance or impedance matrix of the general $2n$-port is well known and is based on the solution of coupled transmission lines equations

$$\frac{\partial v]}{\partial z} = -[Z(\omega)]i] \tag{3.1}$$

$$\frac{\partial i]}{\partial z} = -[Y(\omega)]v] \tag{3.2}$$

where vectors $v]$ and $i]$ represent voltages and currents on the lines and

$$[Z(\omega)] = [R] + j\omega[L], \quad [Y(\omega)] = [G] + j\omega[C]$$

[R], [L], [G], [C] are the per unit length line constant matrices whose elements are in general frequency dependent. The coupled transmission lines equations (1) and (2), are decoupled with the help of voltage and corresponding current eigenvector matrices $[M_V]$ and $[M_I]$ ($[M_I] = [M_V]^{-T}$) respectively, leading to the characterization of the general n lines $2n$-port by its admittance matrix [15] as given by (refer: section-(3.5.1)),

$$[Y] = \begin{bmatrix} [Y_A] & [Y_B] \\ [Y_B] & [Y_A] \end{bmatrix} \tag{3.3}$$

with

$$[Y_A] = [Y_{LM}] * [M_V][coth(\gamma_i l)]_{diag}[M_I]^T$$

$$[Y_B] = [Y_{LM}] * [M_V][-csch(\gamma_i l)]_{diag}[M_I]^T$$

$$[Y_{LM}]_{n\times n} = \begin{bmatrix} Y_{LM11} & Y_{LM12} & . & Y_{LM1n} \\ . & . & . & . \\ . & . & . & . \\ Y_{LMn1} & . & . & Y_{LMnn} \end{bmatrix}$$

where γ_i represents the ith eigenvalue and is the ith normal-mode propagation constant. $[Y_{LM}]$ is the line mode admittance matrix whose element $Y_{LM\,km}$ represents the characteristic admittance of the kth line for mth mode and l is the length of the uniform coupled multiconductor system. The operator '*' was defined in [15] for $[C] = [A] * [B]$, as a product of corresponding terms of matrices $[A]$ and $[B]$. It is readily shown that the admittance matrix of the $2n$-port as given by equation (3) can be decomposed as

$$[Y] = \sum_{m=1}^{n} [Y_m] \tag{3.4}$$

The $[Y_m]$ represents the partial admittance matrix of the $2n$-port corresponding to mode m and can be expressed as

$$[Y_m]_{2n\times 2n} = \begin{bmatrix} coth(\gamma_m l)[Y_{ch}^m] & -csch(\gamma_m l)[Y_{ch}^m] \\ -csch(\gamma_m l)[Y_{ch}^m] & coth(\gamma_m l)[Y_{ch}^m] \end{bmatrix}, \tag{3.5}$$

where

$$[Y_{ch}^m]_{n\times n} = ([Y_{LM}] * [M_V])[D_m]_{diag}[M_I]^T \tag{3.6}$$

and

$$[D_m]_{diag} = \begin{Bmatrix} D_m(j,j) = 0, & j \neq m \\ D_m(j,j) = 1, & j = m \end{Bmatrix}. \tag{3.7}$$

The symmetric matrix $[Y_{ch}^m]$ (refer: section-(3.5.2)) defined in equations (5) and (6) corresponds to the characteristic admittance matrix for mode m, and its (i,j)th element is given by,

$$Y_{ch}^m(i,j) = Y_{LM}(i,m)M_V(i,m)M_I^T(m,j). \tag{3.8}$$

The matrix $[Y_m]$ in (5) is similar to the $2n$-port admittance matrix corresponding to n coupled lines in a homogeneous medium. Recalling that the admittance matrix of a transmission line two port having length l, propagation constant γ and characteristic admittance Y_c is given as

$$[Y]_{2\times 2} = \begin{bmatrix} Y_c\, coth(\gamma l) & -Y_c\, csch(\gamma l) \\ -Y_c\, csch(\gamma l) & Y_c\, coth(\gamma l) \end{bmatrix}. \tag{3.9}$$

Symmetry of $[Y_{ch}^m]$ implies that the $2n$-port network represented by $[Y_m]$ consists of these transmission lines connected in so-called 'configuration-oriented' manner [2]. That is, the partial admittance matrix $[Y_m]$ for mode m is synthesized by a homogeneous configuration-oriented model [2] having transmission lines electrical lengths corresponding to the *m*th mode eigenvalue. The complete network then is obtained as a parallel combination of the *n*, *2n* ports with each $2n$-port corresponding to an orthogonal mode. A similar procedure can be applied to the impedance matrix leading to a dual topology and corresponding network of transmission lines that is equivalent to the multiconductor multiport. It is seen that the admittance or impedance matrix of a n multiconductor transmission lines system can in general be simulated by $n^2(n+1)/2$ transmission lines. In the case of symmetry, the number of lines are reduced depending upon the type of symmetry.

An alternate approach of deriving these circuits involves the use of the characteristic impedance or admittance matrix of the coupled system. These matrices represent a network which terminates all the modes simultaneously on all the lines. The elements of these matrices represent the characteristic immittance of the transmission lines that constitute the equivalent circuit. The length of the transmission lines corresponds to the electrical length of the corresponding mode. Both the $2n$-port and the characteristic immittance matrix based decomposition procedures, of course, lead to the same equivalent circuit representation (refer: section-(3.5.3)).

3.3 NETWORK MODEL FOR UNIFORM COUPLED LINES

The procedure presented in the previous section is applied to general asymmetric and symmetric three lines cases to illustrate the technique and derive closed from expressions for the modal parameters for these two important cases.

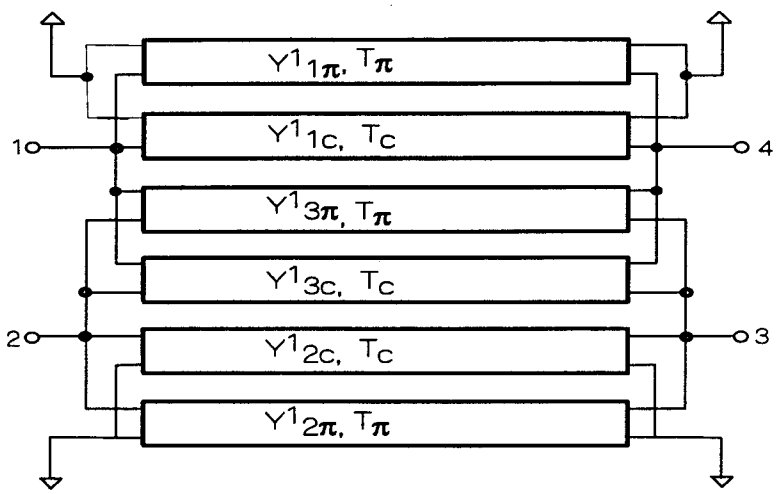

a.)

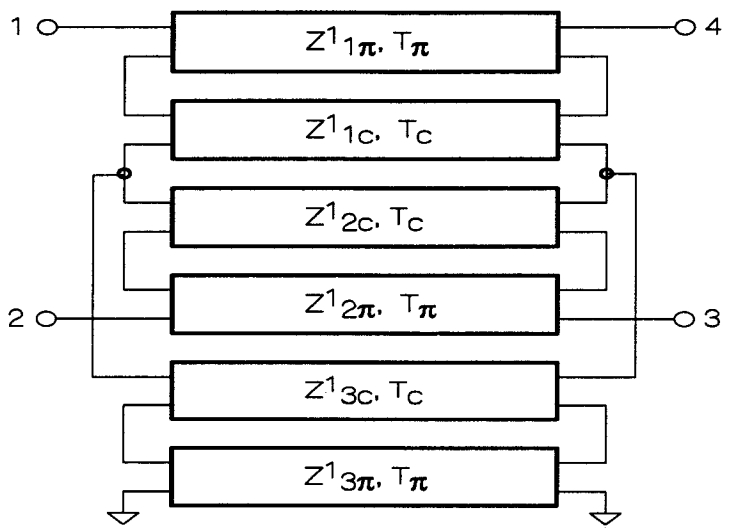

b.)

Figure 3.1. SPICE model for asymmetric coupled lines based on a four port admittance matrix. (b) SPICE model based on four port impedance matrix. T_c and T_π are the time delays associated with the c and π modes. In case of lossy coupled lines the delays and the characteristic admittances of uncoupled transmission lines are function of frequency.

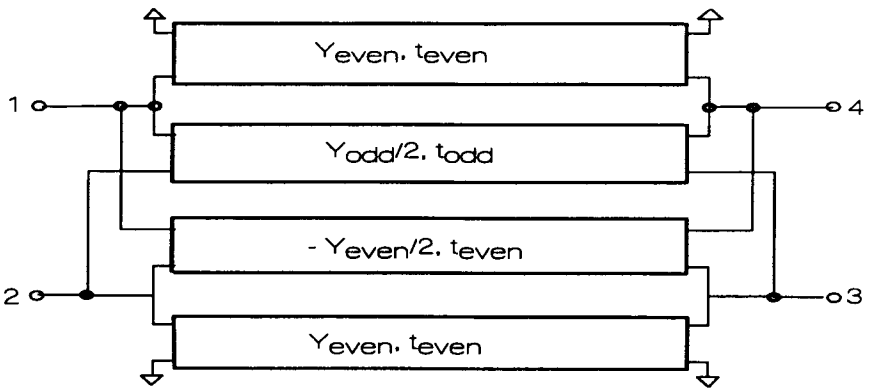

a.)

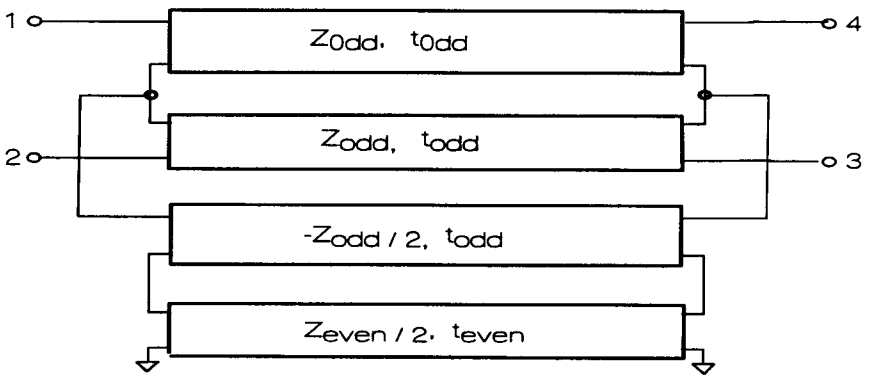

b.)

Figure 3.2. SPICE model for symmetrical coupled lines based on a four port admittance matrix. (b) SPICE model based on four port impedance matrix. t_{even} and t_{odd} are the time delays associated with the even and odd mode. In case of lossy coupled lines the delays and the characteristic admittances of uncoupled transmission lines are function of frequency.

3.3.1 Asymmetric Coupled Lines

A general uniform coupled two line system can be decoupled in terms of two propagating modes π and c [13]. The voltage and the corresponding current eigenvector matrices $[M_V]$, $[M_I]$ can be defined as ([13])

$$[M_V] = \begin{bmatrix} 1 & 1 \\ R_c & R_\pi \end{bmatrix} \text{ and}$$

$$[M_I] = ([M_V]^{-1})^T = \frac{1}{R_\pi - R_c} \begin{bmatrix} R_\pi & -R_c \\ -1 & 1 \end{bmatrix}. \tag{3.10}$$

Where γ_π and γ_c represent eigenvalues and are the normal-mode propagation constants for the π and c modes, R_π and R_c represent the ratio of voltage on line two with respect to line one for π and c modes respectively [13]. The line mode admittance matrix $[Y_{LM}]$ is expressed as

$$[Y_{LM}]_{2\times 2} = \begin{bmatrix} Y_{c1} & Y_{\pi 1} \\ Y_{c2} & Y_{\pi 2} \end{bmatrix}. \tag{3.11}$$

The admittance matrix of the general asymmetric two line system [13] obtained from equations (3),(10) and (11) is expressed as a sum of two matrices corresponding to the two modes using equations (4)-(8), and are found to be

$$[Y]_{4\times 4} = \begin{bmatrix} coth(\gamma_\pi l)[Y^\pi_{ch}] & -csch(\gamma_\pi l)[Y^\pi_{ch}] \\ -csch(\gamma_\pi l)[Y^\pi_{ch}] & coth(\gamma_\pi l)[Y^\pi_{ch}] \end{bmatrix}_\pi + \begin{bmatrix} coth(\gamma_c l)[Y^c_{ch}] & -csch(\gamma_c l)[Y^c_{ch}] \\ -csch(\gamma_c l)[Y^c_{ch}] & coth(\gamma_c l)[Y^c_{ch}] \end{bmatrix}_c, \tag{3.12}$$

where

$$[Y^\pi_{ch}] = \begin{bmatrix} \frac{R_c Y_{\pi 1}}{R_c - R_\pi} & \frac{-Y_{\pi 1}}{R_c - R_\pi} \\ \frac{Y_{\pi 2}}{(R_c - R_\pi)/R_c R_\pi} & \frac{-R_\pi Y_{\pi 2}}{R_c - R_\pi} \end{bmatrix}$$

$$\text{and} \quad [Y^c_{ch}] = \begin{bmatrix} \frac{-R_\pi Y_{c1}}{R_c - R_\pi} & \frac{Y_{c1}}{R_c - R_\pi} \\ \frac{-Y_{c2}}{(R_c - R_\pi)/R_c R_\pi} & \frac{R_c Y_{c2}}{R_c - R_\pi} \end{bmatrix}. \tag{3.13}$$

Each matrix $[Y]_\pi$ and $[Y]_c$ in equation (12) can be synthesized in general by three transmission lines connected at the input and output ends in a π configuration [2]. These two networks connected in parallel yield a complete equivalent circuit as shown in Fig. 3.2a for the coupled line system. The expressions for the characteristic admittance of the transmission lines in the SPICE model in Fig. 3.2a correspond to the admittance matrices given by equation (13) and are given by (see eqns. (37) and (38)),

$$\begin{aligned} Y^1_{1\pi} &= \frac{Y_{\pi 1}(R_c-1)}{R_c-R_\pi}, \quad Y^1_{2\pi} = \frac{R_\pi Y_{\pi 2}(R_c-1)}{R_c-R_\pi}, \\ Y^1_{3\pi} &= \frac{Y_{\pi 1}}{R_c-R_\pi}, \quad Y^1_{1c} = \frac{Y_{c1}(1-R_\pi)}{R_c-R_\pi}, \\ Y^1_{2c} &= \frac{R_c Y_{c2}(1-R_\pi)}{R_c-R_\pi}, \quad Y^1_{3c} = \frac{-Y_{c1}}{R_c-R_\pi}. \end{aligned} \tag{3.14}$$

As noted earlier, the impedance matrix can also be used to construct an alternate equivalent model of the coupled system. The impedance matrix of a general asymmetric coupled line system given in [13] is readily decomposed into two modes

$$[Z]_{4\times 4} = [Z_\pi]_{4\times 4} + [Z_c]_{4\times 4}. \tag{3.15}$$

Each matrix in equation (15) can be modeled by three transmission lines connected in a T configuration for each mode. The complete equivalent circuit is shown in Fig. 3.2b. The expressions for characteristic impedance of the transmission lines in this SPICE model (Fig. 3.2b) are given by,

$$\begin{aligned} Z^1_{1\pi} &= \frac{Z_{\pi 1}R_c}{R_c-R_\pi}(1-R_\pi), \quad Z^1_{2\pi} = \frac{Z_{\pi 2}}{R_c-R_\pi}(1-R_\pi), \\ Z^1_{3\pi} &= \frac{Z_{\pi 1}R_cR_\pi}{R_c-R_\pi}, \quad Z^1_{1c} = \frac{Z_{c1}R_\pi}{R_c-R_\pi}(R_c-1), \\ Z^1_{2c} &= \frac{Z_{c2}}{R_c-R_\pi}(R_c-1), \quad Z^1_{3c} = -\frac{Z_{c1}R_cR_\pi}{R_c-R_\pi}. \end{aligned} \tag{3.16}$$

It should be noted that the characteristic impedance and admittance matrices of the coupled lines system are symmetric and represent a passive n-port network. However, the characteristic impedance of some transmission lines in the equivalent circuit can be

negative depending on modal decomposition. The decomposition of the characteristic admittance matrix (stable and passive network) into the sum of n partial admittance matrices leads to a stable configuration-oriented model in spite of the fact that some of the elements are not passive. This is like having two equal length lines in parallel. For a stable system one of them can have negative characteristic admittance as long as the total combined characteristic admittances of the two lines is positive. These negative impedance transmission lines can be simulated by a positive impedance transmission line elements with the linear dependent sources for the impedance conversion or directly as a negative impedance transmission lines on many CAD tools like LIBRA. Furthermore, in case of symmetric lossless coupled lines ($R_\pi = -1$, $R_c = 1$, $Y_{\pi 1} = Y_{\pi 2}$ and $Y_{c1} = Y_{c2}$ leads to: Y_{odd}=$2Y^1_{3\pi}$ and Y_{even}=Y^1_{1c}) the model reduces to the four transmission lines system presented in [47] (Fig. 3.2a) or to the T equivalent network as shown in Fig. 3.2b (Z_{even}=$2Z^1_{3c}$ and Z_{odd}=$Z^1_{1\pi}$). Similarly for the case of lossless symmetric coupled lines in a homogeneous medium ($\gamma_\pi = \gamma_c$), the equivalent system reduces to a three transmission lines system as in [2].

3.3.2 Symmetric Three-Coupled Lines

For the case of symmetric coupled three-line structures, the voltage and associated current eigenvector matrices corresponding to the three propagating modes a, b and c, are given by [14],

$$[M_V] = \begin{bmatrix} 1 & 1 & 1 \\ 0 & R_{v1} & R_{v2} \\ -1 & 1 & 1 \end{bmatrix} \tag{3.17}$$

and

$$[M_I] = ([M_V]^{-1})^T = \frac{1}{2(R_{v1} - R_{v2})} \begin{bmatrix} R_{v1} - R_{v2} & -R_{v2} & R_{v1} \\ 0 & 2 & -2 \\ R_{v2} - R_{v1} & -R_{v2} & R_{v1} \end{bmatrix}. \tag{3.18}$$

The line mode admittance matrix $[Y_{LM}]$ is

$$[Y_{LM}]_{3\times 3} = \begin{bmatrix} Y_{a1} & Y_{b1} & Y_{c1} \\ Y_{a2} & Y_{b2} & Y_{c2} \\ Y_{a3} & Y_{b3} & Y_{c3} \end{bmatrix}, \tag{3.19}$$

and γ_a, γ_b, γ_c are the propagation constants associated with the normal-modes a, b and c [14]. For three symmetric coupled lines $Y_{a1} = Y_{a3}$, $Y_{b1} = Y_{b3}$ and $Y_{c1} = Y_{c3}$. Substituting equations (17)-(19) in equation (6) leads to the characteristic admittance matrices for the modes a,b and c and are given as (refer: eqn. (39))

$$[Y^a_{ch}] = \begin{bmatrix} \frac{Y_{a1}}{2} & 0 & \frac{-Y_{a1}}{2} \\ 0 & 0 & 0 \\ \frac{-Y_{a3}}{2} & 0 & \frac{Y_{a3}}{2} \end{bmatrix},$$

$$[Y^b_{ch}] = \frac{1}{2(R_{v1}-R_{v2})} \begin{bmatrix} -R_{v2}Y_{b1} & 2Y_{b1} & -R_{v2}Y_{b1} \\ -R_{v1}R_{v2}Y_{b2} & 2R_{v1}Y_{b2} & -R_{v1}R_{v2}Y_{b2} \\ -R_{v2}Y_{b3} & 2Y_{b3} & -R_{v2}Y_{b3} \end{bmatrix}$$

and

$$[Y^c_{ch}] = \frac{1}{2(R_{v1}-R_{v2})} \begin{bmatrix} R_{v1}Y_{c1} & -2Y_{c1} & R_{v1}Y_{c1} \\ R_{v1}R_{v2}Y_{c2} & -2R_{v2}Y_{c2} & R_{v1}R_{v2}Y_{c2} \\ R_{v1}Y_{c3} & -2Y_{c3} & R_{v1}Y_{c3} \end{bmatrix}. \tag{3.20}$$

The six port transmission line network is then readily constructed as three modal networks connected in parallel. The complete network, then, consists of thirteen transmission lines. The expressions for the characteristic admittances for the lines are given below (refer: eqns. (37) and (38)):

Transmission lines between: ports 1 and 4,

$$\frac{Y_{b1}(1-R_{v2})}{R_{v1}-R_{v2}}, \quad \frac{Y_{c1}(R_{v1}-1)}{R_{v1}-R_{v2}}$$

ports 2 and 5,

$$\frac{Y_{b2}R_{v1}(1-R_{v2})}{R_{v1}-R_{v2}}, \quad \frac{Y_{c2}R_{v2}(R_{v1}-1)}{R_{v1}-R_{v2}}$$

ports 3 and 6,

$$\frac{Y_{b3}(1-R_{v2})}{R_{v1}-R_{v2}}, \quad \frac{Y_{c3}(R_{v1}-1)}{R_{v1}-R_{v2}}$$

terminal pairs (1, 2) and (4, 5)

$$\frac{-Y_{b1}}{R_{v1}-R_{v2}}, \quad \frac{Y_{c1}}{R_{v1}-R_{v2}}$$

terminal pairs (2, 3) and (5, 6)

$$\frac{R_{v1}R_{v2}Y_{b2}}{2(R_{v1}-R_{v2})}, \quad \frac{-R_{v1}R_{v2}Y_{c2}}{2(R_{v1}-R_{v2})}$$

terminal pairs (1, 3) and (5, 6)

$$\frac{Y_{a1}}{2}, \quad \frac{R_{v2}Y_{b1}}{2(R_{v1}-R_{v2})}, \quad \frac{-R_{v1}Y_{c1}}{2(R_{v1}-R_{v2})}$$

The electrical length of these transmission lines are given by the corresponding electrical length of the three modes.

3.3.3 Lossy Dispersive Multiconductor Coupled Lines

In general, the coupled line systems have conductor and dielectric losses and therefore the uncoupled transmission lines in the configuration-oriented model have frequency dependent complex propagation constants and the complex characteristic impedances. The multiport SPICE simulation for lossy dispersive multiconductor coupled lines can be accomplished by modeling the uncoupled lines obtained from the formulation presented in section-(3.2) in terms of their two port frequency dependent

network functions such as [Y] or [S] parameters or modeling them in terms of equivalent circuits consisting of ideal lumped and delay elements as shown in [52] for a single microstrip. The frequency dependent complex characteristic parameters (propagation constants, line mode impedances, eigenvector matrices) are computed using a rigorous frequency dependent technique like the Spectral-domain approach [15] or by using CAD-oriented quasi-TEM methods (e.g.,[121]). The model transmission line parameters can be obtained in terms of equivalent frequency dependent self and mutual line constants per unit length as shown in [122]. As an example, for the simple case of identical coupled lines, the even and odd-mode propagation constants and impedances are readily expressed as

$$\gamma_{e,o} = \sqrt{[(R \pm R_m) + j\omega(L \pm L_m)][(G \mp G_m) + j\omega(C \mp C_m)]} \tag{3.21}$$

and

$$Z_{e,o} = \sqrt{\frac{(R \pm R_m) + j\omega(L \pm L_m)}{(G \mp G_m) + j\omega(C \mp C_m)}} \tag{3.22}$$

in terms of the frequency dependent equivalent line constants representing self and mutual inductances, capacitances, resistances and conductances per unit length of the lines. For the case of low losses, equations (21) and (22) can be simplified as

$$Z_{e,o} \approx \sqrt{\frac{L \pm L_m}{C \mp C_m}} \tag{3.23}$$

$$\gamma_{e,o} \approx j\omega\sqrt{(L \pm L_m)(C \mp C_m)} + \frac{R \pm R_m}{2Z_{e,o}} + \frac{G \mp G_m}{2} Z_{e,o}. \tag{3.24}$$

These line constants ($R, R_m, L, L_m, G, G_m, C, C_m$) can be calculated by using quasi–static as well as full wave analysis of the coupled system [15], [121], [122]. For the general asymmetric coupled lines and multiconductor coupled systems the modeling of individual lossy, dispersive lines [52] in terms of network functions, frequency dependent line constants or equivalent circuits is similar to the symmetrical coupled line case.

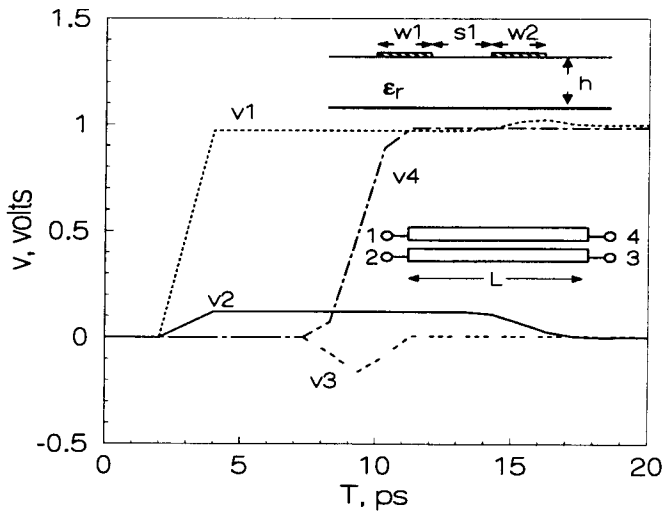

Figure 3.3. Step response of the symmetric lossless coupled microstrip four port.

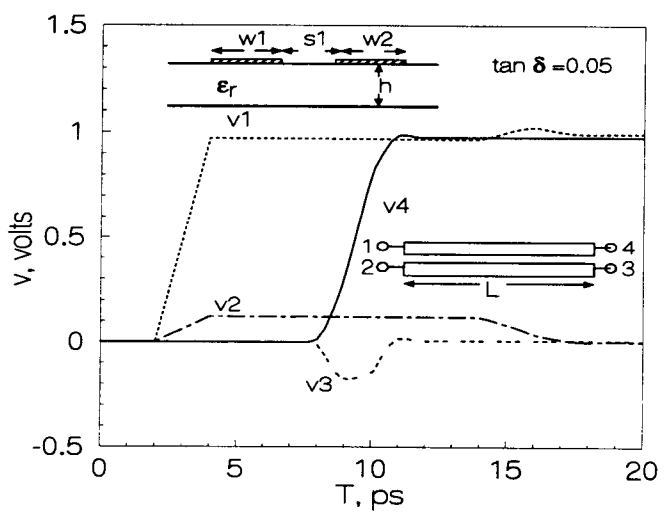

Figure 3.4. Time-domain step response of the symmetric coupled microstrip four port on FR–4 substrate.

3.3.4 The Procedure:

The general procedure for building a configuration-oriented SPICE model of general n line $2n$-ports is summarized below.

- Evaluate propagation constants (γ's), eigenvector matrices $[M_I]$ or $[M_V]$) and line mode admittance matrix ($[Y_{LM}]$) elements using full-wave analysis [122] or compute [R], [L], [G] and [C] matrices using quasi-static analysis [15] and then evaluate propagation constants (γ's) and corresponding voltage eigenvector matrix using eigenvalue equation and $[Y_{LM}]$ line mode admittance matrix whose (k,m)th element corresponds to the characteristic admittance of the kth line for mth mode [13], [14], [15].

- Using equations (4)-(8) decompose the admittance matrix as in equation (3) into a sum of partial admittance matrices $[Y_m]$, each corresponding to the mth mode.

- Each partial admittance matrix corresponding to a propagation mode is synthesized as a $2n$-port network with the two wire transmission lines as in [2] (refer: eqns. (37) and (38)), with the transmission line lengths equal to the electrical length of the respective mode.

- Connect the $2n$-port networks of each partial admittance matrix in parallel to obtain the configuration-oriented SPICE model of a general n-line $2n$-port.

3.4 RESULTS

In order to validate the accuracy of the models and demonstrate their usefulness and versatility, the frequency- and time-domain responses of typical coupled lines structures are presented. Unlike most of the earlier circuit models, the present model can incorporate conductor, dielectric losses and the dispersion due to this losses for the system of n coupled lines. The multiconductor n line system can be represented as $2n$-port (multiport) element, independent of termination conditions at those ports, enabling us

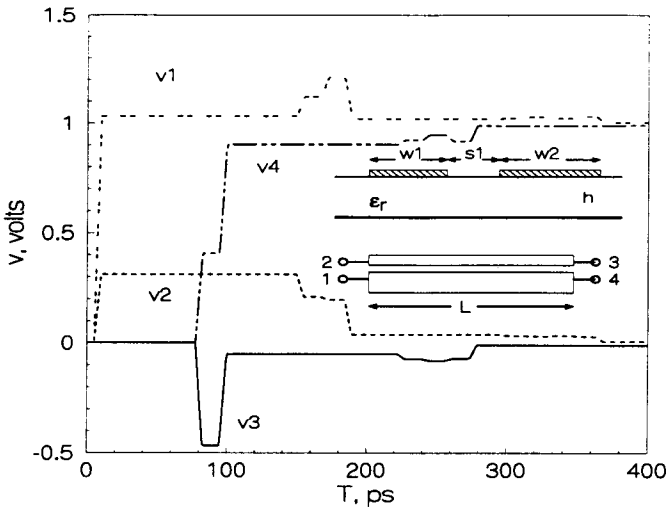

Figure 3.5. Time-domain response of the asymmetric lossless coupled microstrip four port.

to simulate the $2n$-port with linear and nonlinear terminations in a complex circuit environment.

Figure 3.3 shows the time-domain response of a symmetrical lossless microstrip line terminated with the impedances given by z_t ($z_t = \sqrt{z_e z_o}$) at all the four ports. For these calculations ϵ_r*=4.5, w1=w2=0.18 mm, s1=0.04 mm, h=0.1 mm, L=1 mm, strip thickness= 12 μm, and the loss tangent of the dielectric layer, tan δ, is 0.05.* Due to the medium inhomogeneity, both the even and the odd modes are excited and arrive at the terminating ports at different times, generating far end crosstalk. Intuitively, it is can be seen that in the equivalent circuit for the even mode excitation the signal transmission is only through the transmission lines associated with the even mode. Similarly for the odd mode excitation the signal transmission is through the lines associated with the odd mode. The response is exactly the same as that found by using the SPICE model based on the

The time-domain step response of a lossy symmetrical coupled line having both dielectric and conductor losses is shown in Fig. 3.4. Here ϵ_r*=4.5, w1=w2=0.18 mm, s1=0.04 mm, h=0.1 mm, L=1 mm, strip thickness= 12 μm, and the loss tangent of the*

dielectric layer (tan δ) is 0.05. Due to the presence of these losses the uncoupled transmission line expressions given in (14) or (16) are frequency dependent. The approximate expression similar to (23) and (24) are used to simulate the individual (four) uncoupled lossy transmission lines given in (14) and (16). The simulations are performed using the configuration-oriented SPICE models ('π topology': Fig. 3.2a and 'T topology': Fig. 3.2b) with the HP-EEsof CAD tools. As expected, the time-domain waveforms obtained from both the π and T topology based configuration-oriented SPICE models are found to be identical.

The time-domain step response of an asymmetric coupled lossless microstrip structure is shown in Fig. 3.5. For these calculations ϵ_r*=9.8, w1=0.24 mm, w2=0.48 mm, s1=0.04 mm, h=1.0 mm, L=9.3 mm and the strip thickness is 12 μm.* As in the case above, the simulations are performed using the π (eqns (14): Fig. 3.2a) and the T topology (eqns (16): Fig. 3.2b) based configuration-oriented SPICE models. The obtained time-domain waveforms are found to be identical in both the cases. Additionally, the asymmetric coupled microstrip four port in this example is same as that of [3] and validates the accuracy of the present model.

Figure 3.6 shows the frequency response of edge coupled two-section filter simulated by LIBRA using the coupled line model given in Fig. 3.2a. Each section consists of asymmetric coupled microstrips. The effect of dielectric and conductor losses are also included in the simulation. The example demonstrates the application of the configuration-oriented model presented here for the design of general asymmetric and multiconductor coupled line circuits. The values of the [R], [G], [L] and [C] matrices for each asymmetric coupled line section in this filter are obtained by using a CAD oriented quasi-TEM method [121]. The modeling of the individual lossy dispersive lines is done in terms of network functions [52]. The obtained response in Fig. 3.6 is similar to that of response obtained by the simulation of this filter using a full-domain EM tool (HP-EEsof: Momentum). The configuration oriented model can in general include the frequency variations of [R], [G], [L] and [C] matrices and is dependent upon the availability of a single lossy dispersive transmission line model, for which several good CAD oriented techniques are already available.

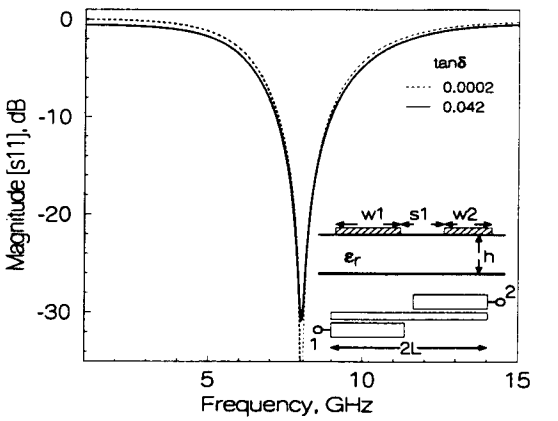

a.)

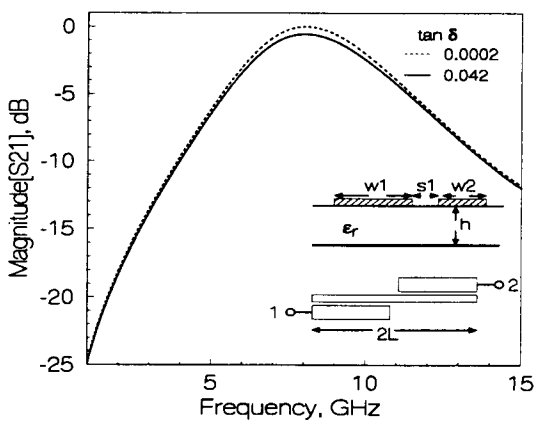

b.)

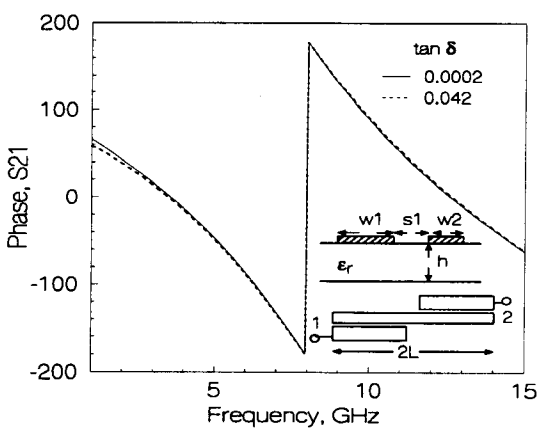

c.)

Figure 3.6. Frequency response of a two-section asymmetric coupled microstrip filter on alumina for different dielectric losses (tan δ= 0.0002 and tan δ= 0.042). (a) Magnitude of S11 in dB. (b) Magnitude of S21 in dB. (c) Phase response of S21. ϵ_r=*9.8, w1=0.4 mm, w2=0.25 mm, s1=0.04 mm, h=0.63 mm, L=3.75 mm* .

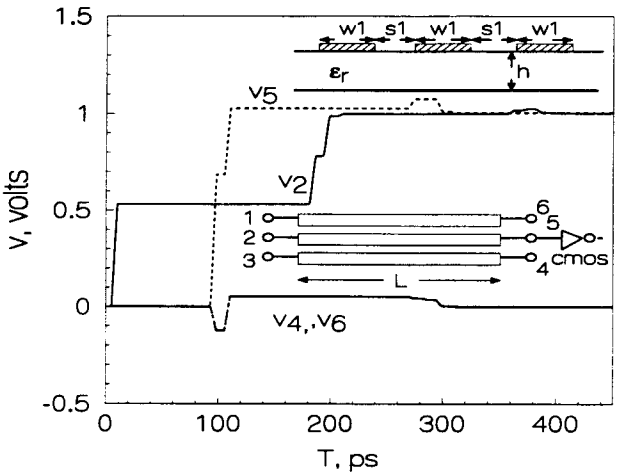

Figure 3.7. Step response of the lossless three symmetric coupled microstrip six ports.

The time-domain response for three symmetrical coupled lossless lines is shown in Fig. 3.7 in order to demonstrate the applicability of the model presented here for the simulation of multiconductor transmission lines in high speed digital circuits. For these calculations ϵ_r= *12.8, w1=0.3 mm, s1=0.3mm, h=0.635 mm and strip thickness is 12* μm. The input and output ports are terminated by 50 Ω impedances except port 5 which drives a high impedance CMOS inverter. The time-domain step response shows signal degradation, coupling and crosstalk effects between the active and passive lines.

3.5 DERIVATIONS & PROOFS

In this section derivations and proofs for some of the results used in this chapter are derived.

3.5.1 Admittance Matrix : n Coupled Lines $2n$-Port System

A procedure similar to that in [13] leads to the solution of n coupled transmission line equations ((1) and (2)) in terms of normal-mode parameters. Using this procedure the expressions obtained for the voltages and the corresponding currents in terms of $2n$ waves is given by,

$$\begin{aligned}[v]_{n\times 1} &= [M_V][e^{-\gamma_i x}]_{diag}[a_r]_{n\times 1} \\ &\quad +[M_V][e^{\gamma_i x}]_{diag}[a_l]_{n\times 1} \qquad (3.25)\\ [i]_{n\times 1} &= ([Y_{LM}] * [M_V])[e^{-\gamma_i x}]_{diag}[a_r]_{n\times 1} \\ &\quad -([Y_{LM}] * [M_V])[e^{\gamma_i x}]_{diag}[a_l]_{n\times 1}. \qquad (3.26)\end{aligned}$$

Where the columns of matrix $[M_V]$ are the voltage eigenvectors, γ_i is the ith normal-mode propagation constant, $[Y_{LM}]$ is the line mode admittance matrix and operator '*' is defined in (3). The admittance matrix for the multiconductor coupled-lines $2n$-port system is obtained by combining (25) and (26). The final expression for the admittance matrix is given in (3).

3.5.2 Proof: $[Y_{ch}^m]$ is Symmetric

It is clear from (25) and (26) that in a system of n coupled lines these $2n$ waves actually consist of two independent sets of n waves each propagating in the opposite direction. Moreover, these n waves satisfy the coupled transmission line equations ((1)and (2)), leading to :

$$[Z][Y][M_V] = [M_V][\gamma_i^2]_{diag} \qquad (3.27)$$

and

$$[Y][Z]([Y_{LM}] * [M_V]) = ([Y_{LM}] * [M_V])[\gamma_i^2]_{diag}. \qquad (3.28)$$

Taking the transpose of (28) and observing that the matrix [Z] and [Y] are symmetric yields

$$([Y_{LM}] * [M_V])^T[Z][Y] = [\gamma_i^2]_{diag}([Y_{LM}] * [M_V])^T. \qquad (3.29)$$

The columns of matrix $[M_V]$ are the right eigenvectors and the rows of matrix $([Y_{LM}] * [M_V])^T$ are left eigenvectors of matrix [Z][Y]. The equation obtained by multiplying on the right hand side of (27) by $([Y_{LM}]*[M_V])^T$ and then subtracting the equation obtained by multiplying on the left hand side of (29) by $[M_V]$ is

$$([Y_{LM}] * [M_V])^T[M_V][\gamma_i^2]_{diag} - [\gamma_i^2]_{diag}$$
$$([Y_{LM}] * [M_V])^T[M_V] = 0. \tag{3.30}$$

Equation (30) shows that $([Y_{LM}] * [M_V])^T[M_V]$ commutes with the diagonal matrix of distinct elements and therefore should be diagonal. Therefore,

$$([Y_{LM}] * [M_V])^T[M_V] = [\lambda_i]_{diag}. \tag{3.31}$$

The values of λ_i depend upon (1) and (2). Combining (31) with (6) gives

$$\begin{aligned}[Y_{ch}^m] &= ([Y_{LM}] * [M_V])[\lambda_i]_{diag}^{-1}[D_m]_{diag}([Y_{LM}] * [M_V])^T \\ &= [M_V]^{-T}[\lambda_i]_{diag}[D_m]_{diag}[M_V]^{-1} = [Y_{ch}^m]^T,\end{aligned} \tag{3.32}$$

where the matrix $[D_m]_{diag}$ is defined in equation (7).

3.5.3 The Procedure: Based on Characteristic Admittance or Impedance Matrix

An alternate approach can also be used in deriving the equivalent circuit with the help of the characteristic impedance matrix $[Z_{ch}]$ or admittance matrix $[Y_{ch}]$ ($[Y_{ch}] = ([Y_{LM}] * [M_V])[M_V]^{-1}$). For example, the characteristic admittance and impedance matrices for the coupled two line structure, as given in [13], are

$$[Y_{ch}] = \begin{bmatrix} \frac{-R_\pi Y_{c1}+R_c Y_{\pi 1}}{R_c-R_\pi} & \frac{Y_{c1}-Y_{\pi 1}}{R_c-R_\pi} \\ \frac{Y_{\pi 2}-Y_{c2}}{(R_c-R_\pi)/R_c R_\pi} & \frac{R_c Y_{c2}-R_\pi Y_{\pi 2}}{R_c-R_\pi} \end{bmatrix} \tag{3.33}$$

and

$$[Z_{ch}] = \begin{bmatrix} \frac{Z_{\pi 1}R_c-Z_{c1}R_\pi}{R_c-R_\pi} & \frac{Z_{c1}-Z_{\pi 1}}{(R_\pi-R_c)/R_c R_\pi} \\ \frac{Z_{c2}-Z_{\pi 2}}{R_c-R_\pi} & \frac{R_c Z_{c2}-R_\pi Z_{\pi 2}}{R_c-R_\pi} \end{bmatrix}. \tag{3.34}$$

Where R_c and R_π are the ratio of voltage on conductor 2 to the voltage on conductor 1 for the two modes, $Y_{c1}, Y_{c2}, Y_{\pi 1}, Y_{\pi 2}$ are corresponding line mode admittances and $Z_{c1}, Z_{c2}, Z_{\pi 1}, Z_{\pi 2}$ are the line mode impedances.

The above impedance or admittance matrix for two coupled lines can be expressed as a sum of two matrices, with the π mode and c mode terms separated, as

$$[Y_{ch}] = \begin{bmatrix} \frac{R_c Y_{\pi 1}}{R_c - R_\pi} & \frac{-Y_{\pi 1}}{R_c - R_\pi} \\ \frac{Y_{\pi 2}}{(R_c - R_\pi)/R_c R_\pi} & \frac{-R_\pi Y_{\pi 2}}{R_c - R_\pi} \end{bmatrix}_\pi + \begin{bmatrix} \frac{-R_\pi Y_{c1}}{R_c - R_\pi} & \frac{Y_{c1}}{R_c - R_\pi} \\ \frac{-Y_{c2}}{(R_c - R_\pi)/R_c R_\pi} & \frac{R_c Y_{c2}}{R_c - R_\pi} \end{bmatrix}_c \tag{3.35}$$

and

$$[Z_{ch}] = \begin{bmatrix} \frac{Z_{\pi 1} R_c}{R_c - R_\pi} & \frac{-Z_{\pi 1}}{(R_\pi - R_c)/R_c R_\pi} \\ \frac{-Z_{\pi 2}}{R_c - R_\pi} & \frac{-R_\pi Z_{\pi 2}}{R_c - R_\pi} \end{bmatrix}_\pi + \begin{bmatrix} \frac{-Z_{c1} R_\pi}{R_c - R_\pi} & \frac{Z_{c1}}{(R_\pi - R_c)/R_c R_\pi} \\ \frac{Z_{c2}}{R_c - R_\pi} & \frac{R_c Z_{c2}}{R_c - R_\pi} \end{bmatrix}_c . \tag{3.36}$$

These matrices are symmetric and singular. From these matrices, each associated with a mode (m), the corresponding configuration-oriented models are obtained by using two wire transmission lines. The characteristic admittance of the transmission line with its one end connected to ports i and k is given by,

$$Y_{ik_m} = -Y_{ch}(i,k)_m \tag{3.37}$$

and the characteristic admittance of the transmission line connecting port i and ground (0) is

$$Y_{i0_m} = \sum_{k=1}^{n} Y_{ch}(i,k)_m. \tag{3.38}$$

The length of transmission lines corresponds to the electrical length of mode. Therefore the matrices $[Y_{ch}]$ and $[Z_{ch}]$ can be synthesized with six transmission lines leading to the same equivalent circuits as shown in Fig. 1 a,b.

The characteristic admittance matrix of symmetrical three coupled lines is derived in a similar manner in terms of the line mode admittance of three lines, the mode volt-

ages and current ratios and propagation constants for the normal-modes, and is given by [14],

$$[Y_{ch}] = \begin{bmatrix} \frac{Y_{a1}(R_{v1}-R_{v2})-Y_{b1}R_{v2}+Y_{c1}R_{v1}}{2(R_{v1}-R_{v2})} & \frac{Y_{b1}-Y_{c1}}{R_{v1}-R_{v2}} & \frac{Y_{a1}(R_{v2}-R_{v1})-Y_{b1}R_{v2}+Y_{c1}R_{v1}}{2(R_{v1}-R_{v2})} \\ \frac{-R_{v1}R_{v2}Y_{b2}+R_{v1}R_{v2}Y_{c2}}{2(R_{v1}-R_{v2})} & \frac{R_{v1}Y_{b2}-R_{v2}Y_{c2}}{(R_{v1}-R_{v2})} & \frac{-R_{v1}R_{v2}Y_{b2}+R_{v1}R_{v2}Y_{c2}}{2(R_{v1}-R_{v2})} \\ \frac{-(R_{v1}-R_{v2})Y_{a3}-R_{v2}Y_{b3}+R_{v1}Y_{c3}}{2(R_{v1}-R_{v2})} & \frac{Y_{b3}-Y_{c3}}{R_{v1}-R_{v2}} & \frac{-(R_{v2}-R_{v1})Y_{a3}-R_{v2}Y_{b3}+Y_{c3}R_{v1}}{2(R_{v1}-R_{v2})} \end{bmatrix} \quad (3.39)$$

Where Y_{a1},Y_{a2},.. etc. are the line mode admittances of three lines for modes a,b and c and the corresponding voltage and current eigenvector matrices are defined in (17). For three symmetric coupled lines $Y_{a1} = Y_{a3}$, $Y_{b1} = Y_{b3}$ and $Y_{c1} = Y_{c3}$. This matrix can be expressed as sum of three matrices for each mode and is readily realized leading to the transmission line network of thirteen transmission lines in a six port network.

3.6 COMMENTS

A new configuration-oriented SPICE model for multiple-coupled microstrip lines and other multiconductor structures in an inhomogeneous medium has been developed and presented. The model is based on the decomposition of the general n-line $2n$-port immittance matrix into a sum of partial immittance matrices corresponding to each mode. The complete equivalent network is obtained by combining the resulting n $2n$-port configuration-oriented models synthesized for each partial immittance matrix. It is observed that n coupled multiconductor lines can in general be simulated $n^2(n+1)/2$ transmission lines. The configuration-oriented SPICE model provides a simple alternate equivalent network in terms of coupled multiconductor characteristic parameters which are readily obtained from rigorous full wave or quasi-TEM computations. This model is compatible with the simulation of lossy, dispersive systems and should be quite helpful in the frequency- and time-domain simulation and design of multiconductor coupled systems. Several frequency- and time-domain simulation examples have been presented for typical interconnect and microwave component structures to demonstrate the applications of the model.

Chapter 4
MODELING AND CHARACTERIZATION OF MULTIPLE COUPLED LINES FROM MEASUREMENTS

4.1 INTRODUCTION

A uniform multiconductor transmission lines (UMCL) are characterized by the characteristic admittance matrix, $[Y_{ch}]$, modal velocities (eigenvalues) and the corresponding modal voltage eigenvectors. All the normal-mode parameters of a UMCL $2n$-port system can be expressed in terms of these parameters. These normal-model parameters are: the line mode admittance matrix, $[Y_{LM}]$, modal voltage eigenvector matrix, $[M_V]$, and the modal delays [3], [13], [14]. Figure 4.1 illustrates a general lossless uniform multiconductor coupled lines (UMCL) $2n$-port system. Here, $[\rho_{in}(0,t]$, is the measured impulse reflection response (IRR) function, $[Y_{in}(0,t)]$, is the input impulse admittance matrix (IIAM) function, $[Y_s]$, is the source admittance matrix corresponding to the source impedances and, $[Y_T]$, is the termination admittance matrix associated with the termination network composed of resistances.

In this chapter, it is shown that in discrete Fourier transform domain (z-domain) the input impulse admittance matrix (IIAM) function of a general UMCL $2n$-port system can be expressed in terms of a rational matrix function. It is assumed that the electrical delay of each mode is an integral multiple of a small time increment $\triangle T$ ($z=e^{-js\triangle T}$). Based on this a synthesis technique is developed to obtain an equivalent UMCL $2n$-port system from the measured discrete time-domain impulse reflection response (IRR). Equivalence between the synthesis technique presented in this chapter and solution of a special case of polynomial algebraic Riccati matrix equation of the form $[A(z)][P][A(z)] = [E(z)]$ is shown [120]. The solution of this algebraic Riccati matrix equation, $[A(z)]$, can lead to the termination resistive network, partial mode admittance matrices and the corresponding modal delays. Instead of finding a general solution of the polynomial algebraic Riccati matrix equation, the proposed technique is based on

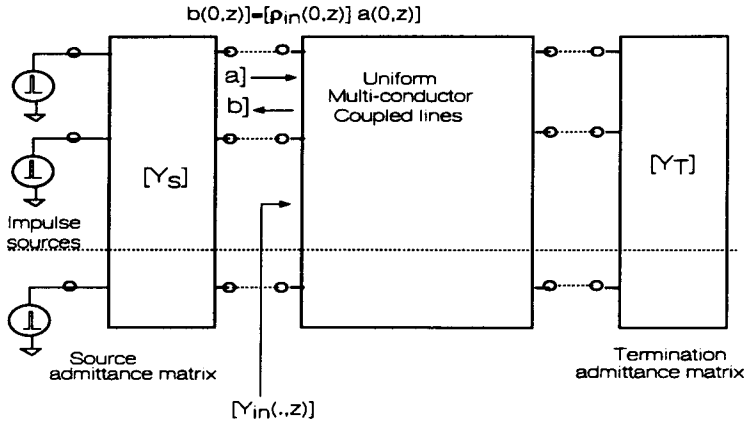

Figure 4.1. A general lossless uniform multiconductor coupled lines (UMCL) $2n$-port system.

the relationships between the IIAM function and the normal-mode parameters which are derived in this chapter. The extracted equivalent UMCL $2n$-port system using the proposed technique is described by the normal-mode parameters which are identical to the actual UMCL $2n$-port system, if terminated in a resistive network that guarantees the satisfaction of necessary and sufficiency conditions presented in this chapter.

This chapter is organized as follows. A decomposition scheme for a general characteristic admittance matrix in terms of partial mode admittance matrices is reviewed. This decomposition scheme has been used in [4] to demonstrate that a n coupled multiconductor lines $2n$-port system can be represented in term of network of single transmission lines, i.e. the basic building block element for the distributed circuit. Also, relation between the equivalent circuit based on the modal decompositions proposed in [3] and configuration-oriented model is derived. The modal decompositions model represents the congruent transformer bank [3] by dependent sources and leads to a circuit model consisting of linear dependent sources and ideal delay elements representing uncoupled transmission lines. The configuration-oriented model consists of only uncoupled transmission lines. The discrete transition matrix function of a uniform MTL $2n$-port system

is derived. The relationship between the measured impulse discrete time-domain reflection response at the input ports of a uniform MTL $2n$-port system and the normal-mode parameters of n coupled multiconductor lines is illustrated. A new feasible synthesis technique for extracting an equivalent uniform MTL $2n$-port system whose response is identical to that of the actual uniform MTL $2n$-port system is proposed. Later, application of this procedure for synthesis of coupled three microstrip line structure from the measured reflection response is demonstrated.

4.2 DECOMPOSITION PROCEDURE : FOR CHARACTERISTIC ADMITTANCE MATRIX

An equivalent n-port resistive network corresponding to a non-singular characteristic admittance matrix, $[Y_{ch}]$, can be decomposed as a sum of n matrices by a set of n linearly independent eigenvectors or vectors. In general, an arbitrary choice of these n linearly independent vectors for the decomposition of characteristic admittance matrix, $[Y_{ch}]$, can lead to the n asymmetric matrices. Thereby, the associated n-port network corresponding to each of these asymmetric matrices do not individually satisfy the condition of reciprocity. The constraint of symmetry on the matrices resulting via decomposition of characteristic admittance matrix limits the choice of n linearly independent voltage or the current vectors to decouple the system. These voltages or current eigenvectors are associated with transmission line equations. In this chapter the set of linearly independent voltage vectors which leads to symmetric matrices for a given characteristic admittance matrix, $[Y_{ch}]$, are described as the modal voltage vectors. For a general UMCL in an inhomogeneous media with characteristic admittance matrix, $[Y_{ch}]$, the modal voltage eigenvectors (ref. [4]) are the elements of this set, consisting of this restricted group of linearly independent voltage vectors (i.e. the modal voltage vectors).

The procedure of decomposing the general n-port resistive network corresponding to the non-singular characteristic admittance matrix, $[Y_{ch}]$, as a sum of n n-port resistive network associated with the each mode is well known [3], [13], [14]. Such a decomposition is based on the choice of n linearly independent modal voltage vectors,

$(\widehat{\zeta}_1, \widehat{\zeta}_2, ., ..\widehat{\zeta}_n)$. Defining the transformations (for the voltages $V]$ and the currents $I]$ at the n ports) as:

$$\begin{aligned} e] &= [M_V^m]^{-1}V] \\ &= \begin{bmatrix} 1 & 1 & . & 1 \\ \zeta_{1,1} & \zeta_{1,2} & . & \zeta_{1,n} \\ \zeta_{2,1} & \zeta_{2,2} & . & \zeta_{2,n} \\ . & . & . & . \\ \zeta_{n-1,1} & \zeta_{n-1,2} & . & \zeta_{n-1,n} \end{bmatrix}^{-1} \begin{bmatrix} V_1 \\ V_2 \\ . \\ . \\ V_n \end{bmatrix} \end{aligned} \tag{4.1}$$

and

$$i] = ([Y_{LM}^m] * [M_V^m])^{-1} I]. \tag{4.2}$$

The constraints on this transformation are given by

$$([Y_{LM}^m] * [M_V^m])^t [M_V^m] = [\lambda_i^m]_{diag} \tag{4.3}$$

and

$$I] = [Y_{ch}]V] = ([Y_{LM}^m] * [M_V^m])[M_V^m]^{-1}V], \tag{4.4}$$

leads to a decoupled system

$$i] = [D]e]. \tag{4.5}$$

Where $[D]$ is an identity matrix, $[Y_{LM}^m]$ is the corresponding line mode admittance matrix for the associated modal voltage matrix, $[M_V^m]$, and subscript 't' is the transpose operator [3], [13], [14]. The columns of $[M_V^m]$ are the modal voltage vectors $(\widehat{\zeta}_i)$. The vectors $V]$ and $I]$ represent voltages and the currents associated with n-ports. The operator '*' was defined in [3] for $[C] = [A] * [B]$, as a product of corresponding terms of matrices $[A]$ and $[B]$. The vectors $e]$ and $i]$ represent decoupled voltage and current. In the subsequent part of this chapter it is assumed that the modal voltage vectors are normalized to a form as represented in (1).

The equivalent circuit corresponding to this non-unique transformation scheme described in (1)-(5) is shown in Fig. 4.2. In case of n coupled transmission lines in

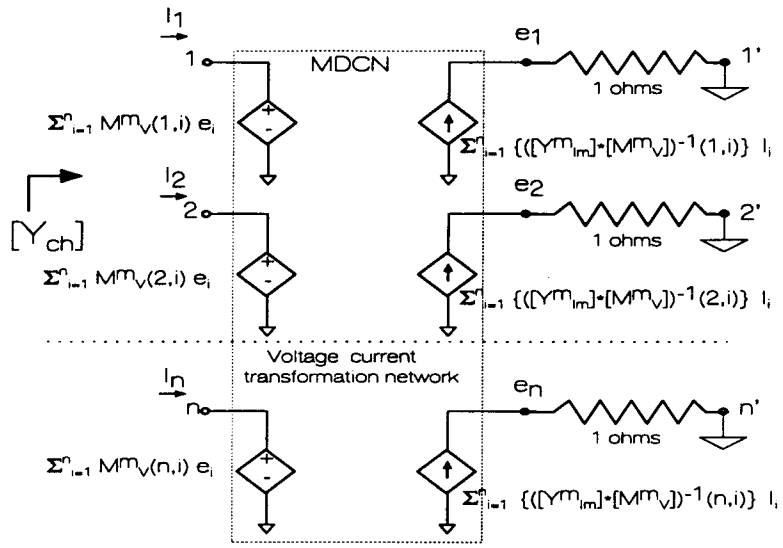

Figure 4.2. Equivalent circuit corresponding to the voltage and current transformation.

a homogeneous media any n linearly independent modal voltage vectors can be used as transformation matrix to decompose the characteristic admittance matrix and hence decouple the UMCL n lines system. The values of the elements of matrix $[\lambda_i^m]_{diag}$ ($\lambda_i^m(i,i) \neq 0$) depends on the choice of the modal voltage vectors. For example, the eigenvectors of the characteristic admittance matrix belong to the set of modal voltage vectors, therefore, they can be used in (1).

Recall, that for a UMCL in an inhomogeneous media these modal voltage vectors are not arbitrary but depend on the eigen-solution of the coupled transmission line equations [3],[12]-[13]. The choice of these modal voltage vectors is then further restricted to the modal voltage eigenvectors ($[M_V]$=$[M_V^m]$). For a UMCL n lines system with n non-degenerate eigenvalues (unequal mode velocities) these modal voltage eigenvectors are complete, i.e. spans n dimensional vector space. The elements of the matrix $[\lambda_i^m]_{diag}$ are the function of the elements of the line mode admittance matrix, $[Y_{LM}]$, ($[Y_{LM}] = [Y_{LM}^m]$) which in turn depends on the coupled transmission line equations [13], [14]. For a UMCL n lines system with q degenerate eigenvalues any q linearly independent modal voltage vectors can be chosen corresponding to these degenerate

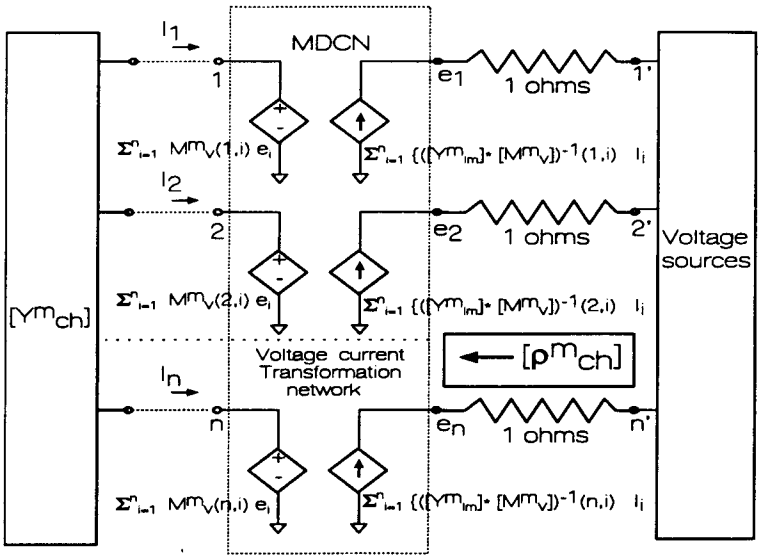

Figure 4.3. Equivalent circuit corresponding to the definition of partial mode admittance matrix, $[Y_{ch}^{m}]$. The internal resistance of the voltage sources in this figure are assumed to be zero.

eigenvalues such that together with the remaining $(n-q)$ non-degenerate eigenvectors are complete. As an aside, note that as illustrated in [3], equations (1) to (5) leads to the SPICE model of a UMCL $2n$-ports system. Moreover, the transformation in (1)-(5), explains the underlining difference between the class of two different UMCL n lines system in a inhomogeneous media with identical characteristic admittance matrices. Based on this transformation a decomposition scheme for the characteristic admittance as a sum of n symmetric matrices, defined as partial mode admittance matrices is derived as shown below.

Partial mode admittance matrix:

A n port network corresponding to the partial mode admittance matrix, $[Y_{ch}^{m}]$, associated with the mode m when used as termination network reflects (reflection coefficient is assumed to be unity) all other modes except the mth mode for which it provides a match condition.

By the above definition (Fig. 4.3):

$$\begin{aligned}[\rho_{ch}^m] &= ([D] - [D_m]) \\ &= ([D] - ([Y_{LM}] * [M_V])^{-1}[Y_{ch}^m][M_V])([D] \\ &\quad + ([Y_{LM}] * [M_V])^{-1}[Y_{ch}^m][M_V])^{-1} \end{aligned} \tag{4.6}$$

with

$$[D_m] = \begin{cases} D_m(i,j) = 0, & i \neq j \\ D_m(j,j) = 0, & j \neq m \\ D_m(j,j) = 1, & j = m \end{cases} . \tag{4.7}$$

Where $[\rho_{ch}^m]$ is the reflection coefficient associated with the mth partial mode admittance matrix. From (6) and (7) the partial mode admittance matrix, $[Y_{ch}^m]$, corresponding to the mode m is given by

$$[Y_{ch}^m] = ([Y_{LM}] * [M_V])[D_m][M_V]^{-1}. \tag{4.8}$$

The expression for the characteristic admittance matrix, $[Y_{ch}]$, in terms of partial mode admittance matrices of a UMCL n lines system is

$$[Y_{ch}] = \sum_{m=1}^{n} [Y_{ch}^m]. \tag{4.9}$$

Equations (1) to (9) provides a general procedure leading to the decomposition of characteristic admittance matrix, $[Y_{ch}]$, as a sum of n symmetric partial mode admittance matrices. The relationship in (9) is utilized in [4] to obtain a configuration-oriented SPICE model for a general UMCL $2n$-port system. This model consists of a network of transmission lines connected in configuration-oriented topological fashion. Therefore, the synthesis procedure of a UMCL $2n$-port system in general is equivalent to realization of all the transmission lines in the configuration-oriented model.

The partial mode admittance matrices of a UMCL are real, symmetric and have rank equal to one. Additionally, the resistive network corresponding to the partial admittance matrices $[Y_{ch}^m]$ is a non-mode converting network. A non-mode converting network does

not introduces inter-mode coupling when utilized as a termination network. Moreover, the vector spanning range space of mth partial mode admittance matrix $[Y_{ch}^{m}]$ is orthogonal to the all other modal voltage vectors (eigenvectors). Therefore,

$$[Y_{ch}^{m}]\zeta_i] = 0], \quad i \neq m. \tag{4.10}$$

Combining (9) and (10) yields

$$([Y_{ch}]\zeta_m])^t\zeta_i] = 0, \quad i \neq m, \tag{4.11}$$

which is the generalization of orthogonality relation between voltage and current for a UMCL n lines system. In general, partial mode admittance matrices with their modal delays are sufficient to completely characterize a UMCL $2n$-port system.

4.3 DISCRETE TRANSITION MATRIX FUNCTION: FOR UMCL

A general SPICE model of a UMCL $2n$-port system can consist of n decoupled transmission lines corresponding to each propagating mode with the current and voltage controlled sources (mode coupling and decoupling network) [3] or network of decoupled $n^2(n+1)/2$ transmission lines of different lengths constituting a configuration-oriented SPICE model [4]. We assume that the travel time through each transmission line is an integral multiple of a small time increment $\triangle$T.

The linear transformation defined in (1) and (2) decouples a UMCL $2n$-port system into n independent transmission line system. Each of these transmission line is associated with a mode and its electrical length corresponds to the respective modal delay. For a UMCL system in an inhomogeneous media the modal voltage vectors in (1) are the modal voltage eigenvectors. The voltage current evolution equation in the z-domain (z-transform) for a single transmission line is given by [8],

$$\begin{bmatrix} v_{in}(.,z) \\ i_{in}(.,z) \end{bmatrix} = \begin{bmatrix} \frac{z^m+z^{-m}}{2} & z_o\frac{z^m-z^{-m}}{2} \\ \frac{z^m-z^{-m}}{z_o 2} & \frac{z^m+z^{-m}}{2} \end{bmatrix} \begin{bmatrix} v_{out}(.,z) \\ i_{out}(.,z) \end{bmatrix}. \tag{4.12}$$

Here z_o is the characteristic impedance of the transmission line and $m\triangle$T is the electrical delay. Likewise, using (12) and (5), the voltage current evolution in the z-domain

for the n independent decoupled transmission lines with the characteristic impedances z_o equal to one ohms leads to,

$$\begin{bmatrix} e_{in}(0,z)] \\ i_{in}(0,z)] \end{bmatrix} = \begin{bmatrix} [A] & [B] \\ [B] & [A] \end{bmatrix} \begin{bmatrix} e_{out}(l,z)] \\ i_{out}(l,z)] \end{bmatrix} \tag{4.13}$$

where,

$$[A] = \begin{bmatrix} \frac{z^{n_1}+z^{-n_1}}{2} & 0 & . & 0 \\ 0 & \frac{z^{n_2}+z^{-n_2}}{2} & . & 0 \\ . & . & . & . \\ 0 & 0 & . & \frac{z^{n_n}+z^{-n_n}}{2} \end{bmatrix}_{n\times n} \tag{4.14}$$

and

$$[B] = \begin{bmatrix} \frac{z^{n_1}-z^{-n_1}}{2} & 0 & . & 0 \\ 0 & \frac{z^{n_2}-z^{-n_2}}{2} & . & 0 \\ . & . & . & . \\ 0 & 0 & . & \frac{z^{n_n}-z^{-n_n}}{2} \end{bmatrix}_{n\times n} . \tag{4.15}$$

Here n_i is an integer associated with the ith mode transmission line electrical delay ($n_i \triangle T$). The vectors $e]_{in}$ and $i]_{in}$ are the voltage and current at the input ports and the vectors $e]_{out}$ and $i]_{out}$ represents the voltage and current at the output ports of the n decoupled transmission lines. Since the linear transformations defined in (1) and (2), (13) can be expressed as ($[M_I] = ([M_V]^{-1})^t$)

$$\begin{aligned} \begin{bmatrix} V_{in}(0,z)] \\ I_{in}(0,z)] \end{bmatrix} &= \begin{bmatrix} [A_z] & [B_z] \\ [C_z] & [D_z] \end{bmatrix} \begin{bmatrix} V_{out}(l,z)] \\ I_{out}(l,z)] \end{bmatrix} \\ &= [T(z)] \begin{bmatrix} V_{out}(l,z)] \\ I_{out}(l,z)] \end{bmatrix}, \end{aligned} \tag{4.16}$$

with

$$\begin{aligned} [A_z] &= ([M_I]^{-1})^t [A][M_I]^t \\ [B_z] &= ([M_I]^{-1})^t [B]([Y_{LM}] * [M_v])^{-1} \\ [C_z] &= ([Y_{LM}] * [M_v])[B][M_I]^t \\ [D_z] &= ([Y_{LM}] * [M_v])[A]([Y_{LM}] * [M_v])^{-1}. \end{aligned}$$

Equation (16) describes the relationship between the input and output ports voltages ($V_{in}(0,z)$] and $V_{out}(l,z)$]) and currents ($I_{in}(0,z)$] and $I_{out}(l,z)$]) of a general UMCL $2n$-port system in terms of the discrete transition matrix function, $[T(z)]$. It is to be noted that the discrete transition matrix function, $[T(z)]$, satisfies reciprocity relationship and therefore is unimodular and can be written as

$$[T(z)] = \sum_{j=1}^{2} \sum_{m=1}^{n} g_{mj}(z)[P_{mj}], \tag{4.17}$$

where,

$$[P_{mj}] = \frac{1}{2} \begin{bmatrix} \left[P_{mj}^{11}\right] & \left[P_{mj}^{12}\right] \\ \left[P_{mj}^{21}\right] & \left[P_{mj}^{22}\right] \end{bmatrix}. \tag{4.18}$$

$$\begin{aligned} \left[P_{mj}^{11}\right] &= ([M_I]^{-1})^t [D_m][M_I]^t \\ \left[P_{mj}^{12}\right] &= (-1)^j ([M_I]^{-1})^t [D_m]([Y_{LM}] * [M_v])^{-1} \\ \left[P_{mj}^{21}\right] &= (-1)^j ([Y_{LM}] * [M_v])[D_m][M_I]^t \\ \left[P_{mj}^{22}\right] &= ([Y_{LM}] * [M_v])[D_m]([Y_{LM}] * [M_v])^{-1} \end{aligned}$$

Here $g_{mj}(z) = z^{(-1)^j n_m}$ is a scalar function associated with the electrical delay of mth mode ($n_m \triangle T$). Additionally the matrices $[P_{mj}]$ satisfy the following relationships:

$$\begin{aligned} [P_{mj}]^2 &= [P_{mj}], \ [P_{mj}][P_{kl}] = [0] \\ &\qquad \text{for} \quad m \neq k \ or \ j \neq l, \end{aligned} \tag{4.19}$$

and

$$\sum_{j=1}^{2} \sum_{m=1}^{n} [P_{mj}] = [D]. \tag{4.20}$$

4.3.1 Input Impulse Admittance Matrix (IIAM) Function :

The Input impulse admittance matrix (IIAM) function, $[Y_{in}(0,t)]$, is defined as a admittance matrix (function of time) of an equivalent resistive network which has a

identical reflection response to that of the actual UMCL $2n$-port system. Assuming, the output end of the given UMCL $2n$-port system's n-ports are terminated with a passive termination network of real resistances. This resistive network is described by a termination admittance matrix, $[Y_T]$, as

$$I_{out}(l,z)] = [Y_T]V_{out}(l,z)]. \tag{4.21}$$

Combining (16) and (21) and defining IIAM function, $[Y_{in}(0,t)]$, in z-domain as $I_{in}(0,z)]$ $= [Y_{in}(0,z)]V_{in}(0,z)]$, leads to

$$\begin{aligned}[Y_{in}(0,z)] = ([Y_{LM}] * [M_V])([D] - [B_1][\rho^T][B_1]) \\ ([D] + [B_1][\rho^T][B_1])^{-1}[M_I]^t\end{aligned} \tag{4.22}$$

with (refer: section-(4.7.1) and section-(4.7.2))

$$\begin{aligned}[\rho^T] = ([D] - ([Y_{LM}] * [M_V])^{-1}[Y_T]([M_I]^{-1})^t) \\ ([D] + ([Y_{LM}] * [M_V])^{-1}[Y_T]([M_I]^{-1})^t)^{-1},\end{aligned} \tag{4.23}$$

and

$$[B_1] = \begin{bmatrix} \frac{z^{-n_1}}{2} & 0 & . & 0 \\ 0 & \frac{z^{-n_2}}{2} & . & 0 \\ . & . & . & . \\ 0 & 0 & . & \frac{z^{-n_n}}{2} \end{bmatrix}_{n\times n}. \tag{4.24}$$

Equation (22) in z-domain represents the IIAM function in terms of a rational matrix function. In a similar fashion an equivalent dual of the IIAM function in terms of the input impulse impedance matrix function, $[Z_{in}(0,t)]$, can also be defined. Now, expressing $[Y_{in}(0,z)]$ in terms infinite power series of decreasing power (Markov expansion) [123] leads to

$$\begin{aligned}[Y_{in}(0,z)] = [Y_0] + \sum_{i=1}^{n}\sum_{j=1}^{n}[Y_{ij}]z^{-n_i-n_j} + \\ \text{Second and higher order terms.}\end{aligned} \tag{4.25}$$

Substituting (25) in (22) and solving for $[Y_{ij}]$ by equating same power of z terms leads to the zero and first-order reflection terms,

$$[Y_0] = ([Y_{LM}] * [M_V])[M_V]^{-1}, \tag{4.26}$$

$$[Y_{ii}] = -2([Y_{LM}] * [M_V])[D_i][\rho^T][D_i][M_V]^{-1} \tag{4.27}$$

and

$$[Y_{ij}] + [Y_{ji}] = -2([Y_{LM}] * [M_V])([D_i][\rho^T][D_j] + [D_j][\rho^T][D_i])[M_V]^{-1}. \tag{4.28}$$

The matrices, $[Y_o]$ and $[Y_{ij}] + [Y_{ji}]$ are real and symmetric given the termination admittance matrix, $[Y_T]$, is real and symmetric. In general, $[Y_{in}(0,t)]$ has a finite or infinite number of terms depending on the source and the termination admittance matrix. The first-order terms can have utmost $(n(n+1)/2)$ terms. Additionally, (22) leads to all the higher order reflection terms in terms of the zero and first-order reflection terms. The inverse z-transformation of (25) leads to the IIAM function, $[Y_{in}(0,t)]$,

$$[Y_{in}(0,t)] = [Y_0]\delta(t) + \sum_{i=1}^{n}\sum_{j=1}^{n}[Y_{ij}]\delta(t-(n_i+n_j)\triangle t) + \text{Second and higher order terms.} \tag{4.29}$$

4.3.2 Measured Impulse Reflection Response (IRR) Matrix Function:

We now derive relationship between the measured IRR matrix function, $[\rho_{in}(0,t)]$, and the IIAM function, $[Y_{in}(0,t)]$. The measured IRR matrix function, $[\rho_{in}(0,t)]$, is constructed by canonically exciting each input port of a UMCL $2n$-port system n ports by a infinitesimal small rise time impulse and measuring the reflection response at the input ports. In general depending on the source and the termination admittance matrix the measured IRR matrix function, $[\rho_{in}(0,t)]$, has a finite or infinite number of terms.

The measured IRR matrix function in terms of IIAM function in z-domain is given by,

$$[\rho_{in}(0,z)] = ([Y_s] - [Y_{in}(0,z)])([Y_s] + [Y_{in}(0,z)])^{-1} \tag{4.30}$$

where $[Y_s]$ is the (non-singular and diagonal) source admittance matrix corresponding to the passive source resistive network. Expressing (30) in terms of infinite power series

with decreasing power (Markov expansion) leads to

$$[\rho_{in}(0,z)] = [\rho_0] + \sum_{i=1}^{n}\sum_{j=1}^{n}[\rho_{ij}]z^{-n_i-n_j} + \text{Second and higher order terms.} \tag{4.31}$$

Solving for $[Y_{ij}]$ in terms of $[\rho_{in}(0,z)]$ by substituting (31) and (25) in (30) and equating same power of z on both sides of the resulting equation, one obtains

$$[Y_0] = ([D] + [\rho_0])^{-1}([D] - [\rho_0])[Y_s], \tag{4.32}$$

$$[Y_{ii}] = -([D] + [\rho_0])^{-1}[\rho_{ii}]([Y_s] + [Y_0]) \tag{4.33}$$

and

$$[Y_{ij}] + [Y_{ji}] = -([D] + [\rho_0])^{-1}([\rho_{ij}] + [\rho_{ji}])([Y_s] + [Y_0]) \tag{4.34}$$

Equations (32)-(34) with (26)-(28) leads to the required relationship between the measured IRR data and the normal-mode parameters of a UMCL n lines system. Taking the inverse z-transform of (31) gives the measured IRR matrix function, $[\rho_{in}(0,t)]$, as

$$[\rho_{in}(0,t)] = [\rho_0]\delta(t) + \sum_{i=1}^{n}\sum_{j=1}^{n}[\rho_{ij}]\delta(t-(n_i+n_j)\triangle T) + \text{Second and higher order terms.} \tag{4.35}$$

4.3.3 The Higher Order Terms

The higher order reflection terms of the IIAM and measured IRR matrix function in (29) and (35) can be evaluated from the zero and first-order reflection terms. These higher order terms can be obtained from (22) and (30). The general expression for the lth order term ($l \geq 1$) of IIAM function, $[Y_{in}(0,z)]_l$, in z-domain is given by,

$$[Y_{in}(0,z)]_l = (-1)^l 2([Y_{LM}] * [M_V])([B_1][\rho^T][B_1])^l[M_V]^{-1}. \tag{4.36}$$

Similarly, the general expressions for the lth order term ($l \geq 2$) of measured IRR matrix function, $[\rho_{in}(0,z)]_l$, in z-domain is given by a recursive relation as,

$$[\rho_{in}(0,z)]_l = -[\rho_{in}(0,z)]_{(l-1)}([Y_s][Y_o]^{-1} - [D])$$
$$([Y_{LM}] * [M_V])[B_1][\rho^T][B_1])$$
$$[M_V]^{-1}([Y_s] + [Y_o])^{-1} \tag{4.37}$$

with

$$[\rho_{in}(0,z)]_1 = -([D] + [\rho_o])[Y_{in}(0,z)]_1([Y_s] + [Y_o])^{-1}. \tag{4.38}$$

Equation (37) shows that in case the source admittance matrix, $[Y_s]$, is equal to the characteristic admittance matrix, $[Y_{ch}]$, the measured IRR matrix function, $[\rho_{in}(0,z)]$ consists of only finite terms associated with the zero and the first-order reflections.

4.4 UMCL SYNTHESIS PROCEDURE : $2n$-Port System

In this section a synthesis procedure for an equivalent UMCL $2n$-port discrete transition matrix from the measured reflection response of a UMCL $2n$-port system with distinct modal delays is presented. The proposed extraction technique is based on the relationship between the normal-mode parameters and the measured IRR data as illustrated in the previous section.

A UMCL $2n$-port system terminated with a unknown resistive network, $[Y_T]$, is considered. Its measured IRR matrix function, $[\rho_{in}^m(0,t)]$, is given by,

$$[\rho_{in}^m(0,t)] = [\rho_o^m]\delta(t) + \sum_{i=1}^{\infty}[\rho_i^m]\delta(t - p_i^m \triangle T). \tag{4.39}$$

Here integer p_i^m corresponds to the modal or inter-modal coupling delays due to the impedance mismatch at the source and the termination end. It is assumed that the unknown termination network, $[Y_T]$, is not equal to the characteristic admittance matrix, $[Y_{ch}]$. The zero, first and all the higher-order reflection terms are included in (39). The IIAM function's zero-order reflection term, $[Y_o]$, is equal to the characteristic admittance matrix, $[Y_{ch}]$. This term can be evaluated by substituting $[\rho_o^m]$ in (32). In case $[Y_s]$

is equal to $[Y_{ch}]$, (39) has only finite terms. These terms are due to the zero and the first-order reflections and can be therefore identified directly.

For a general case, ($[Y_s] \neq [Y_{ch}]$) it is assumed that each modal delay satisfy: $n_i\triangle T >> (n_k - n_l)\triangle T/2$, (for: i, k and $l = 1, ., ..n$). This assumption holds true for microstrip coupled line and similar passive systems [124]. Also it sets a bound on the degree of the system in the corresponding partial realization problem [123]. Using this assumption in (39) the first-order reflection terms, $[\rho_q^m]$, (nj terms) and the delays, $p_q^m\triangle T$, associated with these terms can be obtained. The nj matrices, $[Y_q^m]$, in (34) are given by,

$$[Y_q^m] = -([D] + [\rho_o^m])^{-1}[\rho_q^m]([Y_s] + [Y_o]),$$
$$m = 1, \cdots nj. \tag{4.40}$$

These matrices are the first-order terms of IIAM function, corresponding to the measured IRR matrix function, $[\rho_{in}^m(0,t)]$. The expression of IIAM function, $[Y'_{in}(0,z)]$, for the equivalent UMCL $2n$-port system is given by

$$[Y'_{in}(0,z)] = ([Y_o] + \frac{1}{2}\sum_{i=1}^{nj}[Y_q^i]z^{-p_q^i})[Y_o]^{-1}([Y_o]^{-1}$$
$$- \frac{1}{2}\sum_{i=1}^{nj}[Y_o]^{-1}[Y_q^i][Y_o]^{-1}z^{-p_q^i})^{-1}. \tag{4.41}$$

To extract the modal voltage eigenvector matrix , $[M'_V]$, associated with $[Y'_{in}(0,z)]$ the procedure is: (refer: section-(4.7.3)-(4.7.5))

- Construct matrices, $H_m = [Y_o]^{-1}[Y_q^m][Y_o]^{-1}[Y_q^m]$, for each $[Y_q^m]$, $(m = 1, \cdots nj)$.
- Using the procedure in section-(4.7.4) generate orthogonal matrices, E_i ,$(i = 1, \cdots pj)$.
  - □ If $pj < n$, then the termination resistive network does not satisfy the necessary and sufficiency conditions for the extraction of an equivalent UMCL $2n$-port system (refer: section-(4.7.5)).

- If $pj = n$ then all the normal-mode parameters can be identified from the reflection response data (refer: section-(4.7.5)). Now construct an auxiliary matrix F as

$$\begin{aligned}[F] &= \sum_{k=1}^{n} b_k E_k, b_k \in R \\ &= [G_V][\eta]_{diag}[G_V]^{-1} \end{aligned} \tag{4.42}$$

such that it has n distinct non-zero eigenvalues. It has been shown in section-(4.7.5) that if $pj = n$ such a construction always exists. The eigenvector matrix, $[G_V]$, (normalized to the form as in (1)) of $[F]$ is the voltage eigenvector matrix, $[M'_V]$ of the equivalent UMCL $2n$-port system respectively.

Equation (26) leads to

$$([Y'_{LM}] * [M'_V]) = [Y_o][M'_V], \tag{4.43}$$

and thus set of n^2 algebraic linear equations whose solution leads to the elements of line mode admittance matrix, $[Y'_{LM}]$. From (27) and (28) the matrices, $[\rho_q^{T^m}]$, associated with the matrices, $[Y_q^m]$, are

$$\begin{aligned}[\rho_q^{T^m}] = -\frac{1}{2}([Y'_{LM}] * [M'_V])^{-1}[Y_q^m][M'_V], \\ m = 1, \cdots nj. \end{aligned} \tag{4.44}$$

These matrices $[\rho_q^{T^m}]$ $(m = 1, .., nj)$ associated with the first-order reflections can be resolved as

$$[{\rho_q}^{T^m}] = \begin{cases} ([D_{l_i}][\rho^{T'}][D_{l_i}]) & : \text{matrix is diagonal} \\ ([D_{i_i}][\rho^{T'}][D_{j_i}] + [D_{i_i}][\rho^{T'}][D_{j_i}]) & : \text{matrix is non-diagonal} \end{cases} \tag{4.45}$$

Here the matrix $[\rho^{T'}]$ is equivalent to matrix $[\rho^T]$ in (23) and is given by,

$$[\rho^{T'}] = \sum_{m=1}^{nj} [\rho_q^{T^m}]. \tag{4.46}$$

The resolution leads to the components of modal (l_i) or inter-modal (i_i and j_i) coupled waves at the input end of UMCL $2n$-port system which constitute the first-order

reflection term, $[\rho_q^m]$, at time $t = p_q^m \triangle T$. The linear equation obtained from (45) for evaluating the modal delays is

$$[\rho_q^{T^m}] \rightarrow \begin{cases} 2n'_{l_i} = p_q^m & : \text{matrix is diagonal} \\ n'_{i_i} + n'_{j_i} = p_q^m & : \text{matrix is non-diagonal} \end{cases} \tag{4.47}$$

The solution of n linearly independent equations obtained from the first-order reflection terms leads to the n modal electrical delays, $n'_k \triangle T$, $(k = 1 \text{ to } n)$. These modal electrical delays, $n'_k \triangle T$, corresponding to the matrix, $[M'_V]$, are the modal delays of the equivalent UMCL $2n$-port system. It is to be noted that these n linearly independent equations for the modal delay will always exist given the necessary and sufficiency condition in section-(4.7.5) is satisfied.

The transition matrix, $[T'(z)]$, for the equivalent UMCL $2n$-port system is obtained from (17) and the extracted normal-mode parameters ($[M'_V]$, $[Y'_{LM}]$ and the modal delays $n'_k \triangle T$, $k = 1, \cdots n$).

4.5 RICCATI MATRIX EQUATION: for UMCL $2n$-Port System

The measured impulse reflection response (IRR) and the input impulse admittance matrix function (IIAM) derived earlier can be expressed as a rational matrix functions. The rational matrix function corresponding to the measured impulse reflection response and thereby the input impulse admittance matrix function in the z-domain can be extracted using partial realization techniques developed for system identification [18]. Substituting (23) and (26) in (36) for only the identified first-order terms yields (polynomial algebraic Riccati matrix Equation):

$$\begin{aligned} &([Y_{LM}] * [M_V])[B_1]([Y_{LM}] * [M_V])^{-1}[rh] \\ &\quad ([Y_{LM}] * [M_V])[B_1]([Y_{LM}] * [M_V])^{-1} \\ &\quad = \sum_{i=1}^{n} \sum_{j=1}^{n} [Y_{ij}][Y_o]^{-1} z^{-n_i - n_j} \end{aligned} \tag{4.48}$$

where

$$[rh] = \sum_{i=1}^{n} \sum_{j=1}^{n} [Y_{ij}][Y_o]^{-1} = ([Y_o] - [Y_T])([Y_o] + [Y_T])^{-1}. \tag{4.49}$$

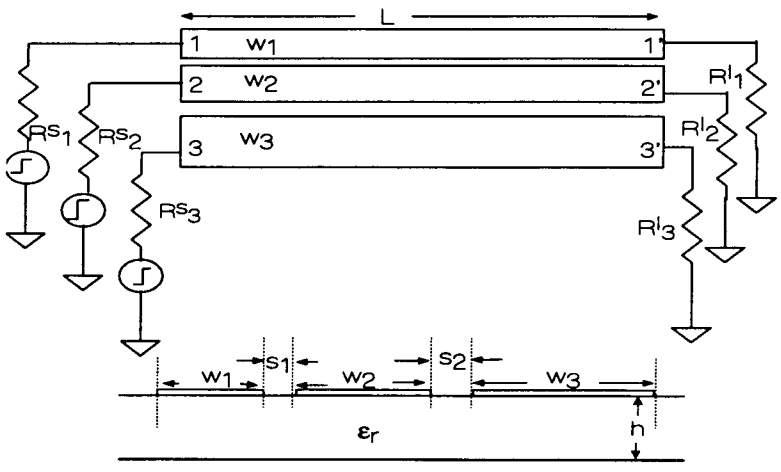

Figure 4.4. Microstrip structure: uniform coupled asymmetric three lines

Equation (48) is of the form $[A(z)][rh][A(z)] = E(z)$, and the solution $[A(z)] = [A_1]z^{-n_1} + \cdots [A_n]z^{-n_n}$, leads to the partial mode admittance matrices, $[Y_{ch}^m] = [A_m][Y_o]$, and the associated degree of z yields the modal delays ($n_m \triangle T$). As alluded earlier in this chapter instead of solving a general polynomial algebraic Riccati matrix equation for identifying the normal-mode parameters of a UMCL $2n$-port system an alternative formulation has been used as presented in the previous section.

4.6 EXAMPLE: UMCL Three Lines System

In order to demonstrate and validate the synthesis procedure proposed in this chapter, an example of three-coupled microstrip line structure is presented.

The normal-mode parameters of three-coupled microstrip line structure as shown in Fig. 4.4 are evaluated by a quasi-static electromagnetic tool and the corresponding equivalent SPICE circuit model [4] is obtained from these normal-mode parameters. The dimen-

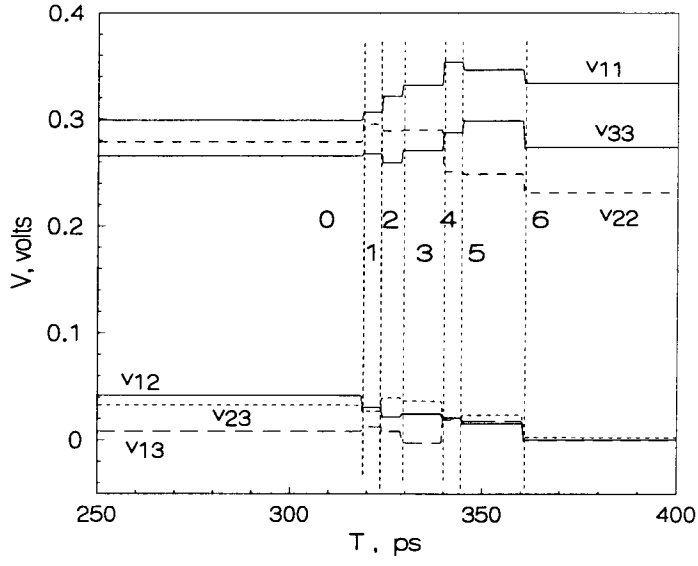

Figure 4.5. Measured reflected voltage response of a uniform coupled asymmetric three lines shown in Fig.4.4 due to the step excitation (excitation voltage: 0.5V)

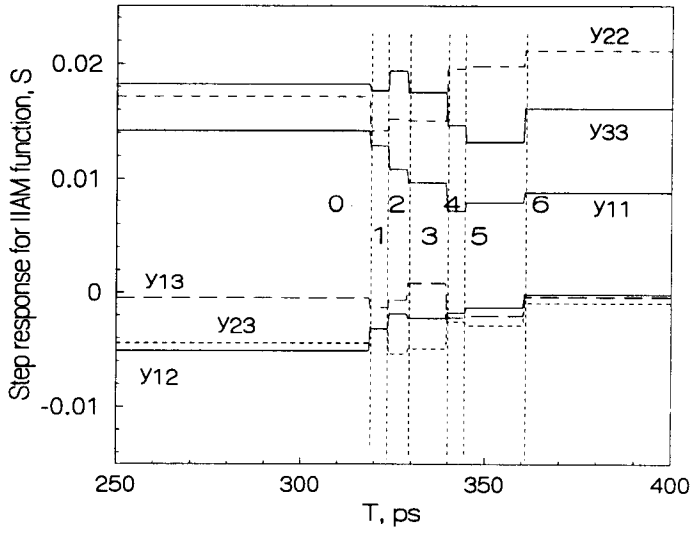

Figure 4.6. The IIAM step-response waveform ($\sum_{m=0}^{j}[Y_q^m]\delta(t-t_j)$) vs time obtained from the measured reflected voltage response shown in Fig. 4.5.

Table 1. IRR function: zero and the first-order terms

m	$\rho_q^m(1,1)$	$\rho_q^m(1,2)$	$\rho_q^m(1,3)$	$\rho_q^m(2,2)$	$\rho_q^m(2,3)$	$\rho_q^m(3,3)$
0	1.950×10^{-1}	1.676×10^{-1}	3.306×10^{-2}	1.147×10^{-1}	1.313×10^{-1}	6.204×10^{-2}
1	3.012×10^{-2}	-4.468×10^{-2}	1.619×10^{-2}	6.620×10^{-2}	-2.399×10^{-2}	8.680×10^{-3}
2	5.972×10^{-2}	-3.567×10^{-2}	-1.564×10^{-2}	-2.540×10^{-2}	5.155×10^{-2}	-3.400×10^{-2}
3	4.096×10^{-2}	1.176×10^{-2}	-4.349×10^{-2}	3.400×10^{-3}	-1.248×10^{-2}	4.612×10^{-2}
4	8.932×10^{-2}	-1.416×10^{-2}	8.609×10^{-2}	-1.542×10^{-1}	-6.410×10^{-2}	6.672×10^{-2}
5	-2.980×10^{-2}	-2.162×10^{-2}	-4.906×10^{-3}	-9.960×10^{-3}	1.247×10^{-2}	4.396×10^{-2}
6	-5.156×10^{-2}	-6.006×10^{-2}	-7.169×10^{-2}	-7.000×10^{-2}	-8.353×10^{-2}	-9.972×10^{-2}

sion of structure shown in Fig. 4.4 and the associated normal-mode parameters are:

$s_1 = 0.2mm, w_2 = 1.0mm, s_2 = 0.3mm, w_3 = 1.5mm, h = 1.0mm, \epsilon_r = 4, L = 3.0cm, R_1^s = R_2^s = R_3^s = 50\Omega, R_1^l = 100\Omega, R_2^l = 40\Omega, R_3^l = 60\Omega)$. The corresponding normal-mode parameters are: $z_{a1} = 123.91\Omega, z_{a2} = 119.13\Omega, z_{a3} = 76.134\Omega, \widehat{\zeta_a} = [1, 1.1137, 1.056]^t, v_a = 1.665 \times 10^8 m/s, z_{b1} = 77.495\Omega, z_{b2} = 80.701\Omega, z_{b3} = 48.63\Omega, \widehat{\zeta_b} = [1, 0.3227, -0.7991]^t, v_b = 1.8251 \times 10^8 m/s, z_{c1} = 46.295\Omega, z_{c2} = 45.775\Omega, z_{c3} = 30.443\Omega, \widehat{\zeta_c} = [1, -1.49, 0.4226]^t, v_c = 1.8837 \times 10^8 m/s.$

The associated time-domain reflection response for this structure for a step excitation is then evaluated via simulating the resulting SPICE model on a circuit simulator. Figure 4.5 shows the time-domain reflection response of a UMCL structure shown in Fig. 4.4. This TDR response (step excitation) is used as a measurement data to validate the synthesis procedure.

The IRR data (eqn. 39) for the structure is extracted from the TDR (step response) waveform (shown in Fig. 4.5) and is given in Table-(1). The corresponding zero and the first-order reflection terms of the IRR are identified and eqn. (40) leads to the matrices, $[Y_q^m]$, associated with the IIAM function's zero and the first-order terms (Table-(2)).

Table 2. IIAM function: zero and the first-order terms

m	$Y_q^m(1,1)$	$Y_q^m(1,2)$	$Y_q^m(1,3)$	$Y_q^m(2,2)$	$Y_q^m(2,3)$	$Y_q^m(3,3)$
0	1.420×10^{-2}	-5.090×10^{-3}	-4.353×10^{-4}	1.717×10^{-2}	-4.438×10^{-3}	1.823×10^{-2}
1	-1.298×10^{-3}	1.957×10^{-3}	-8.343×10^{-4}	-2.949×10^{-3}	1.258×10^{-3}	-5.356×10^{-4}
2	-2.057×10^{-3}	1.231×10^{-3}	6.485×10^{-4}	9.609×10^{-4}	-2.178×10^{-3}	1.682×10^{-3}
3	-1.129×10^{-3}	-3.499×10^{-4}	1.438×10^{-3}	-1.093×10^{-4}	4.456×10^{-4}	-1.829×10^{-3}
4	-2.564×10^{-3}	4.473×10^{-4}	-3.028×10^{-3}	4.476×10^{-3}	2.368×10^{-3}	-2.833×10^{-3}
5	6.843×10^{-4}	5.019×10^{-4}	1.524×10^{-4}	2.456×10^{-4}	-3.221×10^{-4}	-1.497×10^{-3}
6	9.866×10^{-4}	1.142×10^{-3}	1.696×10^{-3}	1.325×10^{-3}	1.964×10^{-3}	2.915×10^{-3}

The resulting IIAM step-response waveform ($\sum_{m=0}^{j}[Y_q^m]\delta(t-t_j)$) vs time is shown in Fig. 4.6. Generating matrices, $H_m(=[Y_q^o]^{-1}[Y_q^m][Y_q^o]^{-1}[Y_q^m]^{-1},\ \mathrm{m} \neq 0)$, and using the orthogonalization procedure (refer: section-(4.7.3)-(4.7.5)) described in section-(4.4), leads to the orthogonal matrices, $[E_i]$ (i=1,2,3),

$$
\begin{aligned}
[E_1] &\simeq \begin{bmatrix} 1.270 \times 10^{-2} & -1.915 \times 10^{-2} & 8.165 \times 10^{-3} \\ -1.894 \times 10^{-2} & 2.855 \times 10^{-2} & -1.217 \times 10^{-2} \\ 5.369 \times 10^{-3} & -8.094 \times 10^{-3} & 3.451 \times 10^{-3} \end{bmatrix} \\
[E_2] &\simeq \begin{bmatrix} 1.336 \times 10^{-2} & 4.133 \times 10^{-3} & -1.699 \times 10^{-2} \\ 4.309 \times 10^{-3} & 1.334 \times 10^{-3} & -5.482 \times 10^{-3} \\ -1.067 \times 10^{-2} & -3.300 \times 10^{-3} & 1.357 \times 10^{-2} \end{bmatrix} \\
[E_3] &\simeq \begin{bmatrix} 3.318 \times 10^{-2} & 3.840 \times 10^{-2} & 5.702 \times 10^{-2} \\ 3.694 \times 10^{-2} & 4.277 \times 10^{-2} & 6.350 \times 10^{-2} \\ 3.504 \times 10^{-2} & 4.057 \times 10^{-2} & 6.023 \times 10^{-2} \end{bmatrix}
\end{aligned} \tag{4.50}
$$

Since there exists three orthogonal matrices, $[E_i]$, the termination resistive network at the receiving end satisfies the necessary and sufficiency conditions given in section-(4.7.5). Thereby, all the normal-mode parameters of the UMCL structure as shown in Fig. 4.4 can be identified from the reflection data. The modal voltage eigenvectors ($\widehat{\zeta_a}, \widehat{\zeta_b}$ and $\widehat{\zeta_c}$) using eqn. (42) are evaluated as:

$$
\begin{aligned}
[F] \simeq \quad & 5[E_1] + [E_2] + 7[E_3] \\
\simeq \quad & \begin{bmatrix} 3.091 \times 10^{-1} & 1.772 \times 10^{-1} & 4.229 \times 10^{-1} \\ 1.682 \times 10^{-1} & 4.435 \times 10^{-1} & 3.782 \times 10^{-1} \\ 2.614 \times 10^{-1} & 2.402 \times 10^{-1} & 4.524 \times 10^{-1} \end{bmatrix} \\
\simeq \quad & \begin{bmatrix} 1.000 & 1.000 & 1.000 \\ 1.113 & 0.3230 & -1.490 \\ 1.056 & -0.7994 & 0.4219 \end{bmatrix} \begin{bmatrix} 0.9532 & 0.000 & 0.000 \\ 0.000 & 0.0283 & 0.000 \\ 0.000 & 0.000 & 0.2235 \end{bmatrix} \\
& \begin{bmatrix} 1.000 & 1.000 & 1.000 \\ 1.113 & 0.3230 & -1.490 \\ 1.056 & -0.7994 & 0.4219 \end{bmatrix}^{-1} \\
\simeq \quad & [\hat{\zeta}_a,\ \hat{\zeta}_b,\ \hat{\zeta}_c] \begin{bmatrix} 0.9532 & 0.000 & 0.000 \\ 0.000 & 0.0283 & 0.000 \\ 0.000 & 0.000 & 0.2235 \end{bmatrix} [\hat{\zeta}_a,\ \hat{\zeta}_b,\ \hat{\zeta}_c]^{-1} \qquad (4.51)
\end{aligned}
$$

From eqn. (43) the line mode admittance matrix, $[Y_{LM}]$, is

$$
[Y_{LM}] \simeq \begin{bmatrix} 8.0716 \times 10^{-3} & 1.2902 \times 10^{-2} & 2.1599 \times 10^{-2} \\ 8.3921 \times 10^{-3} & 1.2399 \times 10^{-2} & 2.1845 \times 10^{-2} \\ 1.3135 \times 10^{-2} & 2.0564 \times 10^{-2} & 3.2870 \times 10^{-2} \end{bmatrix}, \qquad (4.52)
$$

and the linear equations for the modal delays (eqn. (44)-(47)) are given in Table-(3). The solution of linear equations in Table-(3) leads to the normal-mode delays: $n_a\triangle T = 1.8013 \times 10^2 ps$, $n_b\triangle T = 1.6443 \times 10^2 ps$ and $n_c\triangle T = 1.5923 \times 10^2 ps$. The identified normal-mode parameters are in good agreement with the actual normal-mode parameters of the given structure shown in Fig. 4.4. Using (17) the transition matrix , $[T(z)]$ can be synthesized from these normal-mode parameters.

Table 3. Linear equations for evaluating the modal delays: n_a, n_b and n_c

m	$[\rho_q^{T^m}]$: non-zero terms	linear equation	delay: (t_j), $p_q^m \triangle T$, ps
1	(3,3)	$2n_c\triangle T$	3.1846×10^2
2	(2,3) & (3,2)	$(n_b + n_c)\triangle T$	3.2366×10^2
3	(2,2)	$2n_b\triangle T$	3.2886×10^2
4	(1,3) & (3,1)	$(n_a + n_c)\triangle T$	3.3936×10^2
5	(1,2) & (2,1)	$(n_a + n_b)\triangle T$	3.4456×10^2
6	(1,1)	$2n_a\triangle T$	3.6026×10^2

4.7 DERIVATIONS & PROOFS

In this section the derivations and proofs for some of the important results used in this chapter are derived.

4.7.1 Matrix $[\rho^T]$ is Diagonalizable

The matrix $[\rho^T]$ in (23) can be written as

$$[\rho^T] = ([Y_{LM}] * [M_V])^{-1}([Y_{ch}] - [Y_T])([Y_{ch}] + [Y_T])^{-1}([Y_{LM}] * [M_V]) \tag{4.53}$$

The non-singular matrix, $[Y_{ch}]$, corresponding to the characteristic admittance matrix of UMCL represents a passive stable resistive network and therefore positive definite. Similarly the matrix, $[Y_T]$, associated with the passive termination resistance network is positive semi-definite. Moreover, the matrices $[Y_{ch}]$ and $[Y_T]$ are symmetric and therefore both can be simultaneously diagonalized with matrix, $[Q]$, leading to

$$\begin{aligned}\left[\rho^T\right] = & \quad ([Y_{LM}] * [M_V])^{-1}[Q]([\lambda_{Y_{ch}}]_{diag} - [\lambda_{Y_T}]_{diag})([\lambda_{Y_{ch}}]_{diag} \\ & + [\lambda_{Y_T}]_{diag})^{-1}[Q]^{-1}([Y_{LM}] * [M_V]) \\ = & \quad ([Y_{LM}] * [M_V])^{-1}[Q][\lambda_{eqv}]_{diag}[Q]^{-1}([Y_{LM}] * [M_V]) \\ = & \quad [X][\lambda_{eqv}]_{diag}[X]^{-1} \end{aligned} \tag{4.54}$$

and hence the matrix $[\rho^T]$ is diagonalizable. The bounds for the eigenvalues of matrix, $[\rho^T]$, are $\mid \lambda_{eqv}(i,i) \mid \leq 1, i = 1, \cdots n$.

4.7.2 Matrix, $[\lambda_i]_{diag}[\rho^T]$, is Symmetric

The matrix, $[\lambda_i]_{diag}$, is given by (a similar expression as in (3))

$$[\lambda_i]_{diag} = ([Y_{LM}] * [M_V])^t[M_V], \tag{4.55}$$

with non-zero diagonal elements. The symmetric property can be proved by combining (53) and (55) and leads to an important conclusion that if the (i,j)th element of the matrix $[\rho^T]$ is non-zero, the matrix $[\rho^T_{ij}]$=$[D_i][\rho^T][D_j] + [D_j][\rho^T][D_i]$ (i,j) and (j,i)th elements are non-zero. Also the matrix $[\rho^T_{ij}]^2$ is a diagonal matrix whose all the diagonal terms except the (i,i) and (j,j)th element are zero. Moreover the the matrix $[\rho^T_{ij}]^2$ (i,i) and (j,j)th element are equal and the matrix is given by,

$$\begin{aligned}[\rho^T_{ij}]^2 & = ([D_i][\rho^T][D_j] + [D_j][\rho^T][D_i])^2 \\ & = \rho^T(i,j)\rho^T(j,i)([D_i] + [D_j]) = [X^m_q]_{diag}. \end{aligned} \tag{4.56}$$

4.7.3 Inner Product

Let V be a vector space over the field $R^{n\times 1}$ and W be a vector space over the field $R^{n\times n}$. Defining the linear transformation T of V onto W as:

$$\begin{bmatrix} x_1 \\ x_2 \\ . \\ x_n \end{bmatrix} \xrightarrow{T} [S]_{n\times n} \begin{bmatrix} x_1 & 0 & . & 0 \\ 0 & x_2 & . & 0 \\ . & . & . & . \\ 0 & 0 & . & x_n \end{bmatrix}_{diag} [S]^{-1}_{n\times n} \tag{4.57}$$

where matrix $[S]_{n\times n}$ is a nonsingular matrix.

Let α_i, $\beta_i \in R^{n\times 1}$. The above linear transformation, T, leads to: $\alpha_i \xrightarrow{T} S_{\alpha_i}$ and $\beta_i \xrightarrow{T} S_{\beta_i}$, where matrices: $S_{\alpha_i}, S_{\beta_i} \in R^{n\times n}$. Defining the standard inner product [125] $(\alpha_i \,|\beta_i)$ on α_i and β_i by

$$(\alpha_i \,|\beta_i) = \sum_{l=1}^{n} \alpha_i(l,1)\beta_i(l,1), \tag{4.58}$$

and if $\gamma_i, (i = 1, \cdots n)$ be the eigenvalues of matrix $S_{\alpha_i}S_{\beta_i}$ then

$$(\alpha_i \,|\beta_j) =< S_{\alpha_i}, S_{\beta_i} >= \sum_{i=1}^{n} \gamma_i. \tag{4.59}$$

4.7.4 Procedure: Test for Completeness

Let U be a vector space over the field R^n (real diagonal matrices of dimension n), T' be linear transformation of V onto U and T'^{-1} be linear transformation of U onto V defined by

$$\begin{bmatrix} x_1 \\ x_2 \\ . \\ x_n \end{bmatrix} \underset{T'^{-1}}{\overset{T'}{\rightleftharpoons}} \begin{bmatrix} x_1 & 0 & . & 0 \\ 0 & x_2 & . & 0 \\ . & . & . & . \\ 0 & 0 & . & x_n \end{bmatrix}_{diag} \tag{4.60}$$

V is isomorphic to U.

Definition: Let the matrices be of the form $S_a = [S][\chi_a]_{diag}[S]^{-1}$ and $S_b = [S][\chi_b]_{diag}[S]^{-1}$ such that $S_a, S_b \in W$. The matrices are said to be orthogonal matrices if $S_aS_b = S_bS_a = [0]$.

Now, given the matrices $S_i = [S][\chi_i]_{diag}[S]^{-1}$, $(i = 1, \cdots pj, S_i \in W,$ and $[\chi_i]_{diag} \in U)$. The isomorphism in (60) and the property of inner product stated in section-(4.7.3) directly leads to a procedure similar to the Gram-Schmit orthogonalization process [19] for generating the orthogonal matrices, E_k, $(k = 1, \cdots cj \leq pj$ and $E_k \in W)$ corresponding to the matrices S_i. The matrices E_k are of the form $[S][\kappa_k]_{diag}[S]^{-1}$, $[\kappa_k]_{diag} \in U$.

Defining vectors, $[\kappa'_k]$ and $[\chi'_i]$, $([\kappa'_k], [\chi'_i] \in V)$ by

$$[\kappa_k]_{diag}, [\chi_i]_{diag} \xrightarrow{T'^{-1}} [\kappa'_k], [\chi'_i],$$
$$k = 1, \cdots cj \text{ and } i = 1, \cdots pj. \tag{4.61}$$

The procedure is:

- E_1=S_1.
- For constructing E_{j+1}, $(j > 1)$:

$$E_{j+1} = S_{j+1} - \sum_{m=1}^{j} \frac{< S_{j+1}, E_m >}{(< E_m, E_m >)^2} E_m.$$

- If $E_{j+1} = [0]$, then $[\chi'_{j+1}]$ can be expressed as linear combination of $[\chi'_1], \cdots [\chi'_j]$. therefore, exclude S_{j+1} and goto S_{j+2}.

From (58) it is clear that this orthogonalization process is equivalent to extraction of linear independent orthogonal vectors, $[\kappa'_k]$ (or $[\kappa_k]$) from the vectors, $[\chi'_i]$ (or $[\chi_i]$). If the vectors $[\chi'_i]$ are complete then n orthogonal matrices, E_i, $(i = 1, \cdots n)$ will exist. The above procedure provides a test for checking the completeness of $[\chi_i]_{diag}$ over the field of n dimensional real diagonal matrices.

4.7.5 Necessary and Sufficient Conditions: To Identify Normal-Mode Parameters.

1. Necessary conditions: for modal delays:

For the extraction of n distinct modal delays from the first-order reflection terms the **first necessary condition** is

- There should be at least n first-order reflection terms.

The first-order reflection terms contain modal and inter-modal delays. Let nj be the number of matrices, $[Y_q^m]$, $(m = 1, \cdots nj)$ in the first-order terms of the IIAM function. Now construct matrices $H_m = [Y_o]^{-1}[Y_q^m][Y_o]^{-1}[Y_q^m]$ for each $[Y_q^m]$. Using (26)-(28) and (56) the matrix H_m has a form given by $H_m = [M_V][X_q^m]_{diag}[M_V]^{-1}$. To identify the distinct modal delays obtained from the electrical delays of the first-order reflection terms, n linearly independent set of algebraic equations in terms of these modal delays are required. This condition is mathematically equivalent to completeness of matrices $[X_q^m]_{diag}$ over the field of n dimensional real diagonal matrices.

The above requirement translates into the **second necessary condition** given by,

- For a given UMCL $2n$-port system (with distinct modal delays) all the modal delays can be identified from the reflection data if n distinct orthogonal matrices E_i' can be generated from the matrices, $H_m = [Y_o]^{-1}[Y_q^m][Y_o]^{-1}[Y_q^m]$, $(m = 1, \cdots nj)$ using the procedure described in section-(4.7.4).

Necessary condition: for modal voltage eigenvectors:

Let F be the matrix formed from the linear combination of pj orthogonal matrices E_i' generated from the matrices, H_m, using the procedure described in section-(4.7.4) as

$$\begin{aligned}[F] &= \sum_{\text{k=1}}^{pj} b_k E_k', b_k \in R \\ &= [G_V][\eta]_{diag}[G_V]^{-1}. \end{aligned} \tag{4.62}$$

such that it has maximum number of distinct eigenvalues. The **necessary condition** for extraction for modal voltage eigenvector matrix is:

- The number of distinct eigenvalues of F should be equal to n. The eigenvector matrix, $[G_V]$, is then the modal voltage eigenvector matrix, $[M_V]$, of the given UMCL $2n$-port system with n distinct modal delays.

It is to be noted that matrix F with n distinct eigenvalues will always exist if the matrices, $[X_q^m]_{diag}$, $(m = 1, \cdots nj)$ are complete. Therefore the **the necessary and sufficiency condition** of the identification of all the normal-mode parameters of a given UMCL $2n$-port system with n distinct modal delays is:

For a given UMCL $2n$-port system (with distinct modal delays) all the normal-mode parameters can be identified from the reflection data if n distinct orthogonal matrices E_i' can be generated from the matrices, $H_m = [Y_o]^{-1}[Y_q^m][Y_o]^{-1}[Y_q^m]$, $(m = 1, \cdots nj)$ using the procedure (test for completeness) described in section-(4.7.4).

4.8 COMMENTS

A synthesis procedure based on the identification of all the normal-mode parameters of a lossless uniform n multiconductor coupled lines $2n$-port system in an inhomogeneous medium from the reflection response is presented. The necessary and sufficiency conditions for the identification of all the normal-mode parameters from the reflection data are derived and the equivalence between the synthesis procedure presented in this chapter and the solution of special case of polynomial matrix Riccati equation has been established. This procedure establishes a basic framework for the development of multi-dimensional deconvolution techniques for a general lossless non-uniform multiconductor transmission lines structures similar to the already existing deconvolution techniques for a non-uniform transmission line system (Peeling or layer-stripping Algorithm [8], [10], [11], [12] and for the design of general multi-dimensional digital filters.

Chapter 5
ANALYSIS OF MULTILAYER MULTILEVEL MIS TRANSMISSION LINE STRUCTURE

5.1 INTRODUCTION

Modeling of multilayer MIS transmission line structure using quasi-static techniques is a preferable approach for CAD-oriented simulation tools where computational efficiency is of prime concern. In such tools accuracy as well as the range of validity of extracted parameters with the input data are also important. In this chapter, we propose the network analog method [19], [107] as a simple and accurate approach for modeling and design of transmission lines in lossy multi-dielectric layers with multilevel metallization type of substrate environment, particularly applicable to MIS based transmission lines structure.

The proposed approach is based on the solution of magnetic vector potential equation with the magneto-static approximations. This quasi-static formulation based on the network analog approach leads to a computationally efficient and accurate alternative CAD-oriented tool for the design of high performance RF and digital IC's. Moreover, unlike the earlier quasi-static formulations [103], [104], [107], it is demonstrated that the n propagating modes of n coupled lines whose propagation characteristics can be classified into the category of quasi-TEM, slow-wave and the skin-effect modes can all be modeled using this quasi-static method [106]. An efficient diagonalization procedure similar to that presented in [19], [107] which reduces the two-dimensional MIS structure into one-dimensional equivalent structure is shown. Using this diagonalization procedure the expressions for the elements of the impedance matrix can be computed efficiently. It is also shown that the calculated frequency dependent distributed transmission line parameters accurately model the propagation and the impedance characteristics of transmission lines embedded in a multilayer lossy substrate over a wide range of parameter values including the frequency and loss tangents ($\tan\delta$) of the dielectric layers.

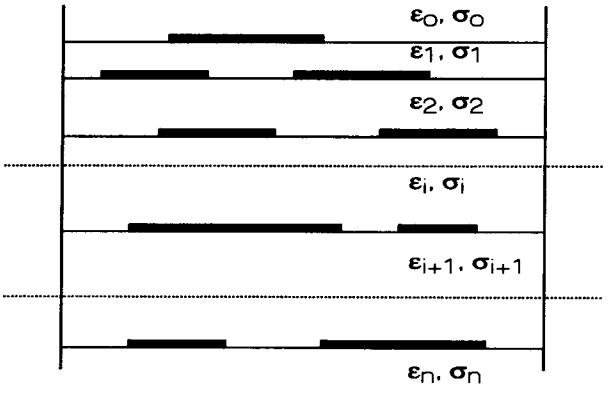

Figure 5.1. A general multilayer multilevel transmission line structure. Here the transmission lines are embedded in the lossy dielectric layers.

Several typical MIS based transmission line structures are analyzed using the network analog approach to illustrate the versatility and the accuracy of the proposed method.

5.2 FORMULATION

A typical multilayer MIS transmission line structure is depicted in Fig. 5.1 and has stacked lossy/lossless dielectric layers with the metallization layers embedded in between them. In case of CMOS based MIS transmission line structure, the lowest layer is made up of highly doped silicon and all the other layers consists of oxide and metallization levels (ref: Fig. 2.5). The magneto-static field equations for the multilayer MIS transmission line structure (for the structure shown in Fig. 5.1) are given by,

$$\nabla \times \vec{B} = \mu_o \vec{J}, \quad \nabla \times \vec{A} = \vec{B}$$
$$\text{and} \quad \vec{J} = \sigma \vec{E} = j\omega\sigma \vec{A} \tag{5.1}$$

subjected to the boundary conditions that the normal and the tangential components of magnetic field, $\vec{B}$, are continuous across the dielectric interface. In a case, when an infinitesimal thin conductors are present in between the dielectric interface layers, the tangential components of, $\vec{B}$, are discontinuous and are related to the surface current density, $\vec{J}_s$,

$$(\hat{n} \times \vec{B})_{interface} = \mu_o \vec{J}_s. \tag{5.2}$$

Here, $\vec{A}$, represents the vector magnetic potential, $\vec{E}$, denotes the electric field, σ, is the conductivity of the media, ω, is the frequency and $\hat{n}$ is a unit vector normal to the infinitesimal thin conductor at the dielectric interface.

Assuming that the surface currents on the strip ($J_{is}\hat{e}_z$) only exists in the z direction and does not change rapidly with time, the magnetic vector potential, $A_i(x,y)\hat{e}_z$, in a lossy dielectric region (μ_o, σ_i) satisfies (ref. Fig. 5.1),

$$\nabla^2 A_i(x,y)\hat{e}_z = j\omega\mu_o\sigma_i A_i(x,y)\hat{e}_z. \tag{5.3}$$

Here, σ_i, is the conductivity of the ith dielectric layer, μ_o, is the permeability of free space, and, ω, is the angular frequency. The boundary conditions for the magnetic vector potential at the dielectric interfaces are

$$\frac{\partial A_{i+1}(x,y)}{\partial y} - \frac{\partial A_i(x,y)}{\partial y} = \begin{cases} \mu_o J_{is} & \text{on the strip} \\ 0 & \text{otherwise} \end{cases}, \tag{5.4}$$

$$\frac{\partial A_{i+1}(x,y)}{\partial x} - \frac{\partial A_i(x,y)}{\partial x} = 0 \tag{5.5}$$

and

$$\frac{\partial A_i(x, y = y_i)}{\partial x} = 0 \tag{5.6}$$

on the perfectly conducting strip. Here y_i is the y-axis coordinate of the dielectric interface layer on which the infinitesimally thin strip is located. Using the finite difference formulation to approximate the Laplacian operator, (3) in the ith layer can be expressed

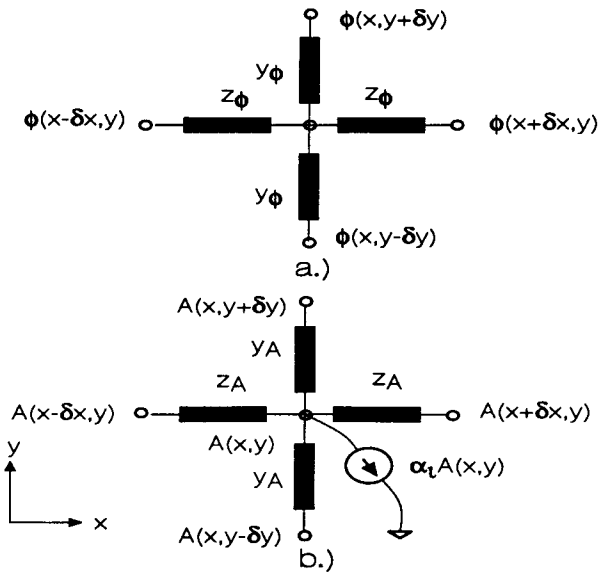

Figure 5.2. The network analog equivalent corresponding to Laplace potential equation. (b.) The network analog equivalent corresponding to magnetic vector potential equation given by (7).

as

$$\frac{A_i(x+\triangle x,y)+A_i(x-\triangle x,y)-2A_i(x,y)}{\triangle x^2}+ \frac{A_i(x,y+\triangle y)+A_i(x,y-\triangle y)-2A_i(x,y)}{\triangle y^2} = j\mu_o\sigma_i\omega A_i(x,y)=\alpha_i A_i(x,y) \tag{5.7}$$

with the boundary condition given by

$$\frac{A_i(x+\triangle x,y)-A_i(x,y)}{\triangle x} \quad \text{and} \quad \frac{A_i(x,y+\triangle y)-A_i(x,y)}{\triangle y} \tag{5.8}$$

are continuous. Combining (7) and (8) with the finite difference approximation of equations (5) and (6) leads to a two dimensional discrete equivalent electrical network analog having branches consisting of resistances and voltage controlled current sources at the nodes to account for the term on the R.H.S of (5). These voltage controlled current sources model the frequency dependent longitudinal substrate current flowing in the

lossy substrate. The solution for magnetic potential, $A_i(x,y)$, and the surface current density, J_{is}, at the conductor surface is represented in terms of node voltages and currents in the equivalent two dimensional discrete electrical network analog. Fig. 5.2 illustrates the network analog equivalent circuit corresponding to the magnetic vector potential equation given by (7). By enforcing the boundary condition given in (4) on the strip (i.e., a constant vector potential, $A(x, y = y_i) = 1$: on the nodes where strip is present), the current flowing in the strip (into the nodes where the strip is present) is determined and the frequency dependent distributed inductive and resistive line parameters are obtained. For example, the expression for the distributed inductance, $L(\omega)$, and resistance, $R(\omega)$, for a single MIS microstrip transmission line system is (given: $\triangle x = \triangle y$),

$$R(\omega) + j\omega L(\omega) = \frac{j\omega\mu_o}{\sum_{i=1}^{N} I^i_{node}} ohms/m, \tag{5.9}$$

where N is number of nodes where the strip is present.

5.3 THE DIAGONALIZATION PROCEDURE

The impedance matrix, $[Z]$, associated with the nodes at any interface can be found in an efficient manner by following a similar diagonalization procedure as given in [107]. Neglecting the details, here the final expressions for the impedance matrix, $[Z]$, using the diagonalization procedure, for both, the single and multilevel metallization MIS transmission lines structure are presented.

5.3.1 Single Level Metallization

In case of single level metallization, the impedance matrix relates the n_c nodes voltage and the associated node currents. Here, n_c, represents the number of columns in the discretization scheme. It is to be noted that the complex substrate currents are already included in the impedance matrix. This impedance matrix, $[Z]_{n_c \times n_c}$, can be diagonalized into a diagonal matrix system, $[\widehat{Z}]_{n_c \times n_c}$, using a involutary matrix, $[P]$,

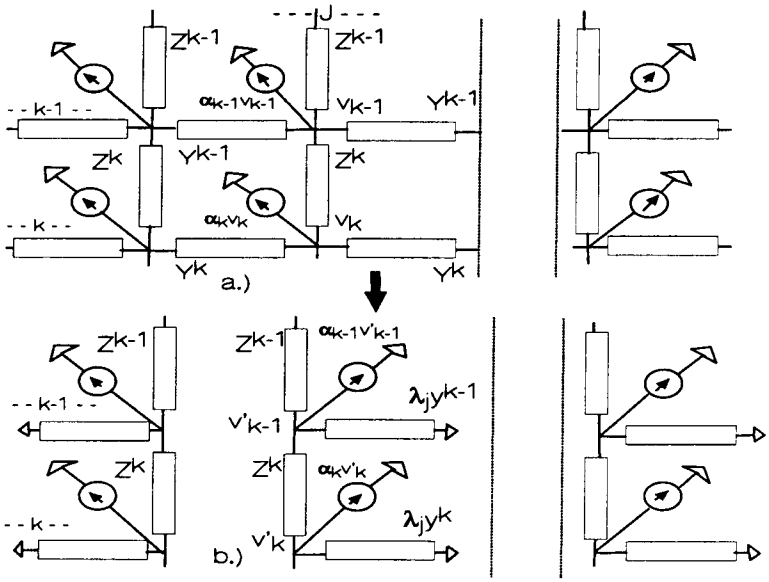

Figure 5.3. The discrete network analog and the algebraically equivalent transformed network after diagonalization.

identical to that given in [107]. Figure 5.3 shows the discrete analog network and the associated algebraically equivalent transformed network after the diagonalization process. The elements of matrix, $[P]$, are given by

$$P(i,j) = \sqrt{\frac{2}{n_c+1}} \sin\left(\frac{ij\pi}{n_c+1}\right), \quad i \text{ and } j = 1, 2, ..., n_c. \tag{5.10}$$

Likewise, the elements of diagonal matrix system, $[\hat{Z}]_{n_c \times n_c}$, at level L are

$$\hat{Z}_j^L = \frac{1}{\frac{1}{(\alpha_u^L)_j} + \frac{1}{(\alpha_l^L)_j} + \lambda_j \frac{y^{L-1}+y^{L+1}}{2} - \frac{\alpha_{L-1}+\alpha_{L+1}}{2}}, \quad j = 1, 2, ..., n_c \tag{5.11}$$

with

$$(\alpha_{u,l}^{k+1})_j = \frac{1}{\frac{1}{(\alpha_{u,l}^k)_j} + \lambda_j y^k - \alpha_k} + z^{k+1},$$

$$(\alpha_{u,l}^1) = z_{u,l}^1,$$

and

$$\lambda_j = 4\sin^2\left(\frac{j\pi}{2(n_c+1)}\right),\ j = 1, 2, ..., n_c. \tag{5.12}$$

Here, α_k is the coefficient of voltage controlled current source at the kth level nodes (ref. eqn. 7), $z^1_{u,l}$ is the impedance associated with the first level from upper (u) and lower (l) side and λ_j is the eigenvalues of the connection matrix in [107]. For an open structures (structures without a ground plane), (11) leads to

$$(\alpha_{u,l})_j = \frac{z}{2}\left\{1 + \sqrt{1 + \frac{4}{z(\lambda_j y - \alpha)}}\right\} \tag{5.13}$$

where z, y and α are the impedance, admittance and the coefficient of voltage controlled current source are the elements of the network in upper and lower open regions respectively.

5.3.2 Multilevel Metallization

Similarly, in case of multilayer multilevel structure the impedance matrix is [107]

$$[z] = \begin{bmatrix} [z]_{11} & [z]_{12} & . & [z]_{1p} \\ [z]_{21} & [z]_{22} & . & [z]_{2p} \\ . & . & . & . \\ [z]_{p1} & [z]_{p2} & . & [z]_{pp} \end{bmatrix}_{pn_c \times pn_c} \tag{5.14}$$

where p is the number of level where metallization exists. The self impedance terms, $[z]_{ii}$, are evaluated by using (11)-(13). The expression for the elements of transfer impedance matrix, $[\hat{z}]_{km}$, in an algebraically equivalent diagonalized domain relating voltage at node at level k to another node at level m in column j are [107],

$$\hat{Z}_{km}(j,j) = \left\{\frac{1}{\frac{1}{(\alpha_u^k)_j} + \lambda_j y^k - \alpha_k}\right\} \left\{\frac{\frac{1}{(\alpha_u^m)_j}}{\frac{1}{(\alpha_u^m)_j} + \frac{1}{(\alpha_l^m)_j} + \lambda_j \frac{y^{m-1}+y^{m+1}}{2} - \frac{\alpha_{m-1}+\alpha_{m+1}}{2}}\right\} \Pi_{q=m+sgn(k-m)}^{q=k-sgn(k-m)} \frac{\frac{1}{(\alpha_u^q)_j}}{\frac{1}{(\alpha_u^q)_j} + \lambda_j y^q - \alpha_q} \tag{5.15}$$

with

$$[z]_{km} = [p][\widehat{z}_{km}][p]. \tag{5.16}$$

Enforcing the boundary conditions on the strips that on the surface of infinitesimal thin strip the magnetic vector potential, A, are constant (i.e. the voltage on the nodes where the strip is located is constant) the currents flowing into the nodes are solved. The inductance matrix is obtained from the evaluated currents flowing into the strip and the magnetic potentials on the surface of infinitesimal thin strip.

5.4 RESULTS

In this section, few popular and useful transmission line structures frequently used in the microwave and interconnect applications are analyzed to demonstrate the accuracy and the versatility of the proposed approach. The typical structures considered here are the microstrip line, coplanar stripline, multilevel stripline, coupled coplanar microstrip lines and the broad-side coupled microstrip lines.

5.4.1 Line Parameters of a MIS Microstrip Line Structure

A MIS microstrip line structure similar to that in [91] is simulated using the network analog method based on the magnetic vector potential equation. Figure 5.4 shows the variation of the frequency dependent distributed line impedance $Z(\omega) = R(\omega) + j\omega L(\omega)$ as a function of the loss tangent of layer 1 ($\tan\delta_1$). The corresponding frequency dependent distributed line admittance $Y(\omega) = G(\omega) + j\omega C(\omega)$ as a function of $\tan\delta_1$ is obtained from the network analog method based on the electric potential equation [107] and is shown in Fig. 5.5. It is seen in Fig. 5.4 and Fig. 5.5 that the imaginary parts of $Z(\omega)$ and $Y(\omega)$ have a step type of response. However, the step transitions occur at different values of $\tan\delta_1$, hence, giving rise to the three mode regions: quasi-TEM, slow-wave, and skin-effect mode. Moreover, it is also observed that the transition from the quasi-TEM to slow-wave mode is due to the change in the imaginary

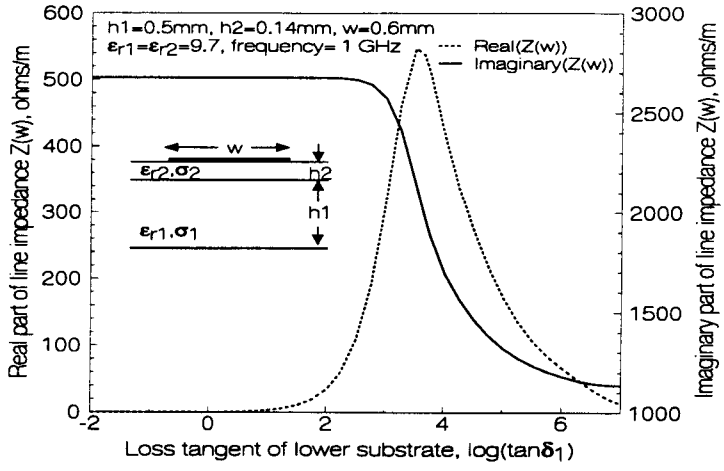

Figure 5.4. Line impedance parameter $Z(\omega)$ $(= R(\omega) + j\omega L(\omega))$ as a function of loss tangent of lower substrate, $\tan\delta_1$ $(\sigma_2 = 0)$.

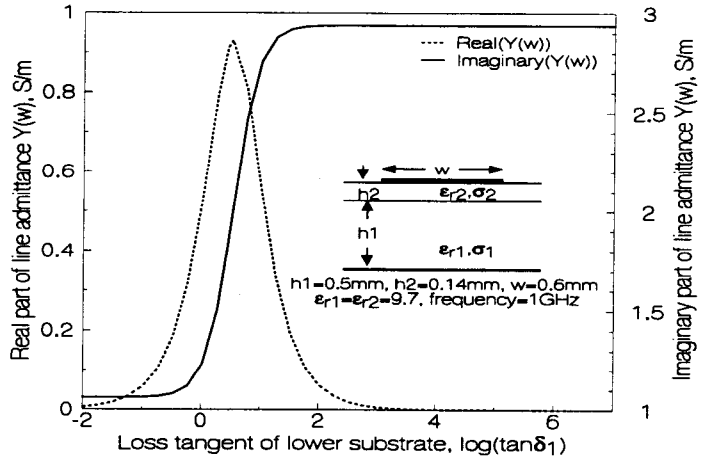

Figure 5.5. Line admittance parameter $Y(\omega)$ $(= G(\omega) + j\omega C(\omega))$ as a function of loss tangent of lower substrate, $\tan\delta_1$ $(\sigma_2 = 0)$.

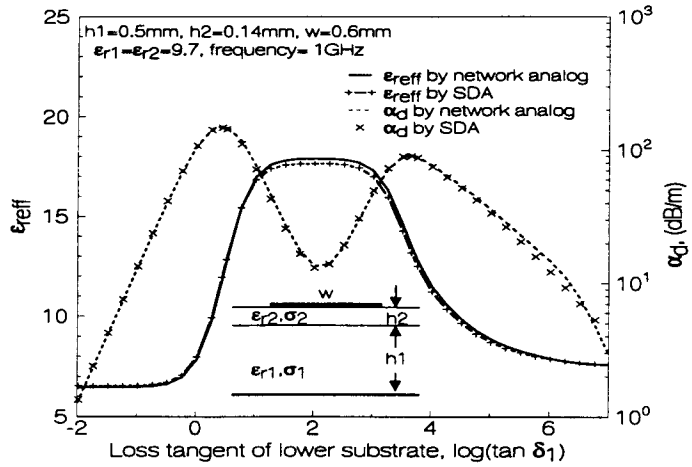

Figure 5.6. ϵ_{reff} and α_d as a function of loss tangent of the lower substrate, $\tan\delta_1$ ($\sigma_2 = 0$).

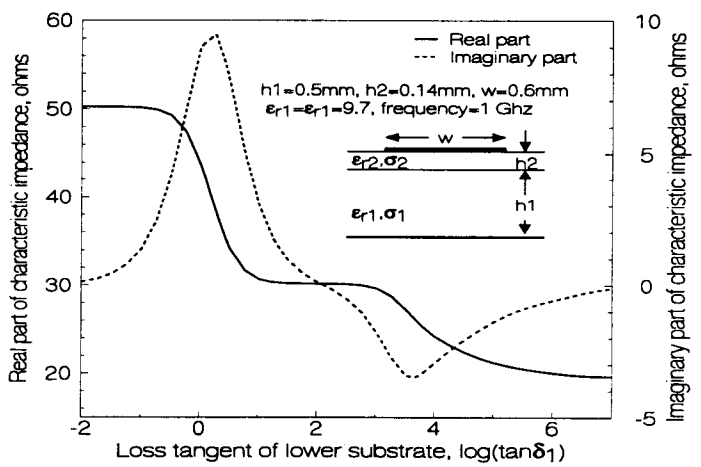

Figure 5.7. Characteristic impedance of the line as a function of loss tangent of the lower substrate, $\tan\delta_1$ ($\sigma_2 = 0$).

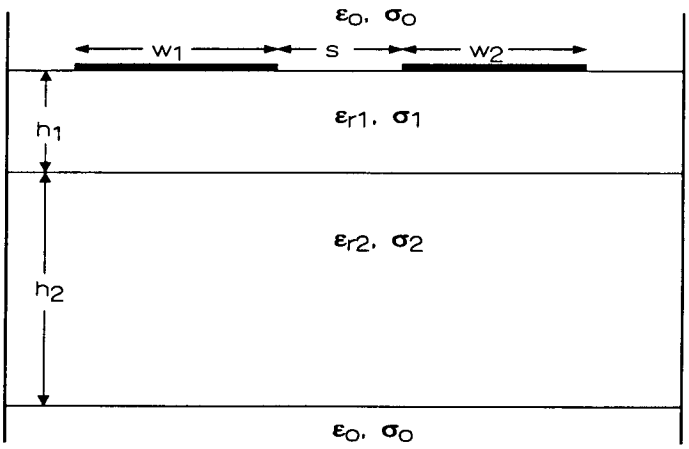

Figure 5.8. A typical MIS based coplanar stripline structure. ($h_1 = 10\mu m$, $h_2 = 200\mu m$, $w_1 = 10\mu m$, $w_2 = 20\mu m$, $s = 10\mu m$, $\epsilon_0 = 1.0$, $\epsilon_{r1} = 3.9$, $\epsilon_{r2} = 9.7$, $\sigma_0 = 0$, $\sigma_1 = 0$).

part of $Y(\omega)$, and in this region the dominant losses are due to the shunt substrate current. Similarly, the transition from the slow-wave mode to the skin-effect mode is due to the change in the imaginary part of $Z(\omega)$, which is in the region where the dominant losses are due to the longitudinal substrate current. Figure 5.6 shows the change in effective dielectric constant, ϵ_{reff}, and attenuation constant, α_d, obtained from the above computed transmission line parameters as a function of $\tan\delta_1$. They are found to be in good agreement with the results of a full-wave Spectral Domain Approach [91]. Figure 5.7 shows the change in the line characteristic impedance obtained from the above transmission line parameters as a function of $\tan\delta_1$. For a lossless case the series transmission line parameter, $Z(\omega)$, of the MIS structure does not depends on the dielectric constant of the dielectric layers. Likewise, in case of lossy substrates the series transmission line parameter, $Z(\omega)$, is also not dependent on the dielectric constant of the dielectric layers but change significantly with the dielectric losses.

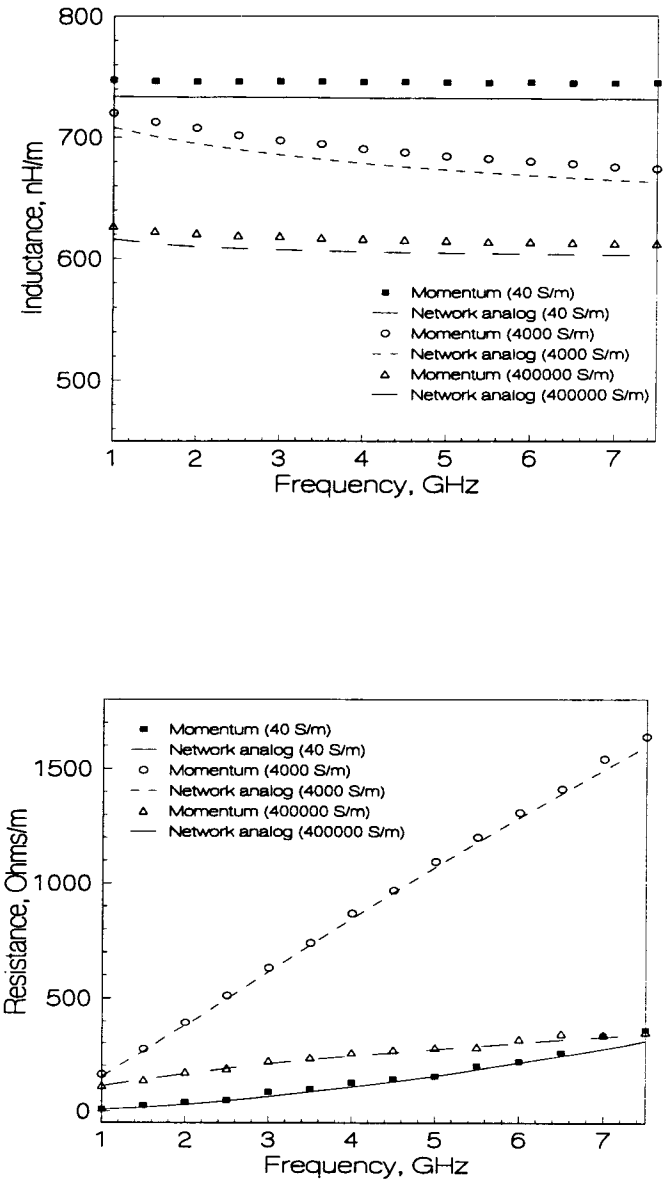

Figure 5.9. The inductive and the resistive transmission line parameters as a function of frequency for different conductivity, σ_2, of the lower Si substrate layer of the structure shown in Fig. 5.8.

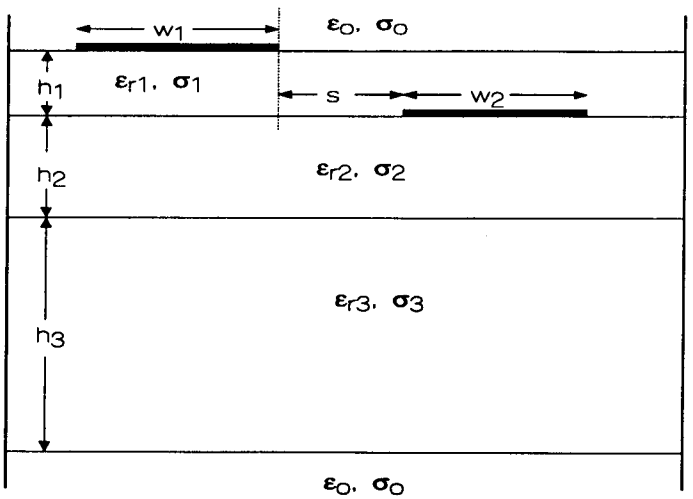

a.)

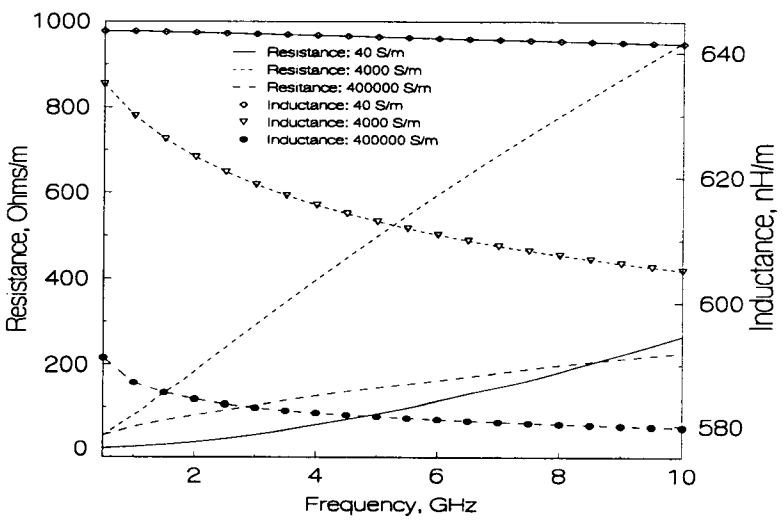

b.)

Figure 5.10. A typical MIS based broad-side stripline structure. (b.) The inductive and the resistive transmission line parameters as a function of frequency for different conductivity, σ_3, of the lower Si substrate layer. ($h_1 = 10\mu m$, $h_2 = 10\mu m$, $h_3 = 200\mu m$, $w_1 = 20\mu m$, $w_2 = 10\mu m$, $s = 3\mu m$, $\epsilon_0 = 1.0$, $\epsilon_{r1} = 3.9$, $\epsilon_{r2} = 3.9$, $\epsilon_{r3} = 9.7$, $\sigma_0 = 0$, $\sigma_1 = 0$, $\sigma_2 = 0$).

5.4.2 Line Parameters of a MIS Based Stripline Structure

An example of MIS based coplanar (ref: Fig. 5.8) and broad-side stripline (ref: Fig. 5.10) structures on $Si - SiO_2$ substrate (for CMOS applications) are analyzed using the proposed approach. Here initially the series line impedance matrix of striplines with respect to the metallic side walls (as a reference) is first evaluated by the network analog approach and is given by,

$$\begin{aligned} v_1 &= (R_{11}(\omega) + j\omega L_{11}(\omega))i_1 + (R_{12}(\omega) + j\omega L_{12}(\omega))i_2 \\ v_2 &= (R_{12}(\omega) + j\omega L_{12}(\omega))i_1 + (R_{22}(\omega) + j\omega L_{22}(\omega))i_2 \end{aligned} \tag{5.17}$$

Later, by enforcing the condition on the resulting impedance matrix that the same current flows on both of the metallic strips, however, the currents have opposite direction leads to the frequency dependent inductive and resistive (series) transmission line parameters associated with the stripline structure. The effects of the lossy substrate and metallic side walls are included in the formulation. Using (17), the expression for the frequency dependent resistance is given by,

$$R(\omega) = R_{11}(\omega) + R_{22}(\omega) - 2R_{12}(\omega). \tag{5.18}$$

Similarly, the expression for the inductance is

$$L(\omega) = L_{11}(\omega) + L_{22}(\omega) - 2L_{12}(\omega). \tag{5.19}$$

In Fig. 5.9 the frequency dependent resistive and inductive transmission line parameters of coplanar stripline structure (shown in Fig. 5.8) are evaluated for different conductivity of Si layer. The obtained values are compared with the results evaluated via a full-wave simulator (HP EEsof: Momentum). These two simulation results are found to be in good agreement. Similarly, the frequency dependent resistive and inductive transmission line parameters of broad-side stripline structure obtained from network analog approach are shown in Fig. 5.10.

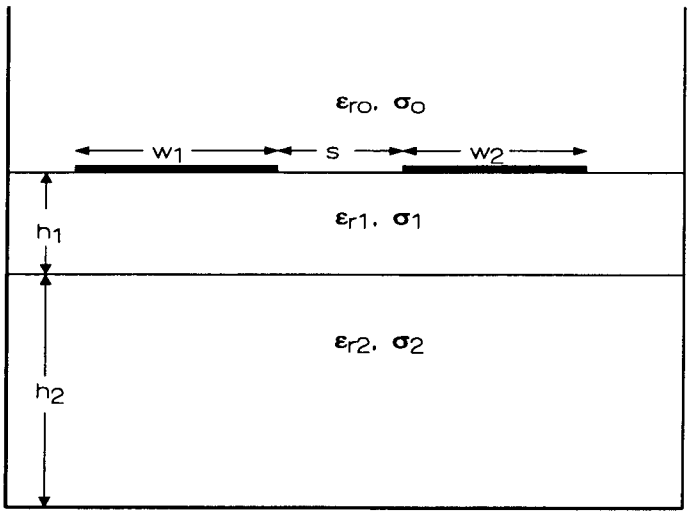

Figure 5.11. A typical MIS based coplanar coupled microstrip line structure. ($h_1 = 10\mu m$, $h_2 = 200\mu m$, $w_1 = 10\mu m$, $w_2 = 20\mu m$, $s = 10\mu m$, $\epsilon_{r0} = 1.0$, $\epsilon_{r1} = 3.9$, $\epsilon_{r2} = 9.7$, $\sigma_0 = 0$, $\sigma_1 = 0$).

5.4.3 Line Parameters of a MIS Based Coupled Microstrip Line Structure

The MIS based coupled microstrip line structure is analyzed using the network analog method proposed in this chapter. In Fig. 5.11, a typical MIS based coplanar coupled microstrip line structure is illustrated. Figure 5.12 shows the obtained frequency dependent elements of resistive and inductive matrices for different conductivity (σ_2) of Si substrate layer (ref: Fig. 5.11). Similarly, in Fig. 5.13, a typical MIS based broad-side coupled microstrip line structure is illustrated and Fig. 5.14 shows the obtained frequency dependent elements of resistive and inductive matrices for different conductivity (σ_2) of Si substrate layer. It is observed that in case of low conductivity ($\sigma_2 = 40S/m$) the corresponding modes (c and the π modes) are in general quasi-TEM or slow-wave region and therefore the associated elements of resistive and inductive matrices vary moderately with change in frequency. In the case of moderate conductivity ($\sigma_2 = 4000S/m$), the associated modes can lie in the transition region (from slow-wave to skin-effect region) and therefore the elements of the resistive and inductive matrices

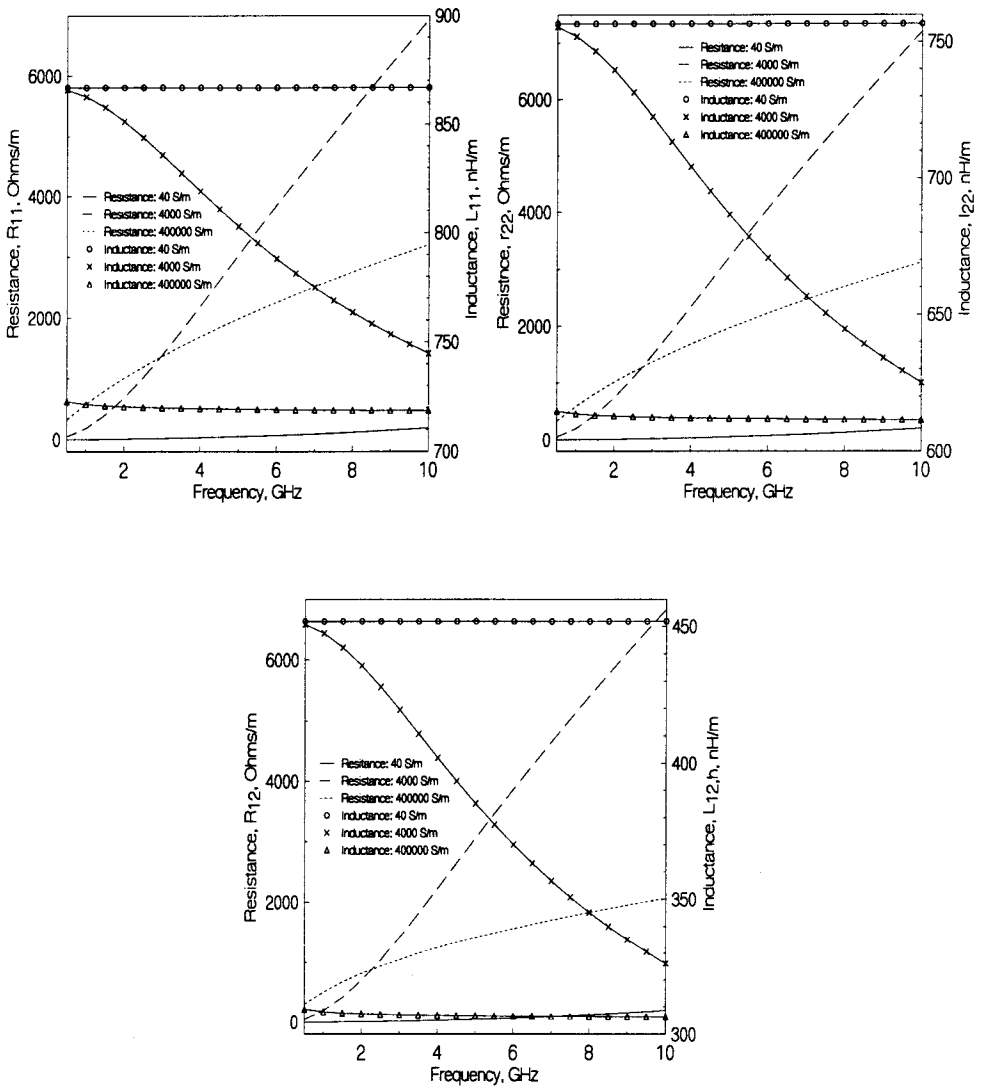

Figure 5.12. The inductive and the resistive transmission line matrix parameters as a function of frequency for different conductivity, σ_2, of the lower Si substrate layer of the structure shown in Fig. 5.11.

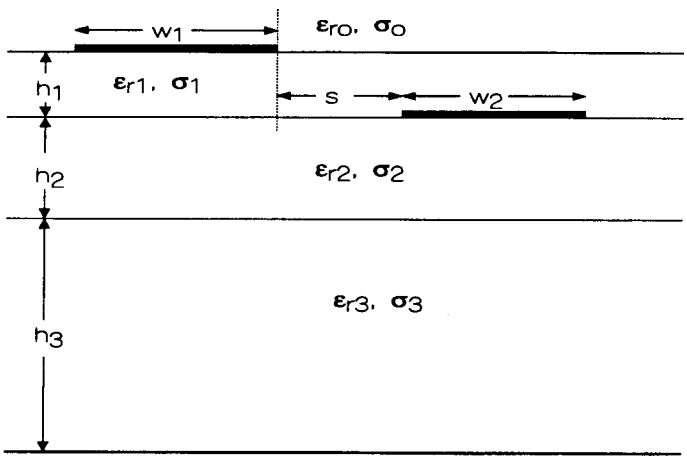

Figure 5.13. A typical MIS based broad-side coupled microstrip line structure. ($h_1 = 10\mu m$, $h_2 = 10\mu m$, $h_3 = 200\mu m$, $w_1 = 20\mu m$, $w_2 = 10\mu m$, $s = 3\mu m$, $\epsilon_{r0} = 1.0$, $\epsilon_{r1} = 3.9$, $\epsilon_{r2} = 3.9$, $\epsilon_{r3} = 9.7$, $\sigma_0 = 0$, $\sigma_1 = 0$, $\sigma_2 = 0$).

can change significantly with change in frequency. For a very high substrate conductivity ($\sigma_2 = 400000 S/m$), the modes are in the skin-effect region and thereby the elements of resistive and inductive matrices do not change significantly with change in frequency. It is also observed that the magnitude of elements of inductance matrix monotonically decrease with increase in the frequency. Moreover, the magnitude of the elements of inductance matrix are at maxima when the conductivity of the Si substrate layer is zero and the modes are in quasi-TEM region. Similarly, the magnitude of the elements of inductance matrix are at minima when the conductivity of Si substrate layer is infinite such that the modes are in the skin-effect region. In case of resistive matrix, the elements attains their maximum value when the associated modes lie somewhere in the slow-wave to skin-effect transition region.

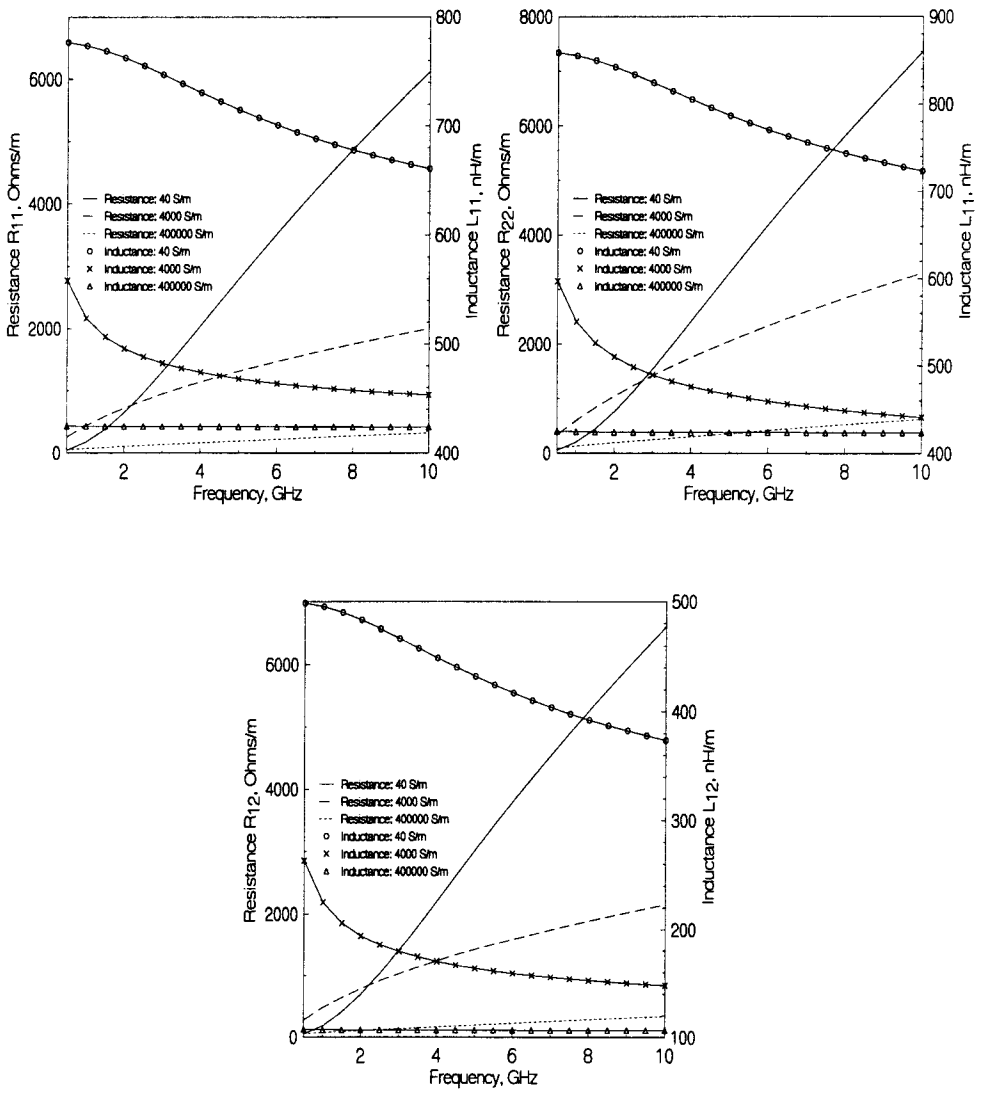

Figure 5.14. The inductive and the resistive transmission line matrix parameters as a function of frequency for different conductivity, σ_2, of the lower Si substrate layer of the structure shown in Fig. 5.13.

5.5 COMMENTS

A network analog method for evaluating distributed inductance and resistance values of a transmission lines associated with the skin-effect mode embedded in a multilayer lossy dielectric substrate has been presented. It has been shown that, when combined with the earlier network analog method for calculating capacitance and conductance, the quasi-static method presented here, accurately models the propagation and impedance characteristics of MIS transmission lines associated with the three mode regions: quasi-TEM, slow-wave, and skin-effect mode. The proposed method is a general one and is applicable to multilevel, multilayer structures including GaAs based MMIC's and silicon based biCMOS and CMOS RFIC's.

Chapter 6
CONCLUSION AND FUTURE WORK

A configuration-oriented equivalent circuit model has been proposed for modeling uniform multiconductor transmission lines (UMCL) system in a homogeneous/ inhomogeneous medium. This model consists of only uncoupled transmission lines and is general enough to include the case of lossy dispersive UMCL system. Moreover, all the earlier models based on the uncoupled transmission lines, proposed in the literature for special cases of UMCL systems, can be derived from the proposed configuration-oriented equivalent circuit model [2], [119]. The model is useful for time- and frequency- domain simulations of interconnects and coupled line components fabricated in the layered structures. Such structures, consists of multi-dielectric layers and multilevel metallization planes, and are typically encountered in high speed digital and RF integrated circuits and printed-circuit boards for mixed-signal applications. Additionally, a general UMCL system can be represented in terms of uncoupled transmission lines and therefore several different formulation and results applicable to single transmission line system can now be possibly extended to the case of UMCL systems. This remains an area for future investigation.

A UMCL $2n$-port system in a homogeneous media, in general, can be fully characterized by the characteristic admittance matrix and the modal delay. Similarly, UMCL $2n$-port system in an inhomogeneous media is fully characterized by normal-mode parameters [13], [14] or by set of n unique symmetric matrices and the respective modal delays associated with these matrices. These matrices are derived and defined as the partial mode admittance matrices. A resistive network corresponding to the characteristic admittance matrix when used as a termination network provides a match condition for all the modes. Likewise, a resistive network corresponding to the partial mode admittance matrix associated with mth mode when used as termination network reflects (reflection coefficient is assumed to be unity) all other modes except the mth mode for which it provides a match condition. Furthermore, it has been demonstrated that the

characteristic admittance matrix of a general UMCL can be represented as a sum of partial mode admittance matrices [4]. The derivation of configuration-oriented model is based on the existence of symmetric partial mode admittance matrices. It is shown that the property of symmetry in the partial mode admittance matrices can be attributed to the inherent symmetric structure of lines matrices, $[R(\omega)]$, $[L(\omega)]$, $[G(\omega)]$ and $[C(\omega)]$ in the coupled transmission line equations [4].

The decomposition scheme for the characteristic admittance matrix as a sum of partial mode admittance matrices can lead to an equivalent algebraic system which consists of decoupled transmission lines. In the z-domain (discrete Fourier transform domain) the discrete transition matrix function of a single transmission line [8] is utilized for each of these decoupled transmission lines to obtain discrete transition matrix function of a n coupled lines $2n$-port system [115]. This discrete transition matrix function, describes a linear operator which relates the input voltages and currents to the output voltages and currents for a given $2n$ ports of n coupled lines respectively. Furthermore, this operator is shown to be diagonalizable and can therefore be decomposed as a direct-sum of $2n$ linear operators (projectors) with the associated characteristics values. The characteristics values of the operator, in general, are only functions of the modal delays. The $2n$ linear operators (projector) are associated with the n distinct modes. A mode is linked with two linear operators (projector), each of which is associated with the right or left propagating wave corresponding to the respective mode in a n coupled lines $2n$-port system.

Using the discrete transition matrix function, in the z-domain the input impulse admittance matrix (IIAM) function is derived in terms of a rational matrix function. Relationship between the measured discrete time-domain impulse reflection response (IRR), input impulse admittance matrix (IIAM) function and the normal-mode parameters is found. The necessary and sufficiency conditions for the identification of all the normal mode parameters from the reflection data are found for a UMCL $2n$-port system terminated with a resistive network. Also, equivalence between the synthesis procedure presented in this thesis and the solution of special case of polynomial matrix Riccati equation has been established. The general realizability and uniqueness proofs

for UMCL $2n$-port system with inductive and capacitive terminations needs further research [78],[79].

A formulation based on the magneto-static field equations has been proposed for evaluating resistive and inductive transmission line parameters of a multilayer multilevel transmission line 2D-structure. In this formulation, magneto-static field equations with the associated boundary conditions are solved using the network analog approach [107]. Frequency dependent transmission line parameters of several typical planar transmission line structures in a lossy multilayer media (MIS structure) are obtained using the proposed approach. It is found that the network analog approach, a method based on quasi-static approximations, can accurately model the propagation and the electrical characteristics of multilayer MIS transmission line structures with lossy substrates. A typical interconnect encountered in a multilayer multilevel structure is basically a 3D-structure. Future work in modifying the 2D network analog approach [107] to the 3D network approach [19] based on magneto-static field equations can be very useful in addressing the present requirement of handling complex interconnection structures encountered in the digital and RFIC's applications.

BIBLIOGRAPHY

[1] M. A. Larsson, "A new equivalent circuit for the analysis of general coupled n-wire transmission lines," *IEEE Trans. Microwave Theory Tech.*, vol. 39, pp. 1855–1861, Oct. 1991.

[2] K. D. Marx and R. I. Eastin, "A configuration-oriented SPICE model for multiconductor transmission lines with homogeneous dielectrics," *IEEE Trans. Microwave Theory Tech.*, vol. 38, pp. 1123–1129, Aug. 1990.

[3] V. K. Tripathi and J. B. Rettig, "A SPICE model for multiple coupled microstrips and other transmission lines," *IEEE Trans. Microwave Theory Tech.*, vol. 33, pp. 1513–1518, Dec. 1985.

[4] A. Tripathi and V. K. Tripathi, "A configuration-oriented SPICE model for multiconductor transmission lines in an inhomogeneous medium," *IEEE Trans. Microwave Theory Tech.*, vol. 46, pp. 1997–2005, Dec. 1998.

[5] Fatima Masot, *et. al.*, "Analysis and experimental validation of a type of three microstrip directional coupler," *IEEE Trans. Microwave Theory Tech.*, vol. 42, pp. 1624–1631, Sept. 1994.

[6] S. Banba and H. Ogawa, "Multilayer MMIC directional couplers using thin dielectric layers," *IEEE Trans. Microwave Theory Tech.*, vol. 43, pp. 1270–1275, Sept. 1994.

[7] J. L. R. Quirarte and J. P. Starski, "A novel phase shifter," *IEEE Trans. Microwave Theory Tech.*, vol. 14, pp. 9–14, Jan. 1993.

[8] A. M. Bruckstein and T. Kailath, "Inverse scattering for discrete transmission-line models," *SIAM Rev.*, vol. 29, pp. 359–389, Sept. 1987.

[9] A. M. Bruckstein and T. Kailath, "An inverse scattering framework for several problems in signal processing," *IEEE ASSP magazine*, pp. 6–20, Sept. 1987.

[10] J. M. Jong and V. K. Tripathi, "Time domain characterization of interconnect discontinuities in high speed circuits," *IEEE Trans. CHMT*, vol. 15, pp. 497–504, Aug. 1992.

[11] J. M. Jong, *et. al.*, "Time domain characterization of coupled interconnects and discontinuities," *IEEE Intl. Microwaves Symp.*, San Diego CA, pp. 1129–1132, June 1994.

[12] A. E. Yagle and B. C. Levy, "Layer-stripping solutions of multi-dimensional inverse scattering problems," *J. Math Phys.*, pp. 1701–1710, 1986.

[13] V. K. Tripathi, "Asymmetric coupled transmission lines in an inhomogeneous medium," *IEEE Trans. Microwave Theory Tech.*, vol. 25, pp. 734–739, Sept. 1975.

[14] V. K. Tripathi, "On the analysis of symmetrical three-line microstrip circuits," *IEEE Trans. Microwave Theory Tech.*, vol. 25, pp. 726–729, Sept. 1977.

[15] V. K. Tripathi and H. Lee, "Spectral–domain computation of characteristic impedances and multiport parameters of multiple coupled microstrip lines," *IEEE Trans. Microwave Theory Tech.*, vol. 37, pp. 215–221, Jan. 1989.

[16] S. Amari, "Capacitance and inductance matrices of coupled lines from modal powers," *IEEE Trans. Microwave Theory Tech.*, vol. 41, pp. 146–148, Feb. 1993.

[17] G. G. Gentili and M. S. Palma, "A definition and computation of modal characteristic impedance in quasi-TEM coupled transmission lines," *IEEE Trans. Microwave Theory Tech.*, vol. 41, pp. 338–343, Feb. 1995.

[18] Everett G. Farr, *et. al.*, "A frequency dependent coupled-mode analysis of multiconductor microstrip lines with applications to VLSI interconnection problem," *IEEE Trans. Microwave Theory Tech.*, vol. 34, pp. 307–310, Feb. 1986.

[19] V. K. Tripathi and R. J. Bucolo, "Analysis and modeling of multilevel parallel and crossing interconnection lines," *IEEE Trans. Electron Devices*, vol. 34, pp. 650–658, Mar. 1987.

[20] K. D. Marx, "Propagation modes, equivalent circuits and characteristic terminations for multiconductor transmission lines with inhomogeneous dielectrics," *IEEE Trans. Microwave Theory Tech.*, vol. 21, pp. 450–457, July 1973.

[21] Guang-Tsai Lei, *et. al.*, "Examination, clarification, and simplification of modal decoupling method for multiconductor transmission lines," *IEEE Trans. Microwave Theory Tech.*, vol. 43, pp. 2090–2099, Sept. 1995.

[22] E. G. Cristal, "Coupled transmission line directional couplers with coupled lines of unequal characteristic impedances," *IEEE Trans. Microwave Theory Tech.*, vol. 14, pp. 337–346, July 1966.

[23] D. J. Gunton and E. G. Paige, "An analysis of the general asymmetric directional coupler with non-mode converting terminations," *Inst. Elect. Engr. J. Microwaves, Opt. and Accoust.*, vol. 2, no. 1, pp. 31–36, 1978.

[24] Y. K. Chin, "Analysis and applications of multiple coupled line structures in an inhomogeneous medium, "*PhD thesis*, Oregon State University, Corvallis, OR, 1982.

[25] F. Sellberg, "Formulas useful for the synthesis and optimization of general, uniform contra-directional couplers," *IEEE Trans. Microwave Theory Tech.*, vol. 38, pp. 1000–1009, Aug. 1990.

[26] Sifen Luo, *et. al.*, "Finline multiport couplers," *IEEE Trans. Microwave Theory Tech.*, vol. 42, pp. 2208–2215, Dec. 1994.

[27] P. K. Ikalainen and G. L. Matthaei, "Design of broad band dielectric waveguide 3-dB couplers,," *IEEE Trans. Microwave Theory Tech.*, vol. 35, pp. 621–628, July 1987.

[28] P. K. Ikalainen and G. L. Matthaei, "Wide band forward coupling microstrip hybrid with high directivity," *IEEE Trans. Microwave Theory Tech.*, vol. 35, pp. 719–725, Aug. 1987.

[29] Abelardo, "Symmetrical and asymmetrical edge-coupled-line impedance transformers with a prescribed insertion loss design," *IEEE Trans. Microwave Theory Tech.*, vol. 34, pp. 1–7, Jan. 1991.

[30] B. Easter and B. S. Shivashankaran, "Some results on the edge-coupled microstrip section as an impedance transformer," *IEE Int. J. Microwave, Opt. Acoust.*, vol. 3, pp. 63–66, Mar. 1979.

[31] D. Kajfez, *et. al.*, "Asymmetric microstrip DC-blocks with rippled response," *MTT-S, Int. Symp. Dig. (Losangles)*, pp. 301–303, June 1981.

[32] Y. Xu and R. G. Bosisio, "A novel structure of tightly coupled lines for MMIC/ MHMIC coupler and phase shifters," *IEEE Trans. Microwave Theory Tech.*, vol. 45, pp. 1594–1599, Sept. 1985.

[33] R. Schwindt and C. Nguyen, "Spectral domain analysis of three symmetric coupled lines and application to a new band pass filter," *IEEE Trans. Microwave Theory Tech.*, vol. 14, pp. 1183–1189, July 1994.

[34] R. Levy, "New equivalent circuits for inhomogeneous coupled lines with synthesis applications," *IEEE Trans. Microwave Theory Tech.*, vol. 36, pp. 1087–1094, June 1988.

[35] Raghu K. Settaluri, *et. al.*, "Compact multilevel folded coupled line RF couplers," Accepted for publication in: *IEEE MTT-S Int. Microwave Symp. Dig.*, June 1999.

[36] J. K. Glib and C. Balanis, "Asymmetric, multiconductor low-coupling structures for high speed high density digital interconnects," *IEEE Trans. Microwave Theory Tech.*, vol. 39, pp. 2100–2106, Dec. 1991.

[37] R. H. Voelker, "Transposing conductors in signal busses to reduce nearest neighbor crosstalk," *IEEE Trans. Microwave Theory Tech.*, vol. 43, pp. 1095–1099, May 1995.

[38] Shidong He, *et. al.*, "Decoupling between two conductor transmission line," *IEEE Trans. Microwave Theory Tech.*, vol. 41, pp. 53–61, Jan. 1993.

[39] R. Seviora, "Equivalent circuit for parallel conductor arrays," *IEEE Trans. Microwave Theory Tech.*, vol. 16, pp. 875–877, Oct. 1968.

[40] R. Sato and E. G. Cristal, "Simplified analysis of coupled transmission-line networks," *IEEE Trans. Microwave Theory Tech.*, vol. 18, pp. 122–131, Mar. 1970.

[41] E. G. Sato, "Coupled-transmission-line directional couplers with coupled lines of unequal characteristic impedances," *IEEE Trans. Microwave Theory Tech.*, vol. 14, pp. 337–346, July 1966.

[42] A. I. Grayzel, "A useful identity for the analysis of a class of coupled transmission-line structure," *IEEE Trans. Microwave Theory Tech.*, vol. 22, pp. 904–906, Oct. 1974.

[43] F.-Y. Chang, "Transient analysis of lossless coupled transmission lines in inhomogeneous dielectric media," *IEEE Trans. Microwave Theory Tech.*, vol. 18, pp. 616–626, Sept. 1970.

[44] C. R. Paul, "Simple SPICE model for coupled transmission lines," *IEEE Int. Symp. Electromagnetic Compatibility, Seattle, WA*, pp. 2–4, Aug. 1988.

[45] D. G. Swanson, "A novel method for modeling coupling between several microstrip lines in MIC's and MMIC's," *IEEE Trans. Microwave Theory Tech.*, vol. 39, pp. 917–923, June 1991.

[46] C. ming Tsai and K. C. Gupta, "A generalized model for coupled lines and its applications to two-layer planar circuits," *IEEE Trans. Microwave Theory Tech.*, vol. 40, pp. 2190–2199, Dec. 1992.

[47] S. Cheng and M. L. Edwards, "TEM equivalent circuits for quasi-TEM couplers," *IEEE MTT-S Int. Microwave Symp. Dig.*, pp. 387–390, June 1990.

[48] F. Romeo and M. Santomauro, "Time-domain simulation of n coupled transmission lines," *IEEE Trans. Microwave Theory Tech.*, vol. 35, pp. 131–137, Feb. 1987.

[49] V. K. Tripathi, "A dispersion model for coupled microstrips," *IEEE Trans. Microwave Theory Tech.*, vol. 34, pp. 66–71, Jan. 1986.

[50] J. F. H. Branin, "Transient analysis of lossless transmission lines," *IEEE Trans. Microwave Theory Tech.*, vol. 55, pp. 2012–2013, Nov. 1967.

[51] Jose I. Alonso, *et. al.*, "A universal model for lossy and dispersive transmission lines for time-domain CAD of circuits," *IEEE Trans. Microwave Theory Tech.*, vol. 40, pp. 938–947, May 1992.

[52] V. K. Tripathi and A. Hill, "Equivalent circuit modeling of losses and dispersion in single and coupled lines for microwave and millimeter wave integrated circuits," *IEEE Trans. Microwave Theory Tech.*, vol. 36, pp. 256–262, Feb. 1988.

[53] J. R. Brews, "Overshoot-controlled RLC interconnections," *IEEE Trans. Electron Devices*, vol. 38, pp. 76–87, Jan. 1981.

[54] S. Voranantakul and J. L. Prince, "Efficient computation of signal propagation delay with overshoot and undershoot control in VLSI interconnections," *in SRC J., Preprint*, Oct. 1992.

[55] R. C. Frye and H. Z. Chen, "Optimal self-damped lossy transmission line interconnections for multichip modules," *IEEE Trans. Circuits and Syst., part-2*, vol. 39, pp. 765–771, Nov. 1992.

[56] Antonijo R. Djordjevic, *et. al.*, "Analysis of lossy transmission lines with arbitrary nonlinear terminal networks," *IEEE Trans. Microwave Theory Tech.*, vol. 34, pp. 660–666, June 1986.

[57] Antonijo R. Djordjevic, *et. al.*, "Time-domain response of multiconductor transmission lines lossy transmission lines with arbitrary nonlinear terminal networks," *Proc. IEEE.*, vol. 75, pp. 743–764, June 1987.

[58] F.-Y. Chang, "Waveform relaxation analysis of nonuniform lossy transmission lines characterized with frequency-dependent parameters," *IEEE Trans. Circuits System*, vol. 38, pp. 1484–1500, Dec. 1991.

[59] F.-Y. Chang, "The generalized method of characteristics for waveform relaxation analysis of lossy coupled transmission lines," *IEEE Trans. Microwave Theory Tech.*, vol. 37, pp. 2028–2038, Dec. 1989.

[60] N. Orhanovic, *et. al.*, "Generalized method of characteristics for time-domain simulation of multiconductor lossy transmission lines," *Proc. IEEE Symp. Circuits System*, May 1990.

[61] J. E. Schutt-Aine and R. Mittra, "Scattering parameter transient analysis of transmission lines loaded with nonlinear termination," *IEEE Trans. Microwave Theory Tech.*, vol. 36, pp. 529–536, Mar. 1988.

[62] J. E. Schutt-Aine and R. Mittra, "Nonlinear transient analysis of a lossy transmission lines," *IEEE Trans. Circuits System*, vol. 36, July 1989.

[63] J. R. Griffith and M. S. Nakhla, "Time-domain analysis of lossy coupled transmission lines," *IEEE Trans. Microwave Theory Tech.*, vol. 38, pp. 1480–1487, June 1990.

[64] L. Lu, "A resetting algorithm for transient analysis of coupled transmission line circuits," *IEEE Trans. Microwave Theory Tech.*, vol. 42, pp. 494–500, Mar. 1994.

[65] K. S. Oh and J. C. Schutt-Aine, "Transient analysis of coupled tapered transmission line with arbitrary nonlinear termination," *IEEE Trans. Microwave Theory Tech.*, vol. 41, pp. 168–273, Feb. 1993.

[66] L. T. Pillage and A. Rohrer, "Asymptotic waveform evaluation for timing analysis," *IEEE Trans. Computer-Aided-Design*, vol. 9, pp. 352–366, Apr. 1990.

[67] T. K. Tang, *et. al.*, "Analysis of lossy multiconductor transmission lines using asymptotic waveform evaluation technique," *IEEE Trans. Microwave Theory Tech.*, vol. 39, pp. 2107–2116, Dec. 1991.

[68] J. E. Bracken, *et. al.*, "Interconnect simulation with asymptotic waveform evaluation (AWE)," *IEEE Trans. Circuits System*, vol. 39, pp. 869–878, Nov. 1992.

[69] M. Celik, *et. al.*, "An all-purpose transmission-line model for interconnect simulation in SPICE," *IEEE Trans. Microwave Theory Tech.*, vol. 45, pp. 1857–1867, Oct. 1997.

[70] R. Sanaie, "A fast method for frequency and time-domain simulation of high speed VLSI interconnects," *IEEE Trans. Microwave Theory Tech.*, vol. 42, pp. 2562–2571, Dec. 1994.

[71] J.-F. Mao and Z.-F. Li, "Analysis of the time response of multiconductor transmission lines with frequency-dependent losses by the method of convolution characteristics," *IEEE Trans. Microwave Theory Tech.*, vol. 40, pp. 637–644, Apr. 1992.

[72] O. A. Palusinki and A. Lee, "Analysis of transients in nonuniform and uniform multiconductor transmission lines," *IEEE Trans. Microwave Theory Tech.*, vol. 37, pp. 127–138, Jan. 1989.

[73] M. Celik, *et. al.*, "Pole-zero computation in microwave circuits using multi-point Pade approximation," *IEEE Trans. Circuits and System, part-1*, vol. 42, pp. 6–13, Jan. 1995.

[74] M. Celik and A. C. Cangellaris, "Simulation of dispersive multiconductor transmission line by Pade approximation via Lanczos process," *IEEE Trans. Microwave Theory Tech.*, vol. 44, pp. 1480–1487, Dec. 1996.

[75] H. Braunisch and H. Grabinski, "Time-domain simulation of large lossy interconnect systems on conducting substrates," *IEEE Trans. Circuits and System, part-1*, vol. 45, pp. 909–918, Sept. 1998.

[76] J. Zheng, *et. al.*, "CAD-oriented equivalent circuit modeling of on-chip interconnects for RF integrated circuits in CMOS technology," accepted for publication in: *IEEE MTT-S Int. Microwave Symp. Dig.*, June 1999.

[77] S. C. Burkhart and R. W. Wilcox, "Arbitrary pulse shape synthesis using stripline nonuniform transmission line," *IEEE Trans. Microwave Theory Tech.*, vol. 38, pp. 1514–1518, Oct. 1990.

[78] D. C. Youla, "Analysis and synthesis of arbitrarily terminated loss less nonuniform lines," *IEEE Trans. Circuit Theory, CT-2*, vol. 11, pp. 363–372, Sept. 1964.

[79] M. R. Wohlers, "Analysis and synthesis of arbitrarily terminated lossless nonuniform lines," *IEEE Trans. Circuit Theory*, vol. 13, pp. 356–363, Sept. 1966.

[80] M. Kobayashi and N. Sawada, "Analysis and synthesis of tapered microstrip transmission lines," *IEEE Trans. Microwave Theory Tech.*, vol. 40, pp. 1642–1646, Aug. 1992.

[81] B. Gopinath, "Inversion of the telegraph equation and the synthesis of nonuniform lines," *Proc. IEEE*, pp. 383–392, Sept. 1987.

[82] S. I. Orlov, "Concerning the theory of nonuniform transmission lines," *Translated by American Physical Society, Sov. Phys. Tech.*, vol. 1, pp. 2284–2294, 1957.

[83] J. L. Frolik and A. E. Yagle, "Forward amd inverse scattering for discrete layered lossy and absorbing media," *IEEE Trans. on circuits & systems, part-2*, vol. 44, pp. 710–722, Sept. 1997.

[84] L. A. Hayden and V. K. Tripathi, "Characterization and modeling of multiple line interconnection from time-domain measurement," *IEEE Trans. Microwave Theory Tech.*, vol. 42, pp. 1737–1743, Sept. 1994.

[85] S. D. Corey and A. T. Yang, "Automatic netlist extraction for measurement based characterization of off-chip interconnects," *IEEE Trans. Microwave Theory Tech.*, vol. 45, pp. 1434–1440, Aug. 1997.

[86] S. Sercu and L. Martins, "A new approach for the experimental circuit modeling of coupled interconnection structures based on causality," *IEEE Trans. Microwave Theory Tech.*, vol. 45, pp. 1977–81, Oct. 1997.

[87] P. P. Roberts and G. E. Town, "A design of microwave filters by inverse scattering," *IEEE Trans. Microwave Theory Tech.*, vol. 43, pp. 739–743, Apr. 1995.

[88] L. A. Hayden, *et. al.*, "Measurement and characterization of multiple coupled interconnection lines in hybrid and monolithic integrated circuits," *International*

Conference on Advances in Interconnection and Packaging, vol. 1389, pp. 205–211, 1990.

[89] Jun-Fa Mao, *et. al.*, "Synthesis of coupled transmission lines," *IEEE Trans. on Circuits and Systems-(1), Fundamental Theory and Applications*, vol. 44, pp. 327–337, Apr. 1997.

[90] A. Tripathi and V. K. Tripathi, "Characterization and modeling of multiple coupled lines in an inhomogeneous medium from time domain reflection measurements," submitted to: *IEEE Trans. Circuits and System, part-1.*

[91] J. P. K. Gilb and C. A. Balanis, "MIS slow-wave structures over a wide range of parameters," *IEEE Trans. Microwave Theory Tech.*, vol. 40, pp. 2148–2154, Dec. 1992.

[92] Frank Olyslager, *et. al.*, "Rigorous analysis of the propagation characteristics of lossless or lossy multiconductor transmission lines in multilayered media," *IEEE Trans. Microwave Theory Tech.*, vol. 41, pp. 79–88, Jan. 1993.

[93] Tsung-Chang Mu, *et. al.*, "Characteristic of multiconductor asymmetric slow-wave microstrip transmission lines," *IEEE Trans. Microwave Theory Tech.*,vol. 34, pp. 1471–1477, Dec. 1986.

[94] T. Kitazawa and T. Itoh, "Propagation characteristics of coplanar type transmission lines with lossy media," *IEEE Trans. Microwave Theory Tech.*, vol. 39, pp. 694–1700, Oct. 1991.

[95] Ching-Kuang and T.-P. Tseng, "A full wave mixed potential mode matching method for the analysis of planar or quasi-planar transmission line," *IEEE Trans. Microwave Theory Tech.*, vol. 39, pp. 1701–1711, Dec. 1991.

[96] Mattan Kamon, *et. al.*, "Fasthenry: A multipole accelerated 3D inductance extraction program," *IEEE Trans. Microwave Theory Tech.*, vol. 42, pp. 1950–1958, Sept. 1994.

[97] Kyung Suk Oh, *et. al.*, "Capacitance computation in a multilayered dielectric medium using closed form spatial Green's functions," *IEEE Trans. Microwave Theory Tech.*, vol. 42, pp. 1443–1453, Aug. 1994.

[98] H. Klingbeil and W. Henrich, "Calculation of CWP ac resistance and inductance using a quasi-static mode matching approach," *IEEE Trans. Microwave Theory Tech.*, vol. 42, pp. 1004–1007, July 1994.

[99] Enrique Drake, *et. al.*, "Improved quasi-TEM spectral domain analysis of boxed coplanar multiconductor microstrip lines," *IEEE Trans. Microwave Theory Tech.*, vol. 41, pp. 261–267, Feb. 1993.

[100] Young R Knon, *et. al.*, "Quasi-TEM analysis of slow-wave mode propagation on coplanar microstructure MIS transmission lines," *IEEE Trans. Microwave Theory Tech.*, vol. 35, pp. 545–551, June 1987.

[101] Ganzalo Plaza, *et. al.*, "Quick computation of $[C]$, $[L]$, $[G]$ and $[R]$ matrices for multiconductor and multilayer transmission lines," *IEEE Trans. Microwave Theory Tech.*, vol. 43, pp. 1623–1626, July 1995.

[102] M. J. Tsuk, *et. al.*, "A hybrid method for the calculation of the resistance and inductance of transmission lines arbitrary cross-section," *IEEE Trans. Microwave Theory Tech.*, vol. 39, pp. 1338–1347, Aug. 1991.

[103] Cao Wei, *et. al.*, "Multiconductor transmission lines in multilayered dielectric media," *IEEE Trans. Microwave Theory Tech.*, vol. 4, pp. 439–449, Apr. 1984.

[104] V. K. Tripathi, *et. al.*, "Quasi-TEM spectral domain analysis of thick microstrip for microwave and digital integrated circuits," *Electron. Lett.*, vol. 25, pp. 1253–1254, Apr. 1989.

[105] Ichichik Toyoda, *et. al.*, "Three dimensional master slice MMIC on Si substrates," *IEEE Trans. Microwave Theory Tech.*, vol. 45, pp. 2524–2530, Dec. 1997.

[106] M. F. H. Hasegawa and H. Yanai, "Properties of microstrip line on Si-SiO_2 system," *IEEE Trans. Microwave Theory Tech.*, vol. 19, pp. 869–881, Nov. 1971.

[107] V. K. Tripathi and R. Bucolo, "A simple network analog approach for the quasi-static characteristics of general lossy, anisotropic, layered structures," *IEEE Trans. Microwave Theory Tech.*, vol. 33, pp. 1458–1464, Dec. 1985.

[108] A. C. Reyes, "Coplanar waveguides and microwave inductors on silicon substrates," *IEEE Trans. Microwave Theory Tech.*, vol. 43, pp. 2016–2021, Sept. 1995.

[109] Dylan F. Williams, *et. al.*,"Accurate characteristic impedance measurement on silicon," *IEEE MTT-S Int. Microwave Symp. Dig.*, pp. 1917–1920, June 1998.

[110] R. A. Lawton and W. T. Anderson, "Two layer dielectric microstrip line structure: SiO_2 on Si and $GaAs$ on Si: modeling and measurement," *IEEE Trans. Microwave Theory Tech.*, vol. 36, pp. 545–551, Apr. 1988.

[111] J. N. Burghartz, *et. al.*, "Microwave inductors and capacitors in standard multilevel interconnect silicon technology," *IEEE Trans. Microwave Theory Tech.*, vol. 44, pp. 100–104, Jan. 1996.

[112] J. R. Long and M. A. Copeland, "The modeling, characterization and design of monolithic inductors for silicon RFIC's," *IEEE J. Solid State Circuits*, vol. 32, pp. 357–369, Mar. 1997.

[113] Christoph Warns, *et. al.*, "Transmission lines and passive elements for multilayer coplanar circuits on silicon," *IEEE Trans. Microwave Theory Tech.*, vol. 46, pp. 616–622, May 1998.

[114] Veljko Milanovic, *et. al.*, "Characterization of broad-band transmission for coplanar waveguides on CMOS silicon substrates," *IEEE Trans. Microwave Theory Tech.*, vol. 46, pp. 632–640, May 1998.

[115] Alok Tripathi, *et. al.*, "A quasi-TEM spectral domain approach for calculating distributed inductance and resistance of microstrip on Si-SiO_2 substrate," Electron. Lett., vol. 34, pp. 1330–1331, June 1998.

[116] R. D. Lutz, *et. al.*, "Modeling of spiral inductors on lossy substrates for RFIC applications," *IEEE MTT-S Int. Microwave Symp. Dig.*, pp. 1855–1858, June 1998.

[117] Ke-Wu, *et. al.*, "Hybrid-mode analysis of homogeneously and inhomogeneously doped low loss slow-wave coplanar transmission lines," *IEEE Trans. Microwave Theory Tech.*, vol. 39, pp. 1348–1360, Aug. 1991.

[118] Jun-Wu Tao, *et. al.*, "Full-wave description of propagation and losses in quasi-planar transmission lines by quasi analytical solution," *IEEE Trans. Microwave Theory Tech.*, vol. 42, pp. 1246–53, July 1994.

[119] W. I. Bowman and J. M. McNamee, "Development of equivalent π and T matrix circuits for long untransposed transmission lines," *IEEE Trans. Power Apparatus Syst.*, vol. 39, pp. 625–632, June 1964.

[120] S. B. Hanti, *et. al.*, The Riccati Equation. *Springer Verlag*, 1991.

[121] G. L. Matthaei and G. C. Chinn, "Approximate calculation of the high-frequency resistance matrix for multiple coupled lines," *IEEE MTT-S Int. Microwave Symp. Dig.*, pp. 1353–54, June 1992.

[122] V. K. Tripathi and N. Orhanovic, "Time domain characterization and analysis of dispersive dissipative interconnects," *IEEE Trans. on circuits & systems, part-1*, vol. 39, pp. 938–945, Nov. 1992.

[123] R. E. Kalman, *et. al.*, Topics in Mathematical System Theory. *New York: McGraw-Hill*, 1969.

[124] L. A. Hayden, "Characterization and electrical circuit modeling of interconnections and packages using time domain network analysis," *PhD thesis*, Oregon State University, Corvallis, OR, 1993.

[125] K. Hoffman and R. Kunze, Linear Algebra, *Pretince-Hall, Inc.*, 1991 (reprint).